POLITECNICO DI TORINO
Repository ISTITUZIONALE

Powder Degradation and Recycling Strategies for Aluminum Alloys in Additive Manufacturing: A Comprehensive Review

Original
Powder Degradation and Recycling Strategies for Aluminum Alloys in Additive Manufacturing: A Comprehensive Review / Rezaei, S., Biamino, S., Bondioli, F., Ugues, D., Fino, P., Lombardi, M.. - In: APPLIED SCIENCES. - ISSN 2076-3417. - 16:13(2026), pp. 1-53. [10.3390/app16136822]

Availability:
This version is available at: 11583/3013348 since: 2026-07-21T12:08:09Z

Publisher:
Multidisciplinary Digital Publishing Institute (MDPI)

Published
DOI:10.3390/app16136822

Terms of use:

This article is made available under terms and conditions as specified in the corresponding bibliographic description in the repository

Publisher copyright

(Article begins on next page)

25 November 2026

applied sciences

MDPI

Review

Powder Degradation and Recycling Strategies for Aluminum Alloys in Additive Manufacturing: A Comprehensive Review

Sina Rezaei *, Sara Biamino, Federica Bondioli, Daniele Ugues, Paolo Fino and Mariangela Lombardi *

Department of Applied Science and Technology, Politecnico di Torino, Corso Duca degli Abruzzi 24, 10129 Turin, Italy; sara.biamino@polito.it (S.B.); federica.bondioli@polito.it (F.B.); daniele.ugues@polito.it (D.U.); paolo.fino@polito.it (P.F.)

* Correspondence: sina.rezaei@polito.it (S.R.); mariangela.lombardi@polito.it (M.L.)

Abstract

The growing adoption of additive manufacturing (AM) has increased the demand for efficient and sustainable powder management, particularly for aluminum alloys used in lightweight and high-performance applications. Despite their attractive strength-to-weight ratio, corrosion resistance, and recyclability, aluminum powders are highly sensitive to degradation during repeated reuse. This review examines the main physical and chemical changes occurring in aluminum alloy powders during AM, including oxidation, morphological evolution, agglomeration, moisture uptake, contamination, and porosity-related effects. Their influence on powder flowability, spreadability, packing behavior, laser absorption, and final part quality is critically discussed. The study also reviews current and emerging powder recycling and reconditioning strategies, including sieving, top-up blending, Hydride–Dehydride processing, plasma spheroidization, annealing, and chemical surface treatments. In addition, best practices for powder handling, storage, and quality assessment are summarized to support reliable reuse. Particular attention is given to aluminum powders used in laser powder bed fusion. Unlike earlier reviews that address powder degradation, recycling, or aluminum AM separately, this review provides an integrated framework connecting degradation mechanisms, reconditioning strategies, and qualification methods for reused aluminum powders. It also highlights key knowledge gaps and future directions for developing more reliable and sustainable powder lifecycle management in aluminum-based AM.

Keywords: additive manufacturing; aluminum alloys; powder degradation; powder recycling; laser powder bed fusion; sustainable manufacturing

Check for updates

Academic Editor: Manoj Gupta

Received: 21 May 2026
Revised: 22 June 2026
Accepted: 1 July 2026
Published: 7 July 2026

Copyright: © 2026 by the authors. Licensee MDPI, Basel, Switzerland. This article is an open access article distributed under the terms and conditions of the Creative Commons Attribution (CC BY) license.

1. Introduction

Additive manufacturing (AM) is a layer-wise manufacturing approach in which components are produced directly from digital model data [1,2]. Over the past decades, AM has evolved from a rapid prototyping tool into a broader manufacturing platform capable of producing functional components with complex geometries, reduced material waste, and high design flexibility [3,4]. Among its different process families, metal AM has gained particular importance for high-value engineering applications where material efficiency and geometric complexity are critical.

In metal AM, powder-based routes such as laser powder bed fusion (L-PBF), directed energy deposition (DED), electron beam powder bed fusion, and binder jetting are commonly used, each with specific requirements regarding powder size, morphology, chemistry,

and flow behavior [5,6]. Among metallic feedstocks, aluminum alloys are especially attractive because of their low density, high specific strength, recyclability, and industrial relevance in transportation and aerospace sectors. At the same time, they are among the most challenging powders to manage because of their high reflectivity, high thermal conductivity, strong affinity for oxygen, and sensitivity to moisture-related degradation during repeated reuse and handling [7–12].

Aluminum plays a crucial role in energy transitions and lightweight applications, particularly in the transportation and aerospace industries. Recognized for its high strength-to-weight ratio, durability, and recyclability, aluminum is a key material for sustainable development [13,14]. Recycling aluminum requires only 5% of the energy needed for primary production, significantly reducing carbon emissions and overall energy consumption [15]. Its lightweight properties further enhance energy efficiency, leading to lower fuel consumption and emissions in the automotive and aerospace sectors. Beyond transportation, aluminum is also vital in energy-efficient buildings, solar panels, and electric vehicles, reinforcing its significance in promoting global efficiency and environmentally friendly industries [16–19]. Currently, some of the key alloying elements used in the production of important aluminum alloys, such as silicon, magnesium, and scandium, are classified as critical raw materials (CRMs). Additionally, aluminum holds significant economic importance. Although its current supply risks are relatively low, it remains a material of strategic interest, already recognized as a CRM by U.S. authorities and considered a potential CRM for the European Union in the near future [20,21]. Processing aluminum alloys through L-PBF offers significant opportunities to reduce environmental impacts, particularly in industries where weight reduction is critical, such as automotive and aerospace [22]. However, despite these advantages, only a limited number of aluminum alloy systems have so far achieved robust processability in powder-based AM, which makes powder selection, powder reuse, and powder quality control particularly important for this class of materials.

Because of these material-specific challenges, powder reuse in aluminum AM cannot be discussed in the same way as powder reuse in broader multi-metal systems [23–25]. Although previous reviews have addressed powder recycling, reuse strategies, or aluminum additive manufacturing separately, a more focused discussion linking degradation mechanisms, reconditioning approaches, and powder qualification methods for reused aluminum powders remains limited [26,27]. This review was therefore undertaken to provide an integrated overview of powder degradation and recycling strategies for aluminum alloy powders in additive manufacturing, with particular emphasis on L-PBF, where aluminum powder reuse is both most relevant and most extensively documented [28–30]. This emphasis on L-PBF was adopted because it remains the most mature and most widely used powder-based AM route for aluminum alloys, and it also provides the most substantial body of literature on powder reuse, degradation behavior, and powder qualification [31–33]. The discussion is centered primarily on Al–Si-based powders, especially AlSi10Mg, AlSi7Mg, and AlSi12, because these remain the most mature and most extensively studied aluminum systems in powder-based AM and form the main basis of current reuse and recycling investigations, while selected emerging systems such as Scalmalloy and modified high-strength aluminum alloys are discussed more selectively to illustrate future alloy-development opportunities [33–38]. In addition to summarizing degradation pathways and reconditioning methods, the present work highlights aluminum-specific challenges, discusses their implications for powder-bed behavior and final part quality, and identifies key research gaps and future directions for more reliable and sustainable powder lifecycle management. For this reason, the review intentionally combines a concise mechanistic overview of powder degradation and recycling with an aluminum-specific analysis, so that broader powder-reuse concepts are included only where they are necessary to interpret the behavior of

reused aluminum powders. The scope of the present review is limited to reused aluminum alloy powders in powder-based additive manufacturing, with primary emphasis on L-PBF and secondary reference to DED only where it provides useful comparative context. The discussion is centered mainly on Al–Si-based powders, especially AlSi10Mg, AlSi7Mg, and AlSi12, because these systems currently provide the most robust basis for analyzing degradation, reuse, and reconditioning behavior. Non-aluminum systems are referred to only when they offer mechanistic insight that is not yet sufficiently documented for aluminum powders.

Review Methodology

This manuscript was prepared as a focused critical narrative review addressing powder degradation, reuse, recycling, reconditioning, and qualification strategies for aluminum alloy powders in powder-based additive manufacturing. The review was structured to prioritize studies directly relevant to reused aluminum powders, with primary emphasis on laser powder bed fusion (L-PBF) and secondary reference to directed energy deposition (DED) only where it provides useful comparative context. Particular attention was given to Al–Si-based systems, especially AlSi10Mg, AlSi7Mg, and AlSi12, because these alloys currently provide the most substantial body of evidence on degradation behavior, powder reuse, reconditioning, and final part performance.

The reviewed literature was organized thematically according to the main objectives of the manuscript, including degradation mechanisms, recycling and reconditioning strategies, powder handling and storage, aluminum-specific powder behavior, quality assessment methods, and the influence of reused powder on final part microstructure and mechanical properties. Priority was given to peer-reviewed journal articles and recent review papers reporting experimentally supported observations relevant to reused aluminum powders. Broader studies on other metallic systems were retained only when they provided mechanistic insights not yet sufficiently documented for aluminum powders. Accordingly, this review is intended to provide an integrated, aluminum-centered critical synthesis rather than an exhaustive systematic survey of all metal-powder reuse literature.

Powder reuse in additive manufacturing involves recovery of the unfused feedstock after a build, removal of out-of-spec fractions such as spatter, agglomerates, or excessive fines, optional blending with virgin powder, and re-qualification before reuse. The suitability of the recycled powder depends on whether key properties such as particle size distribution, morphology, flowability, and chemical condition remain within an acceptable processing window. As summarized schematically in Figure 1, this workflow is not a single recovery step but a controlled sequence of extraction, reconditioning, qualification, storage, and reintroduction into the next build cycle. Because repeated reuse can progressively alter powder characteristics and thereby affect process stability and final part quality, effective reuse requires systematic monitoring and application-specific quality control throughout the powder lifecycle [23,24,39–47].

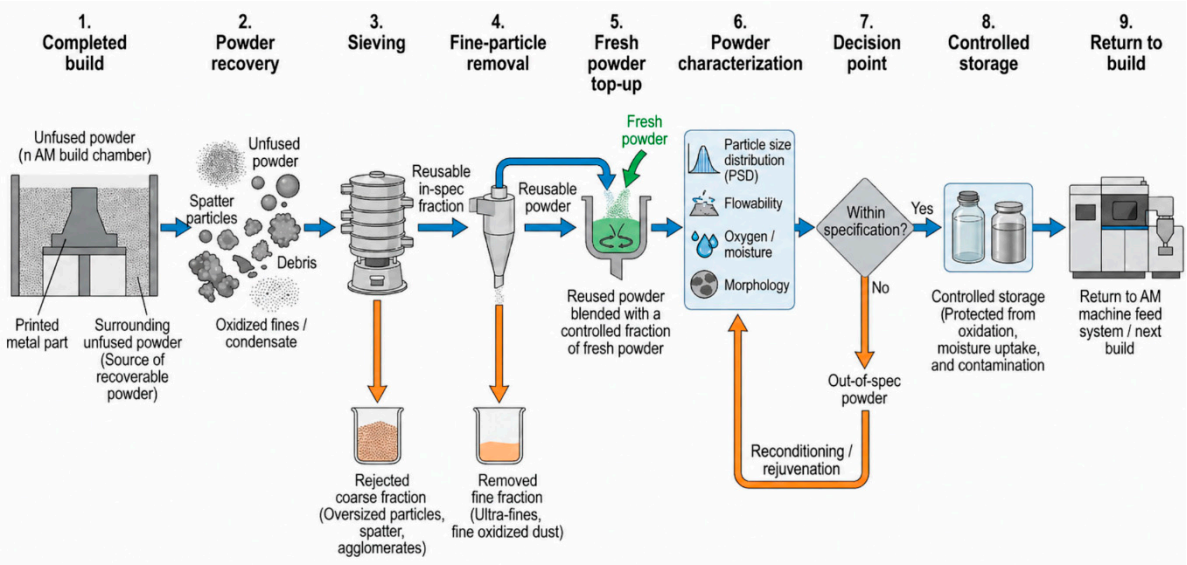

Figure 1. Schematic illustration of the powder reuse workflow in AM.

2. Powder Degradation Mechanisms

Although many powder degradation mechanisms are broadly relevant to metal additive manufacturing, the present section discusses them primarily from the perspective of aluminum alloy feedstocks and their reuse in powder-based AM. Cross-material examples are retained only where they clarify mechanistic aspects that are not yet sufficiently documented for aluminum itself. Particular emphasis is placed on oxidation, morphology evolution, sintering/agglomeration, moisture uptake, and contamination, because these mechanisms are the most consistently linked to powder-bed behavior, reuse stability, and final part quality in aluminum AM [25,43]. Figure 2 schematically summarizes the main degradation pathways relevant to repeated reuse of aluminum alloy powders in powder-based additive manufacturing and their effects on powder properties, process stability, and final part quality.

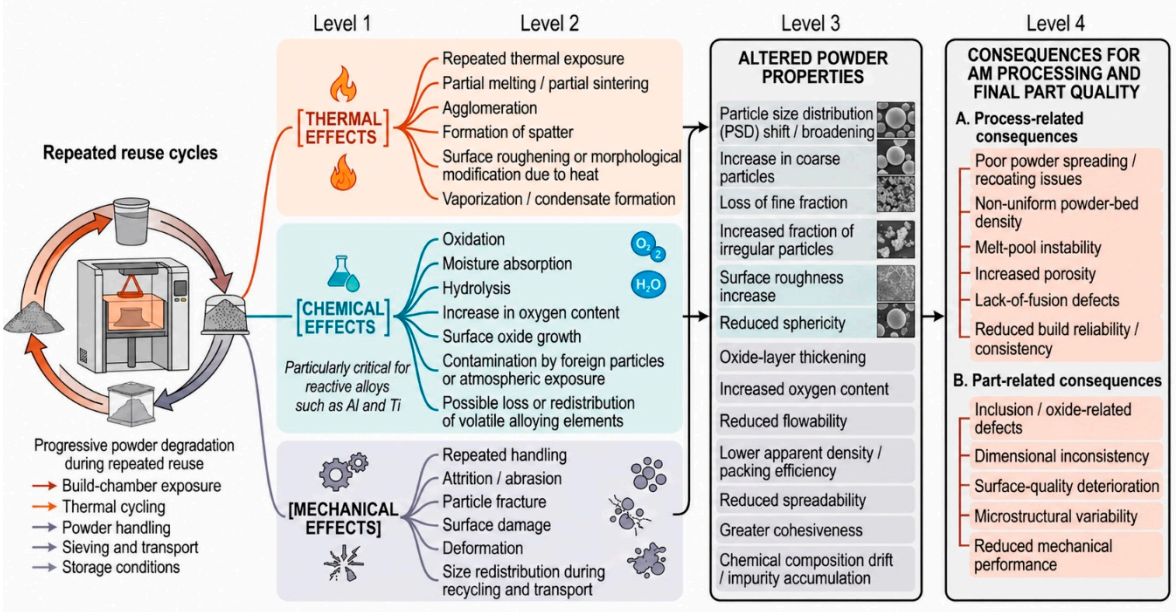

Figure 2. Schematic illustration of the main powder degradation pathways relevant to repeated reuse of aluminum alloy powders in powder-based additive manufacturing and their effects on powder properties, process stability, and final part quality.

2.1. Thermal Effects

2.1.1. Oxidation of Powder Feedstock

Oxidation involves the formation of oxide layers or the absorption of oxygen by metal particles. This phenomenon is particularly pronounced in reactive metals such as titanium and aluminum, which are highly susceptible to oxidation upon exposure to oxygen, whether at ambient or elevated temperatures. In AM processes like L-PBF and DED, powders are subjected to high temperatures and may come into contact with atmospheric oxygen or residual gases within the build chamber. Even in environments that are nominally inert, trace amounts of oxygen or moisture can still promote oxidation. With repeated reuse, oxygen accumulation becomes more significant, leading to the development of thicker oxide layers on the powder surface or the diffusion of oxygen into the subsurface of the particles [48]. Oxidation is a significant concern in PBF processes, both laser-based and electron beam-based (E-PBF), as well as in DED, particularly when shielding is inadequate. In L-PBF, the build chamber is typically filled with an inert gas such as argon or nitrogen to minimize oxidation. However, impurities or residual oxygen and moisture in the shielding gas can still lead to unintended oxidation of the metal powder [49,50]. In E-PBF, which operates under a partial vacuum, oxygen ingress during the build process is minimal. However, moisture retained in the powder or within the build chamber can decompose under high temperatures, releasing oxygen and thereby contributing to oxidation [51,52]. DED processes, such as laser cladding, also employ inert gas shrouds to protect the molten material. However, any exposure to air either before or during powder delivery can result in oxidation of the heated particles, whether in flight or upon deposition on the build surface [53]. Oxidation alters the chemical composition of the powder by increasing its oxygen content and by thickening the oxide film that covers the particle surface. In reactive alloys, especially aluminum, this oxide layer is particularly detrimental because it behaves as a refractory barrier during both solid-state contact and laser melting. In the case of aluminum powders, the native Al_2O_3 film remains solid at temperatures far above the melting point of aluminum itself, so it can hinder intimate metallic contact between neighboring particles and reduce effective wetting during melting. As a result, inter-particle bonding becomes less efficient, particle coalescence is delayed, and the continuity of the molten region may be locally disrupted. During partial melting or sintering, such oxide films can also restrict mass transport across contact points, thereby slowing neck growth and limiting densification. During full melting, oxide skins may remain partially intact on molten droplets or break into fine entrained oxide fragments, which can then act as inclusions inside the melt pool. These oxide-related barriers and inclusions may interfere with melt-pool flow, weaken bonding between adjacent molten regions, and promote lack-of-fusion defects or pore formation in the final part [54–56]. Consequently, oxidation is closely monitored in studies involving reused powders, with oxygen content often serving as a critical quality indicator. For example, one study found that the oxygen concentration in Ti-6Al-4V powder increased from 0.08 wt% to 0.19 wt% after 21 reuse cycles, a change that is correlated with a measurable decline in the ductility of the produced parts. Therefore, effective oxidation management through storage in inert environments, controlled atmosphere handling, and strict limitations on powder reuse cycles is essential to preserving both powder integrity and the mechanical performance of the final components [48].

2.1.2. Morphological Changes (Particle Shape and Size Evolution)

By examining the effects of thermal degradation caused by the interaction between the energy beam and the powder (Figure 3), it becomes evident that the primary impact is associated with the formation of molten metal droplets. These droplets are rapidly expelled

from the energy source and solidify almost instantly, contributing to degradation phenomena [57,58]. In this scenario, several phenomena simultaneously influence the powder composition as well as its size and geometry. For instance, a molten metal droplet may be ejected directly from the melt pool. Upon ejection, the droplet undergoes independent solidification, and depending on the degree of overheating reached by the metal, this can result in the formation of a new crystalline structure or a phase transformation [59]. During AM processing and subsequent powder recycling, the physical shape and PSD of the powder can undergo significant changes. Studies on reused AM powders consistently show that morphology evolves away from the near-spherical and tightly controlled condition typical of virgin gas-atomized feedstock. For example, studies cited in [60,61] reported PSD shifts toward coarser sizes during reuse, mainly because of fine-particle depletion and agglomerate formation. Likewise, ref. [48] associated repeated reuse with reduced sphericity and increased surface roughness, while [42,62] linked these changes to both thermal exposure and mechanical actions such as sieving, scraping, and powder recovery.

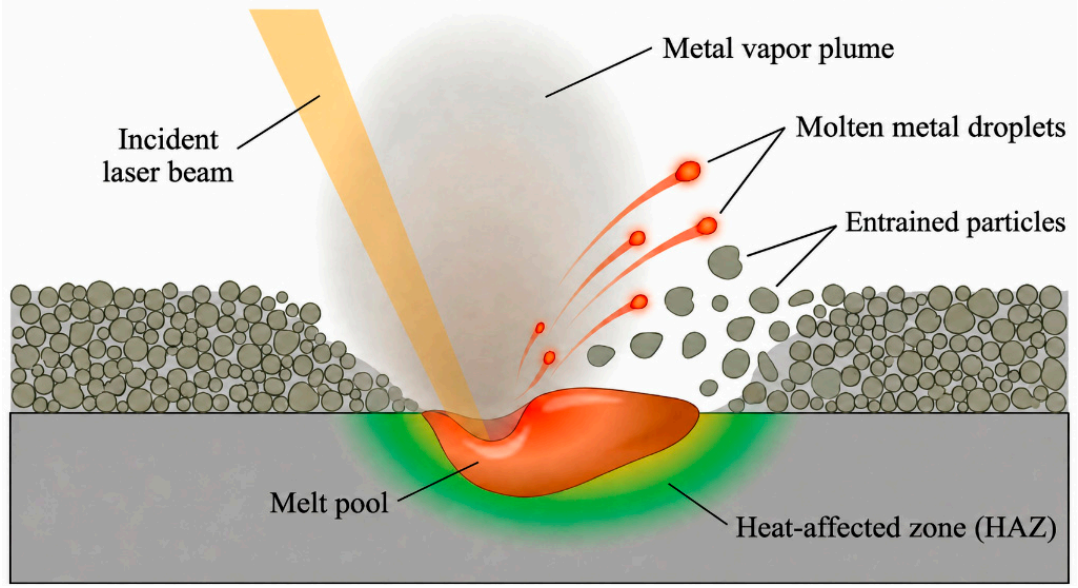

Figure 3. Simplified illustration of the interaction between a high-energy beam and metallic powders. The green area indicates the heat-affected zone (HAZ), while the red region represents the melted material.

The consequences of these changes are not purely geometric. As reported in [48] rougher and less spherical particles generally show poorer flowability and packing behavior than smooth spherical particles. However, ref. [60] also noted that flowability may occasionally improve after reuse when the loss of ultra-fine particles reduces cohesive interparticle forces. This indicates that the net effect of reuse on powder flow depends on the balance between shape degradation and fines depletion, rather than on a single morphological descriptor alone.

Specific observations further illustrate this point. In a Ti-6Al-4V study, it was found that repeated reuse increased particle surface roughness while the overall particle shape remained largely spherical, and few large agglomerates were formed. The same study emphasized that such roughened particles may trap more air or moisture and exhibit altered thermal absorption behavior, which increases the likelihood of incomplete melting and local lack-of-fusion defects [43]. In contrast, the effects of adhered spatter, condensate, and other foreign particulates are discussed separately in Section 2.2.2, where contamination-related chemical and compositional changes are addressed more directly.

2.1.3. Sintering and Agglomeration of Particles

Partial sintering is also recognized as a form of thermal degradation in metal AM processes [63]. Partial melting or thermal fusion of particles is a common form of degradation in AM. When particles are exposed to temperatures approaching their melting point for extended periods, they can undergo sintering, forming solid necks at points of contact or even fuse completely into larger clusters. In metal PBF processes, this phenomenon may occur either by design or unintentionally as a result of the processing conditions. For example, E-PBF is carried out at elevated powder-bed temperatures and typically produces a sintered powder cake that must be mechanically broken apart after the build. Even in L-PBF, particles located close to the melt pool or exposed to local overheating may partially sinter. In practice, this behavior is usually observed in two forms: satelliting and agglomeration. Satelliting occurs when small particles attach to the surfaces of larger ones, whereas agglomeration refers to several particles, often of comparable size, joining together to form a single irregular mass. In both cases, the underlying cause is usually partial melting at particle contact points, followed by solidification that creates bridges between them [43]. Although controlled partial sintering can sometimes be beneficial for improving powder flowability, packing density, and interlayer bonding, excessive or uncontrolled sintering is generally harmful. These include reduced flowability, increased porosity, poor surface finish, and dimensional inaccuracies in the final parts. Therefore, it is crucial to precisely control and optimize thermal conditions during the AM process to minimize the adverse effects of partial sintering and maintain the quality and structural integrity of AMed components [63–65]. Agglomerated particles effectively act as "oversized" powder, skewing the PSD toward larger, often irregular shapes. This gives rise to several adverse effects. First, large agglomerates flow poorly through recoaters or nozzles and can disturb powder spreading, producing surface irregularities such as streaks or local bumps in the powder bed. Second, these agglomerates may be retained by fine sieves during powder recycling, which leads to material loss; if they are not removed, they can also block powder delivery systems and interfere with process stability. Third, because of their larger size, agglomerated particles generally require more energy to melt completely. When process parameters are tuned for smaller, individual particles, these larger clusters may melt only partially, increasing the risk of inclusions or lack-of-fusion defects in the final part. Finally, sintered clusters may exhibit thermal conductivity and absorption behavior that differ from that of individual particles, which can alter their interaction with the laser or electron beam during the build process. Overall, powder sintering reduces the volume of free-flowing, reusable powder and concentrates alloying elements into fewer, larger masses, potentially leading to microsegregation and reduced material homogeneity [66–69].

2.2. Chemical Effects

2.2.1. Moisture Absorption and Hydrolysis

Many powders exhibit hygroscopic behavior, meaning they easily absorb moisture from the surrounding air. This moisture can either physically adhere to the surface of the particles or become chemically adsorbed. Fine powders, which have a high surface area, are especially prone to absorbing moisture quickly [70]. In metal powders, moisture usually refers to a thin film of water coating the particles. Upon heating, this moisture can initiate oxidation reactions, as water serves as a source of both oxygen and hydrogen [71]. Moisture can enter metal powders during storage, particularly if containers are not properly sealed or lack desiccants, as well as during handling between build cycles. In PBF systems, once a build is complete and the chamber is opened, the exposed powder can rapidly absorb moisture from the ambient air. Within just a few minutes of exposure, fine metal powders are capable of adsorbing a measurable amount of water [72]. Moisture alone can cause

powders to clump or cake. When water molecules form bridges between particles, capillary forces cause them to adhere to one another, leading to the formation of larger agglomerates. This negatively impacts both flowability and spreadability of the powder [73]. When heated, moisture within the powder can vaporize, potentially generating pressure that disrupts powder layering or leads to spattering. More critically, moisture introduces both oxygen and hydrogen. In reactive metals such as titanium or aluminum, the presence of water on the powder surface promotes oxidation (metal + $H_2O \rightarrow$ metal oxide + H_2). The resulting hydrogen gas can dissolve into the melt pool or form pores if it escapes as bubbles, ultimately compromising the integrity of the final part [49,74]. Aluminum alloys are particularly sensitive to moisture adsorption. A study on Al-6061 powder used in L-PBF found that even slight increases in powder moisture could lead to the formation of aluminum hydroxides and result in small spherical pores within the printed parts. Although the moisture content of reused aluminum powder was reported to be comparable to that of virgin powder in the study, the researchers emphasized that any moisture uptake could increase the risk of porosity-related defects in aluminum components [25].

2.2.2. Contamination (Foreign Particles and Impurities)

Another chemical degradation mechanism in AM is powder contamination, which can alter the chemical composition of the material and negatively impact the quality and performance of the final part [75–77]. Contamination refers to the presence of unwanted foreign materials or impurities introduced into the powder. This can result from various sources, including process byproducts such as spatters or condensates, mechanical wear from components like recoater blades or nozzles, environmental exposure to dust and dirt, or cross-contamination with different types of powders. Such contaminants can alter the powder's chemical and physical properties, potentially compromising the integrity and performance of the final printed parts [78]. Contaminants can be detrimental in several ways. For instance, large spatter particles mixed into the powder can behave like agglomerates, disrupting the smoothness of the powder layer and potentially failing to fully melt during processing, which can lead to defects in the final part [79]. If the spatter has a different chemical composition, such as being rich in oxides, it can lead to the formation of inclusions within the final microstructure, potentially compromising the material's mechanical properties and performance [80]. Fine condensate particles can coat otherwise good powder particles, potentially hindering proper melting or altering the local chemical composition during processing [81]. Overall, contamination often results in increased porosity and reduced mechanical properties in the final parts. This occurs because foreign particles may not melt and fuse properly, leading to voids or lack-of-fusion defects around them. Alternatively, if they do melt, they can form brittle phases or inclusions that compromise the structural integrity of the material [82–84].

2.3. Mechanical Effects

In AM, mechanical degradation of powder specifically refers to the decline in powder quality and characteristics caused by repeated use, handling, and exposure to environmental factors throughout the manufacturing process. Unlike the mechanical degradation of finished parts, powder degradation affects the feedstock material itself, which in turn can impair the mechanical properties and overall performance of the final AMed components [27,43,85].

The mechanical degradation of powder in AM primarily results from several interconnected factors. Repeated recycling causes deformation, fragmentation, and size variation in powder particles, which diminishes flowability and packing density [43,86]. Additionally, mechanical handling and thermal exposure can lead to particle fracture or agglomeration,

resulting in irregular shapes and clusters that disrupt layer uniformity and hinder smooth powder flow [62]. Environmental exposure further introduces contaminants such as moisture and gases, while promoting oxidation of particle surfaces; these changes adversely affect the thermal and mechanical behavior of the powder, ultimately reducing the mechanical performance of the printed parts [87]. Over successive usage cycles, powder particles also experience surface roughening, which increases inter-particle friction and leads to poor flowability and uneven powder layer deposition [27].

Mechanical degradation of powder can negatively affect both the AM process itself and the quality of the final components [43]. As the powder deteriorates, its flowability tends to decline, which can result in uneven spreading, irregular layer formation, and defects such as porosity and incomplete fusion. At the same time, changes in particle morphology and PSD can further increase porosity in the printed material, creating stress concentration sites that reduce mechanical strength and fatigue resistance [27]. Degraded powder may also lead to less uniform thermal behavior during processing, which can intensify residual stress buildup and increase the likelihood of crack initiation and growth in the final part [88]. In addition, powder degradation can introduce microstructural heterogeneity, which may adversely affect key properties such as ductility, toughness, and tensile strength, ultimately reducing the reliability and overall performance of AMed components [89].

Several measures can be adopted to limit powder degradation and preserve the mechanical properties of AM parts. A controlled recycling strategy typically involves restricting the number of reuse cycles, monitoring changes in particle morphology, and periodically adding virgin powder to maintain feedstock consistency [90,91]. Regular quality checks, including PSD measurements, chemical composition analysis, and morphological inspection, are also important for identifying early signs of degradation [92]. Proper storage and handling under controlled conditions, such as vacuum or inert atmospheres, can further reduce the risk of oxidation and contamination [72]. In addition, careful optimization of process parameters, including scan speed, laser power, and layer thickness, can help offset variations in powder condition and support stable, high-quality part production [93].

A common form of mechanical powder degradation in AM is attrition, which occurs when repeated handling and mechanical agitation during storage, transport, or processing gradually abrade and fragment the particles [94,95]. This can alter PSD, particle shape, and surface roughness, all of which negatively influence flowability and packing behavior. The problem may be intensified by friction between the powder and machine components, such as feed systems, recoaters, and metallic blades, which can cause wear on both the powder and the equipment. These interactions often generate fine debris and airborne particles, increasing the risk of contamination and further reducing feedstock consistency. Taken together, these effects can compromise the quality, repeatability, and mechanical performance of the final AMed parts [27].

3. Powder Recycling Strategies and Advances in Powder Recycling Techniques

For aluminum alloy powders, recycling and reuse strategies are especially important because powder degradation can directly affect flowability, oxidation state, melt-pool stability, and the quality of AMed parts. Although many recycling concepts were originally developed across broader metal AM systems, their relevance to aluminum varies significantly because aluminum powders are particularly sensitive to oxide growth, moisture pickup, and morphology-related spreadability problems. In Section 3, therefore, reviews the main recycling and reconditioning routes with emphasis on their practical relevance to aluminum powders, especially in L-PBF, while retaining a limited number of broader metal-AM examples only where they provide useful comparative context [26,48]. Figure 4

provides an overview of the main powder recycling methods used in metal additive manufacturing, including mechanical, thermal, and chemical approaches discussed in this section.

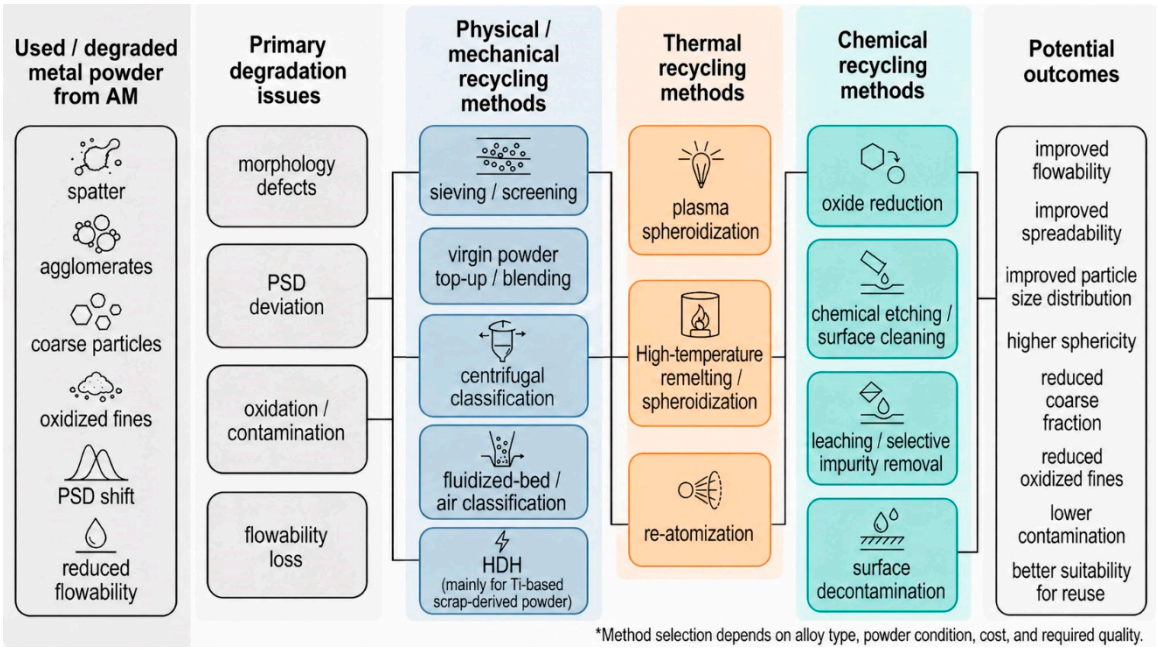

Figure 4. Overview of the main powder recycling methods in metal additive manufacturing.

3.1. Methods for Powder Recycling

Powder recycling methods used in additive manufacturing can be broadly classified into mechanical, thermal, and chemical approaches, depending on whether powder recovery is achieved mainly through physical separation and reshaping, heat-based restoration, or chemically assisted cleaning and reduction. For clarity and direct comparison, the main recycling routes discussed in this review are summarized in Table 1. The comparison includes not only technical advantages and limitations, but also economic feasibility, scalability, and practical suitability for aluminum alloy powders.

Table 1. Summary of the main powder recycling methods used in additive manufacturing.

Recycling Category	Method	Main Principle	Main Advantages	Main Limitations/Risks	Typical Suitability/Remarks	Economic Feasibility	Industrial Applicability/Suitability for Aluminum Powders	Scalability/ Implementation Level
Mechanical	Reuse and blending/top-up	Recovery of unfused powder followed by contaminant removal and reuse, often with controlled addition of virgin powder	Simple, industrially practical, low cost, and preserves most of the original feedstock	Does not fully restore degraded morphology or chemistry; requires strict quality monitoring	Widely used in PBF workflows; effective when degradation is still moderate	High	Very high; currently the most practical route for routine aluminum L-PBF reuse under controlled qualification	High; already widely implemented in industrial powder-handling workflows
Mechanical	Ball milling/ mechanical grinding	Conversion of bulk scrap, machining chips, or oversized particles into finer powder by mechanical comminution	Cost-effective route for turning scrap into powder feedstock	Produces irregular or angular particles; may introduce contamination from milling media; usually requires further treatment	More suitable for routes that tolerate non-spherical powders; less suitable for L-PBF without post-treatment	Medium	Limited for direct aluminum L-PBF reuse because irregular morphology usually requires additional reconditioning	Medium; scalable for bulk powder production or scrap conversion, but less suitable as a direct in-line AM reuse route

Table 1. *Cont.*

Recycling Category	Method	Main Principle	Main Advantages	Main Limitations/Risks	Typical Suitability/Remarks	Economic Feasibility	Industrial Applicability/Suitability for Aluminum Powders	Scalability/ Implementation Level
Mechanical/ hybrid	Hydride–Dehydride (HDH)	Hydrogenation of Ti scrap to form brittle hydride, followed by crushing or milling and dehydrogenation	Enables direct recycling of titanium scrap with limited alloy loss	Often produces angular particles; oxygen pickup and further conditioning may be required	Particularly relevant for Ti-based systems; may require sieving or spheroidization before PBF use	Medium	Low for aluminum; mainly relevant to titanium-based systems rather than routine aluminum powder reuse	Medium; scalable in dedicated powder-production chains, but not commonly implemented for routine aluminum AM reuse
Mechanical	Centrifugal separation	Particle separation based on density differences under high-speed rotation	High-throughput bulk classification	Limited efficiency for removing fine contaminants such as oxides, satellites, or broken particles	More common in conventional powder processing than in AM-specific workflows	Medium	Moderate for bulk classification, but limited as a standalone solution for oxidation- or morphology-driven aluminum degradation	Medium to high; scalable for bulk classification, though limited in selectivity for AM-specific degradation features
Thermal	Plasma spheroidization/ICP spheroidization	Surface or full melting of degraded particles in a high-temperature plasma, followed by spheroidization through surface tension and rapid solidification	Improves sphericity, flowability, packing density, and may reduce attached satellites	High energy demand; requires tight control of atmosphere and temperature; risk of further oxidation or coalescence if poorly controlled	Suitable for restoring morphology of irregular or degraded powders	Low to medium	Promising for severely morphology-degraded aluminum powders, but currently more specialized than routine industrial reuse	Low to medium; scalable mainly in specialized external powder-treatment facilities
Thermal	Annealing/ vacuum thermal treatment	Heat treatment under controlled atmosphere to reduce adsorbed species, relax surface-related degradation, and partially restore powder behavior	Less resource-intensive than full re-atomization; may improve flowability and surface condition	Cannot fully recover severely degraded powder; risk of oxidation, sintering, or microstructural changes if improperly controlled	Useful when degradation is mainly surface-related rather than morphological	Medium	Potentially useful for aluminum powders when degradation is mainly surface-related, but requires careful oxidation control	Medium; potentially scalable with batch furnace systems, but dependent on atmosphere control and powder sensitivity
Thermal	Re-atomization/ remelting-based recovery	Melting of scrap or degraded powder followed by atomization into new powder particles	Can substantially reset powder morphology and particle size distribution	High cost and energy demand; effectively closer to re-manufacturing than routine in-house reuse	More suitable when powder is heavily degraded or large waste volumes accumulate	Low	Limited to high-value or large-volume recovery scenarios; not generally suitable for routine in-house aluminum powder reuse	Low to medium; scalable mainly at large industrial volumes or centralized recovery operations
Chemical	Acid etching/surface cleaning	Selective removal of oxide layers or surface contaminants by controlled chemical treatment	Can clean oxidized particle surfaces and improve powder usability	Risk of hydrogen uptake, residue contamination, or morphology alteration during washing and drying	Promising for oxidized powders if carefully controlled	Low to medium	Scientifically promising for oxidized aluminum powders, but industrial adoption remains limited by residue control and safety concerns	Low; industrial scalability is limited by wet-chemical handling, washing, drying, and waste-treatment requirements

Table 1. *Cont.*

Recycling Category	Method	Main Principle	Main Advantages	Main Limitations/Risks	Typical Suitability/Remarks	Economic Feasibility	Industrial Applicability/Suitability for Aluminum Powders	Scalability/ Implementation Level
Chemical	Oxide reduction using reducing atmospheres	Removal or thinning of oxide layers through hydrogen-containing or otherwise reducing environments	May restore cleaner surfaces and reduce oxygen-related degradation	Risk of sintering, hydrogen pickup, and safety or processing complexity	More relevant for reactive alloys and heavily oxidized powders	Medium	Potentially relevant for oxidized aluminum feedstocks, but requires strict control because of hydrogen-related risks and process complexity	Low to medium; scalability depends on strict atmosphere control, safety management, and alloy sensitivity
Chemical	Leaching/ selective impurity removal	Chemical dissolution of undesirable species or contamination from degraded powder streams	Can target specific contaminant phases	Requires hazardous chemicals and waste handling; not always practical for routine AM workflows	More suitable for external recycling or specialized recovery operations	Low	Limited for routine aluminum AM; more suitable for specialized external recovery rather than standard powder reuse workflows	Low; generally more suitable for specialized off-line recovery than routine industrial powder reuse

Mechanical recycling methods are generally the simplest and most industrially accessible approaches for powder recovery. They are mainly based on physical separation, screening, classification, blending, or reuse-oriented conditioning, and are particularly useful when powder degradation is still moderate. Their main advantage lies in their practicality and relatively low cost; however, they cannot fully restore severe morphological degradation or surface-related chemical changes.

Thermal recycling methods become more relevant when powder degradation extends beyond simple contamination or PSD deviation and includes more severe morphology-related changes, such as reduced sphericity, satellite formation, or surface roughening. In these cases, the objective is not only powder cleaning but also morphological restoration through melting, remelting, or spheroidization. Representative process schematics for selected thermal routes are shown in Figures 5 and 6.

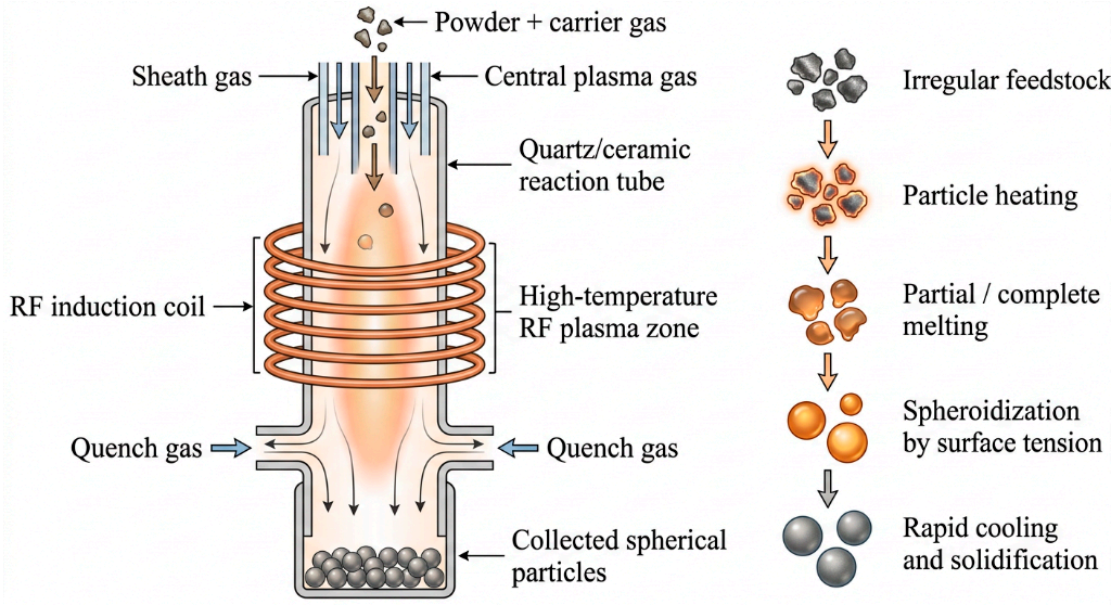

Figure 5. Schematic of the RF plasma spheroidization process.

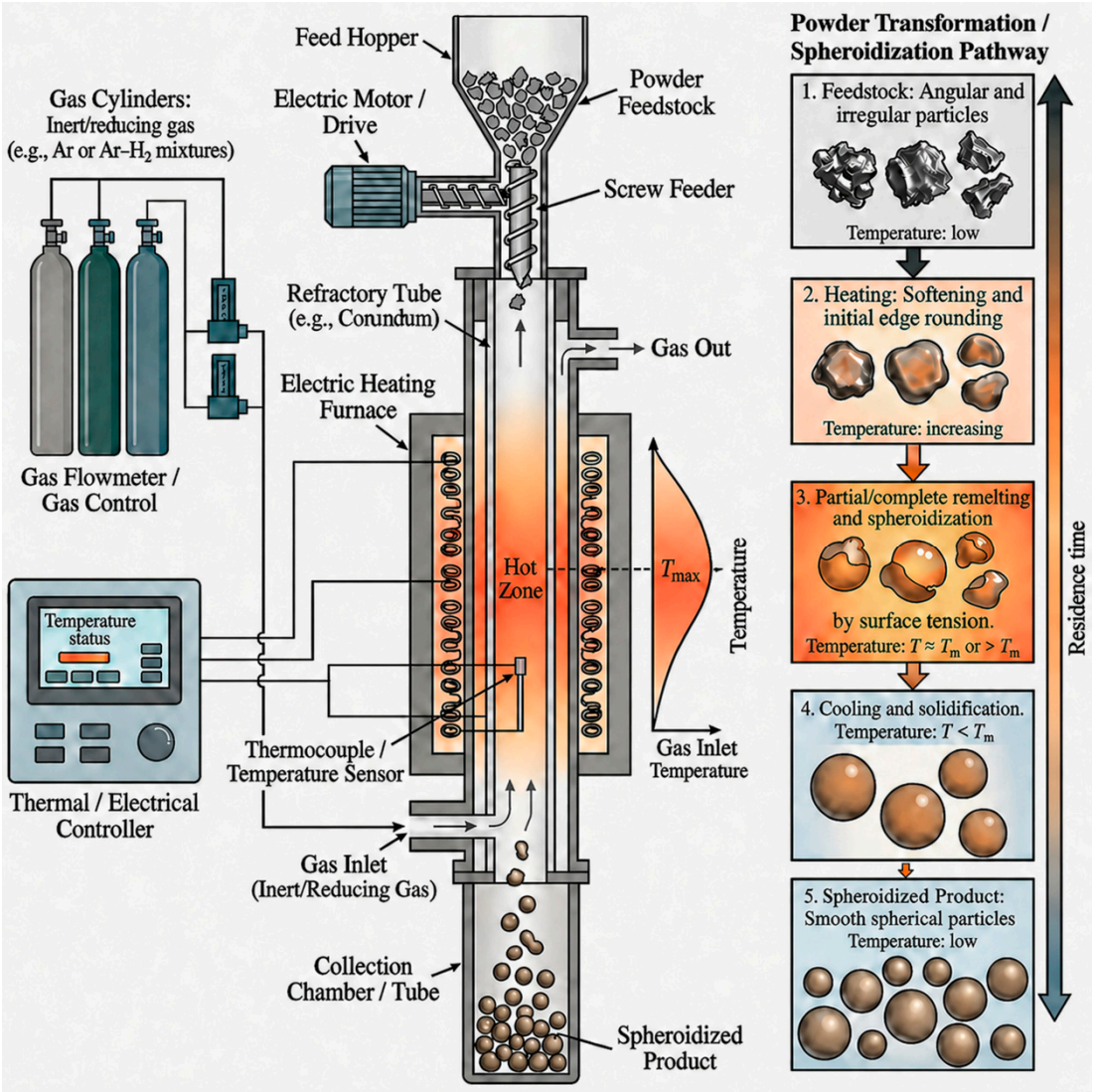

Figure 6. Schematic diagram of the HTRS device and process.

Figure 5 illustrates a plasma-based spheroidization route, in which irregular feedstock particles are exposed to a high-temperature plasma and are reshaped into more spherical particles through melting and surface-tension-driven solidification. This type of process is mainly valuable when poor particle morphology has become a dominant limitation for reuse.

Figure 6 shows the HTRS device and process, representing a hydrogen-assisted thermal treatment route intended for oxide reduction and powder surface recovery rather than direct morphological spheroidization. Compared with direct powder reuse or simple sieving-based reconditioning, such approaches are more intensive but may be effective when powder degradation is dominated by surface oxidation and chemically altered surface layers.

Chemical recycling methods are mainly intended to remove oxide layers, surface contamination, or specific impurity phases that cannot be adequately addressed by purely mechanical approaches. These methods can be effective when degradation is dominated by surface chemistry rather than severe particle-shape changes, but they generally require tighter process control, careful post-treatment, and attention to residue management and safety considerations.

From a critical standpoint, the currently most industrially viable powder-management route for aluminum AM is not aggressive powder regeneration, but controlled reuse supported by sieving, top-up blending, drying, and oxidation-aware handling. These approaches are attractive because they can be integrated directly into existing L-PBF workflows, require comparatively limited process complexity, and match the dominant degradation pattern observed in Al–Si powders, which is usually gradual surface oxidation, fines-related flow deterioration, and moderate morphology evolution rather than catastrophic bulk chemistry loss [23,26,27,54]. For this reason, the practical strategy for aluminum powders is often not to "fully restore" every degraded particle, but to keep powder quality within an acceptable processing window through regular reconditioning and qualification.

By contrast, more intensive thermal and chemical recovery routes offer higher restoration potential but currently have narrower industrial windows for aluminum powders. Plasma spheroidization and remelting-based routes may improve particle morphology and flowability, yet their higher energy demand and added equipment complexity can limit their economic attractiveness for routine in-house reuse. Likewise, chemical oxide-removal or reduction approaches are scientifically promising for severely oxidized powders, but their wider industrial implementation for aluminum remains constrained by residue control, hydrogen-related risks, waste handling requirements, and the lack of broadly accepted post-treatment qualification criteria [27,96–98]. A major knowledge gap, therefore, lies in defining aluminum-specific decision thresholds: when simple reconditioning is sufficient, when intensive recovery becomes justified, and when the powder should be retired. Future work should also extend beyond the currently dominant AlSi10Mg datasets and establish cost-aware, alloy-specific, and application-specific qualification frameworks for reused aluminum powders [26,29,99].

3.2. Powder Sieving, Filtration, and Reconditioning

For aluminum alloy powders, the most practically relevant reconditioning routes are those that can be integrated directly into routine additive manufacturing workflows with limited process complexity. In most industrial settings, powder reuse is therefore based primarily on sieving, optional top-up blending with virgin powder, and drying or controlled de-gassing before reuse. These measures are intended to remove spatter and agglomerates, limit the accumulation of excessive fines or oxidized debris, and maintain acceptable flowability, spreadability, and powder-bed consistency over repeated build cycles [23,26,27,54,96].

Among these methods, sieving remains the most widely adopted first-line strategy because it is simple, inexpensive, and effective in removing oversized particles and fused debris that would otherwise disturb recoating and melt-pool stability [25,27,100–103]. Blending with virgin powder is likewise important when repeated reuse begins to shift particle size distribution or surface condition beyond the desired processing window [26,104,105]. Drying is particularly relevant for aluminum powders because moisture adsorption can aggravate cohesion, surface reactions, and hydrogen-related defect risks during melting [72,74,96,106,107].

More advanced approaches may provide additional control in specific situations, especially when finer debris or weak agglomerates accumulate. In this context, fluidized-bed-assisted classification can help remove highly cohesive fine particles and weak clusters while preserving the build-relevant powder fraction. As shown schematically in Figure 7, this approach relies on controlled gas flow to separate lighter particles from the denser reusable fraction [108–110]. For aluminum powders, however, such methods should be viewed mainly as auxiliary options rather than as the core of a reuse strategy. In practice, the

key issue is not the adoption of increasingly complex reconditioning routes, but maintaining powder quality within an acceptable processing window through simple, repeatable, and application-oriented control measures [23,26,27,54,96].

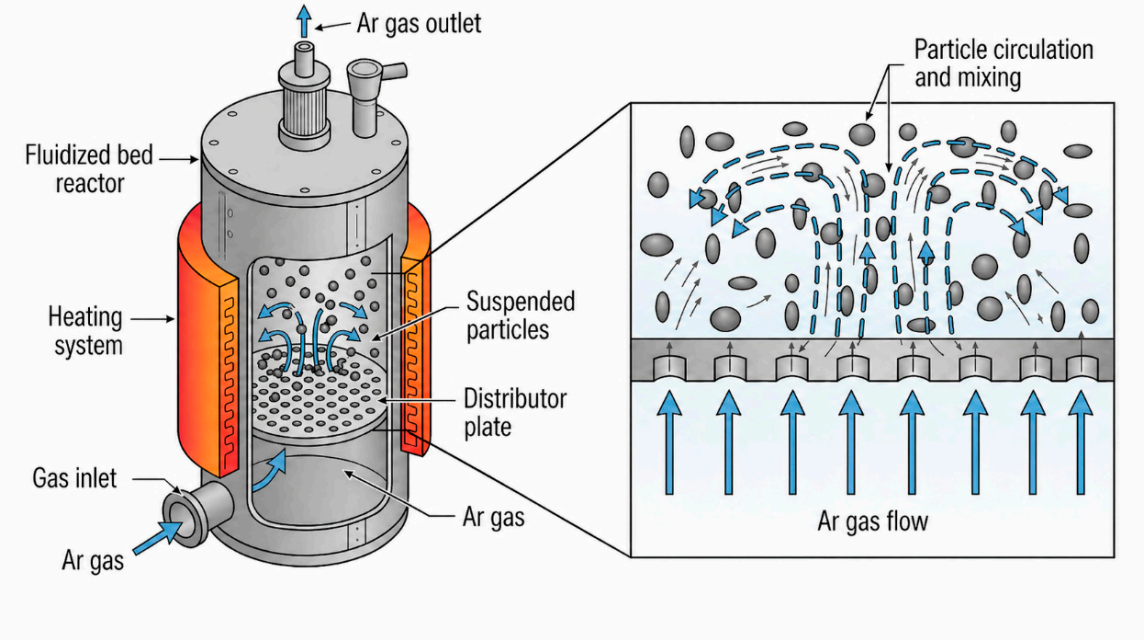

Figure 7. Schematic illustration of fluidized-bed-assisted powder classification and fine-particle removal.

3.3. Powder Handling and Storage Considerations

Effective powder recycling of aluminum alloy powders depends not only on reconditioning operations such as sieving, blending, drying, or classification, but also on proper handling and storage throughout the reuse cycle. Because aluminum powders are highly sensitive to oxygen and moisture uptake, even brief exposure during transfer, depowdering, storage, or reuse can accelerate oxidation, promote moisture adsorption, and increase particle cohesion, thereby reducing flowability and compromising the consistency of subsequent builds. For this reason, powder reuse protocols should be supported by controlled environmental conditions, including humidity management, clean handling practices, and minimization of unnecessary air exposure [72,106,107,111–113]. In practice, maintaining inert-gas protection during sensitive powder-handling steps is one of the most effective ways to preserve powder integrity between build cycles. Sealed containers, argon-purged handling systems, gloveboxes, and oxygen-controlled transfer procedures can all help reduce further oxidation and limit chemical drift during reuse. These measures are particularly relevant for aluminum powders, where progressive oxide-layer thickening can alter wetting, flow behavior, and process stability if reuse is not carefully controlled. In addition, safe handling procedures remain essential, both to reduce the risk of introducing foreign contamination and to protect operators during powder recovery, sieving, and transfer operations [97,106,114–117].

Storage time and recycling logistics also play an important role in powder quality preservation. Reused powder should be stored in sealed, moisture-limited conditions, retested when held for extended periods, and handled promptly during recycling operations to avoid unnecessary degradation. In particular, delays between depowdering and sieving may allow partially sintered particles to consolidate into harder agglomerates or permit fine particles to absorb moisture, both of which can reduce reuse quality. Accordingly, proper powder handling and storage should be regarded not as an independent

recycling route, but as enabling conditions that determine whether a nominal recycling strategy can remain effective and reliable under real AM production conditions [97,117].

3.4. Emerging Technologies and Future Perspectives

Future improvements in aluminum powder recycling are expected to rely on more integrated, alloy-specific strategies rather than isolated recovery steps. In particular, closed-loop powder handling, better monitoring of oxygen and moisture pickup, and selective reconditioning methods tailored to the degradation behavior of aluminum feedstocks may improve reuse reliability while reducing unnecessary powder discard. Because these developments are closely linked to broader qualification and sustainability challenges, their implications are discussed further in Section 6.

4. Aluminum Powder in Am

Aluminum and its alloys have emerged as essential materials in metal AM owing to their superior strength-to-weight ratio and the growing demand in aerospace and automotive applications [31]. Despite these advantages, the AM of aluminum remains challenging due to its high thermal conductivity, low laser absorptivity, and the persistence of a stable oxide layer. These inherent properties collectively constrain the range of aluminum alloys that can be processed efficiently through AM technologies [28]. To date, only a limited number of aluminum alloys have exhibited consistent compatibility with AM, whereas traditional high-strength grades, such as the 7xxx series, are susceptible to hot cracking, porosity, elemental vaporization, and other processing-related defects in the absence of tailored modifications [29]. Although recent progress has introduced promising solutions to overcome these limitations in high-performance aluminum alloys, the predominant feedstocks in AM continue to be those with excellent castability and weldability, most notably Al–Si–Mg casting alloys [30].

4.1. Aluminum Alloys Commonly Used in Am and Processes Utilizing

Aluminum Powder

Among aluminum powders used in additive manufacturing, Al–Si-based alloys remain the most relevant reference systems for powder reuse studies, particularly AlSi10Mg, AlSi7Mg, and AlSi12. Their importance stems not only from their comparatively good printability but also from the fact that they currently provide the most consistent body of literature on powder degradation, reuse behavior, reconditioning, and final part performance. By contrast, higher-strength or more specialized systems, including Scalmalloy and modified 7xxx-series alloys, are increasingly attracting research interest but remain less established from the perspective of repeated powder reuse and lifecycle management [28–38].

Figure 8 illustrates a representative application-oriented example of aluminum AM. Its relevance in the context of the present review is not primarily the specific component itself, but the fact that such lightweight structural applications are highly sensitive to defects, porosity, and process inconsistency. This makes powder condition and reuse reliability especially important when aluminum AM is considered for function-critical parts [118].

Among powder-based AM routes, L-PBF is by far the dominant process for aluminum powder reuse studies and therefore serves as the primary reference framework throughout this review. This is because L-PBF combines high industrial relevance with the largest available evidence base on powder aging, oxidation, morphology evolution, spreadability, defect formation, and the resulting implications for part quality. DED is also relevant as a secondary comparative route, particularly for larger-scale deposition and repair-oriented applications, but it remains less systematically documented in the specific context of

repeated aluminum powder reuse [29,31,32,119]. Table 2 summarizes the aluminum alloy systems and AM routes most commonly reported in the literature.



Figure 8. (**a**) Topology-optimized AlSi10Mg bracket produced by L-PBF; (**b**) conventional AlSi10Mg bracket manufactured by machining, showing geometry adapted to traditional processes. (Reproduced from [118], licensed under CC BY 4.0).

Table 2. List of the most common alloys used in 3D printing and their techniques.

Alloys	Ref	Technique
AlSi10Mg	[120,121]	L-PBF
	[122–124]	DED
	[125]	BJ
AlMg1SiCu	[126]	L-PBF
AlSi12	[127–129]	L-PBF
AlSi7Mg	[130]	L-PBF
	[131]	BJ
2024	[132,133]	L-PBF
2011	[134]	L-PBF
2219	[135]	L-PBF
3003	[136]	L-PBF
3104	[137]	DED
5005	[138]	L-PBF
5052	[138]	L-PBF
5183	[139]	L-PBF
5087	[140,141]	L-PBF
5754	[140]	L-PBF
	[142]	DED
6061	[143–145]	L-PBF
	[146]	DED

Table 2. *Cont.*

Alloys	Ref	Technique
6063	[147–149]	L-PBF
6082	[150]	L-PBF
7075	[151]	L-PBF
	[152]	DED
7050	[153]	L-PBF
	[38]	DED

From the perspective of powder degradation and recycling, the main practical implication of this alloy/process landscape is that current evidence is strongest for Al–Si-based powders processed by L-PBF. These systems, therefore, provide the most robust basis for discussing how repeated reuse affects powder condition, process stability, and final part performance. The following sections are consequently focused primarily on these aluminum systems rather than on a broad survey of all printable aluminum alloys.

A concise quantitative trend can also be identified from the aluminum-specific studies reviewed in this work. Fresh gas-atomized AlSi10Mg powders typically show native oxide thicknesses of about 2–5 nm and oxygen contents at or below about 0.05 wt.%, whereas long-term reused powders may reach oxygen levels of about 0.06–0.12 wt.% and oxide thicknesses approaching 38 nm, with bulk oxygen increasing from roughly 500 to 1250 ppm. Even so, under controlled reuse conditions, AlSi7Mg0.6 and AlSi10Mg systems often retain low porosity, high density, and largely stable tensile properties over moderate reuse intervals, while more noticeable mechanical losses are mainly reported for long-term or poorly controlled reuse conditions [54,99,154,155].

4.2. Morphological and Physical Characteristics and Powder Reusability of Aluminum Alloy Powders

4.2.1. Morphological Characteristics

The morphological characteristics of aluminum alloy powders, such as their degree of sphericity, surface smoothness, and the presence of satellites or agglomerates, play a critical role in determining not only the efficiency of powder handling and layer deposition but also the quality and mechanical performance of the final parts. High-quality aluminum powders with controlled morphology ensure enhanced process stability, reduced defect formation, and improved microstructural homogeneity. On the other hand, deviations in morphology can cause poor powder bed density, incomplete melting, or defects such as porosity and cracking in the AMed components [128].

Powder Size Distribution

Powder size is a fundamental physical parameter that represents the average equivalent diameter of a powder batch. For spherical particles, this diameter can be measured directly. However, in the case of irregularly shaped particles, an equivalent diameter is typically calculated to characterize their size [156]. Powder size varies depending on the specific AM method, primarily due to differences in the process energy and deposition mechanisms. For example, L-PBF commonly utilizes powders with particle sizes ranging from 15 to 53 μm, whereas DED processes typically employ coarser powders, with sizes ranging from 20 to 200 μm [157]. PSD is a widely used parameter to characterize powder size, providing a statistical description of particle dimensions within a given powder batch. PSD plays a crucial role in determining the density and compactness of the fabricated part, directly influencing the quality and mechanical properties of AMed components [158]. As illustrated in Figure 9, beyond the commonly observed Gaussian distribution, powder

batches can also exhibit skewed and multi-modal distributions depending on the sieving or mixing methods used during preparation [159]. In the case of a Gaussian distribution, shown in Figure 9a, the curve features a single central peak with an axis of symmetry, where the peak corresponds to the mean particle size of the batch. For skewed distributions, depicted in Figure 9b,c, the peak shifts positively or negatively relative to the mean size, indicating a predominance of either coarser or finer particles, respectively. In multi-modal distributions, such as bi-modal or tri-modal cases shown in Figure 9d,e, two or three distinct peaks are present, reflecting multiple dominant particle size ranges within the powder batch.

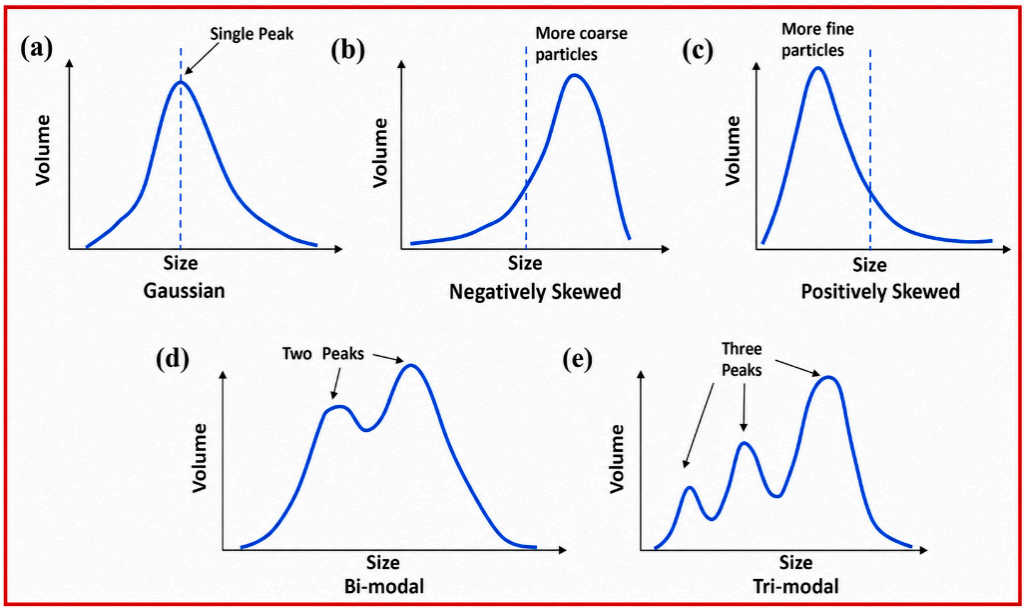

Figure 9. Examples of powder size distribution (PSD) types: (**a**) Gaussian distribution; (**b**) positively skewed distribution; (**c**) negatively skewed distribution; (**d**) bimodal distribution; and (**e**) trimodal distribution. (Reproduced from [159], licensed under CC BY-NC-ND 4.0—non-commercial use only).

The PSD of aluminum alloy powders is a critical factor influencing flowability, packing density, and layer uniformity in AM processes. For L-PBF applications, powders with a narrow PSD, typically ranging from 10 to 45 μm, are preferred to ensure stable process conditions. A study on L-PBF of 6061 aluminum alloy powders demonstrated that most particles within this size range contributed to consistent layer deposition and minimized the occurrence of defects in the final parts [160].

Surface Roughness

Given that AM is intrinsically a layer-by-layer process, the quality and integrity of each deposited layer critically affect the subsequent build and the overall performance of the component. Surface roughness is widely recognized as a key parameter for assessing single-layer formability. Owing to the high energy input and steep thermal gradients inherent in AM, surface roughness often emerges as a major challenge, adversely affecting surface quality. Excessive roughness not only weakens interlayer adhesion but also degrades the mechanical performance of the manufactured part, most notably by reducing its fatigue resistance [161].

Surface roughness represents a significant challenge in AM of aluminum alloys, especially in processes such as L-PBF and DED, due to the intrinsic physical properties of aluminum [162]. Alloys such as AlSi10Mg and Scalmalloy possess high thermal conductivity and reflectivity, which complicate laser–material interactions and promote process

instabilities, including balling and spattering [163]. Additionally, the presence of a native aluminum oxide (Al_2O_3) layer on particles impedes complete melting and fusion, often leading to partially sintered particles adhering to the component surface and increasing surface roughness [164]. Geometric factors, such as the stair-stepping effect on inclined and curved surfaces, further degrade surface finish, especially when larger layer thicknesses are employed. Consequently, as-built surface roughness values for aluminum alloys typically range from 10 to 25 µm (Ra), which is higher than those observed in titanium or steel alloys fabricated under similar conditions [165].

To address these challenges, various strategies are implemented, including the optimization of laser power, scan speed, and layer thickness, as well as advanced techniques like contour scanning and laser remelting to improve surface quality. Nevertheless, post-processing methods such as machining, abrasive blasting, chemical etching, and laser polishing are often essential to meet the surface finish requirements for functional applications [166,167]. Achieving consistent surface quality, however, necessitates a careful balance between powder characteristics, process parameter optimization, and effective post-processing techniques [118].

Porosity

Powder porosity denotes the presence of small internal voids within individual particles, which must be distinguished from the porosity observed in the AMed components. It is typically quantified either as the volume fraction or as the number of pores contained within the powder material. A range of characterization techniques has been employed to examine and quantify porosity in metal powders intended for AM [168]. For instance, in the case of AlSi10Mg powder, researchers employed a combination of optical microscopy, SEM, and transmission electron microscopy (TEM) to identify entrapped gas pores within individual particles. Their analysis revealed spherical gas inclusions with diameters ranging from sub-micrometer to several micrometers, originating primarily from the atomization process. These pores were shown to reduce the apparent density of the powder and to influence powder flowability, which in turn affected the homogeneity of powder bed layers during L-PBF. The study further emphasized the strong link between powder internal porosity and the occurrence of defects, such as lack-of-fusion or gas-induced pores, in the final AlSi10Mg components [169]. A representative example of internal porosity in aluminum powder particles is shown in Figure 10. These internal defects are inherited from powder production and should be distinguished from process-induced porosity in the final AMed component. However, trapped gas within powder particles may still contribute to residual porosity in the final part.

Porosity is one of the most critical defects in AMed aluminum alloys because it can significantly reduce tensile strength, ductility, and especially fatigue life [170]. Alloys such as AlSi10Mg and Scalmalloy are particularly vulnerable to this issue because of their high thermal conductivity, low density, and the presence of a stable Al_2O_3 film on the powder surface. These characteristics make complete melting and wetting more difficult during laser processing, which in turn promotes lack-of-fusion defects and increases internal porosity [171,172]. In addition, the high reflectivity of aluminum limits laser energy absorption, often producing a shallower and less stable melt pool than those typically observed in materials such as titanium or steel [32]. In aluminum AM, the most common pore types are keyhole pores, which are associated with excessive laser power and localized vaporization, and lack-of-fusion pores, which arise from insufficient energy input or poor bonding between adjacent layers [173]. Gas entrapment, originating from entrained gases within the powder or the processing atmosphere, also contributes to the formation of spherical gas pores. In general, the volumetric porosity of as-built aluminum parts ranges from 0.5 to

3%, depending on factors such as process parameters and powder quality [174]. Advanced process control strategies, including the optimization of laser power, scan speed, and hatch spacing, as well as preheating the build plate to mitigate thermal gradients, have proven effective in reducing porosity in aluminum AMed [175]. Moreover, post-processing techniques such as Hot Isostatic Pressing (HIP) and heat treatments are commonly employed to eliminate internal porosity and enhance the mechanical integrity of AMed aluminum components. Despite these mitigation methods, porosity continues to be a significant challenge, particularly in critical applications within aerospace and automotive industries, where high reliability and structural performance are essential [176].

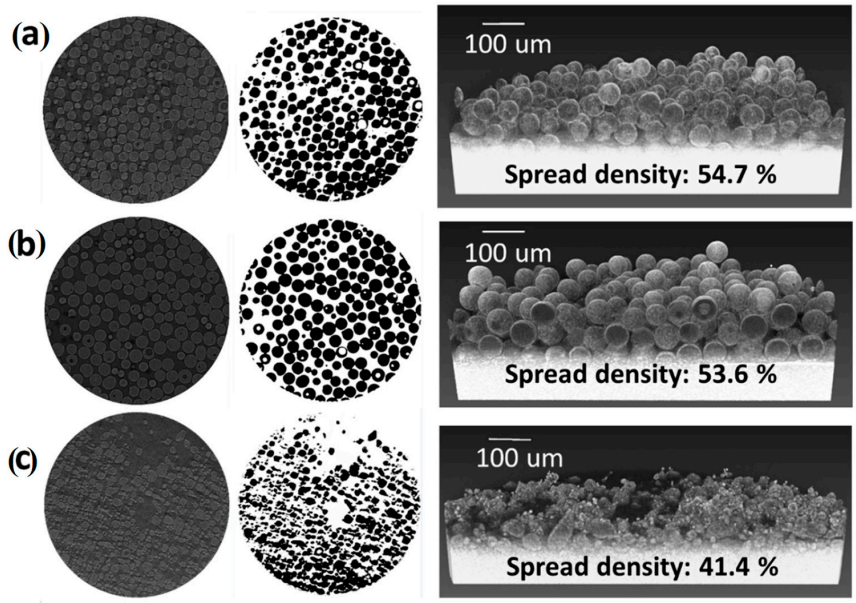

Figure 10. Representative images of aluminum alloy powder particles showing internal porosity and trapped gas: (**a**) 2D image of powder particles with internal pores; (**b**) 3D reconstructed image highlighting trapped gas and internal porosity within the particles; and (**c**) magnified view of an individual powder particle showing internal trapped gas pores. (Reproduced from [130], licensed under CC BY 4.0).

Satellite Particles

Satellite particles refer to small particles that become attached to the surfaces of larger primary particles in powders used for AM processes [177], as highlighted in Figure 11. In aluminum alloys, satellites are especially common due to the low viscosity of molten aluminum and the turbulent conditions during gas atomization [178,179]. These attached satellites negatively affect powder flowability, resulting in irregular powder layering and inconsistent recoating during PBF processes [68,180]. In addition, satellite particles may detach during powder spreading and contribute to defects such as higher surface roughness, lack-of-fusion porosity, and inclusions in the AMed part. Their irregular shape also increases interparticle friction, which lowers apparent density and reduces packing efficiency. As a result, powder layer uniformity is compromised, and the interaction with the laser can become less consistent, ultimately affecting the overall quality of the fabricated component [68,181]. From a quality-control standpoint, satellite particles are also problematic because they increase the total surface area of the powder, which can accelerate oxidation and promote the growth of thicker Al_2O_3 films. These oxide layers further limit proper melting and bonding during the AM process, making it more difficult to produce parts of consistently high quality [155]. To reduce the presence of satellites and improve powder quality, advanced powder production and conditioning methods such as plasma atomization and ultrasonic sieving are often employed [182]. Despite their relatively small size,

satellite particles in aluminum alloys present a considerable challenge to achieving high surface quality, dimensional accuracy, and mechanical reliability in AMed components [68].

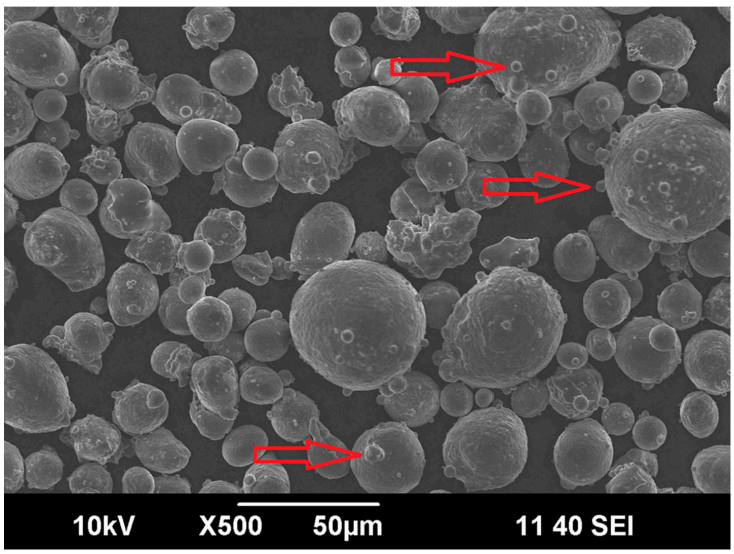

Figure 11. Topography of the as-received AA7075 showing a mostly spherical morphology with some satellite particles. (Reproduced from [183], licensed under CC BY 4.0).

Agglomeration and Clustering

In aluminum powders, agglomeration and clustering are mainly observed as soft or hard particle assemblies formed by oxide-covered fines, moisture-assisted adhesion, or partially sintered contacts between particles. The general degradation mechanism and its process-related origins were discussed earlier in Section 2.1.3. In the present aluminum-focused context, the main significance of agglomeration is morphological and practical: it reduces powder mobility, disturbs recoating uniformity, and can locally alter energy absorption during processing. These effects are particularly relevant in fine aluminum powders because surface oxidation and particle cohesion can intensify clustering during reuse and storage. Therefore, for aluminum alloy feedstocks, agglomeration is best regarded as an indicator of declining powder handling quality and reuse stability rather than as a separate degradation mechanism in itself [68,107,184–187]. The main morphological characteristics of aluminum alloy powders and their associated challenges in additive manufacturing are summarized in Table 3.

Table 3. Summary of the main morphological characteristics of aluminum alloy powders and their associated challenges in additive manufacturing.

Morphological Characteristic	Typical Manifestation in Aluminum Powders	Main Challenge in AM	Representative Consequences	Ref.
Powder size distribution (PSD)	Excessively fine particles, broad distributions, or poorly balanced size ranges	Increased cohesiveness, moisture uptake, and unstable powder spreading	Reduced flowability, non-uniform powder bed, increased porosity, and inconsistent part quality	[158,159,188]
Particle shape /sphericity	Irregular, angular, or rough-surfaced particles instead of smooth spherical ones	Greater interparticle friction and mechanical interlocking	Lower apparent density, poor packing efficiency, and less uniform recoating	[68,128,181,189]

Table 3. *Cont.*

Morphological Characteristic	Typical Manifestation in Aluminum Powders	Main Challenge in AM	Representative Consequences	Ref.
Internal porosity	Gas-filled voids trapped within individual powder particles	Reduced powder quality and potential gas contribution during melting	Lower density and possible residual porosity in the AMed part	[169,170]
Satellite particles	Small particles attached to larger primary particles	Disturbed powder flow and increased effective surface area	Irregular layer deposition, oxidation sensitivity, inclusions, lack-of-fusion defects, and poorer surface quality	[68,155,177–182]
Agglomeration /clustering	Soft or hard clusters formed by fines, oxide-covered particles, or moisture-assisted adhesion	Poor powder mobility and non-uniform energy absorption during processing	Reduced powder-bed uniformity, melt-pool instability, porosity, lack of fusion, and poor surface finish	[68,107,184–187]

4.2.2. Physical Characteristics

Apparent Density

The apparent density of aluminum powder, defined as the mass per unit volume in its loose and uncompacted state, is a critical parameter for assessing its processability in powder-based AM techniques such as L-PBF. For commonly used aluminum powders, including AlSi10Mg and Scalmalloy, apparent density values typically fall within the range of 1.0–1.5 g/cm^3, depending on factors such as the production route (e.g., gas atomization) and the resulting powder morphology [190]. Owing to aluminum high surface reactivity, particles frequently develop a thin Al_2O_3 layer, which influences interparticle interactions and may further lower the apparent density, particularly in the presence of irregular morphologies or satellite particles [128].

Spherical morphology is essential for achieving higher apparent density, as it promotes efficient packing and smooth powder flow [69]. However, aluminum powders frequently exhibit surface roughness and satellite particles due to their low melt viscosity during atomization. These satellites prevent the close packing of particles and introduce voids, which lead to a lower apparent density [181]. Fine aluminum powders, especially those below 20 µm, often show even lower apparent densities due to increased cohesiveness, which further reduces flowability and packing uniformity in the powder bed [188].

Low apparent density in aluminum powders can adversely affect layer uniformity during AM, often resulting in defects such as incomplete melting, lack-of-fusion porosity, and a consequent reduction in the mechanical performance of the fabricated part. In contrast, powders with optimized apparent density enable uniform spreading, improved laser energy absorption, and minimized porosity, all of which are essential for producing dense and mechanically robust components [191,192]. However, excessively high apparent density may also be undesirable, as it can reflect the presence of oversized particles or agglomerates, potentially reducing resolution and promoting particle segregation during the recoating process [189].

Therefore, controlling and optimizing the apparent density of aluminum powders through careful selection of atomization parameters, powder classification, and moisture-

free storage is essential to ensure process stability and mechanical reliability in aluminum-based AM applications [193].

Flowability

Flowability describes the ease with which metallic powders spread to form a smooth and uniform layer during the recoating stage of powder bed AM. This property is essential for ensuring consistent layer thickness, geometric accuracy, and reliable mechanical performance of the final component [69]. In the case of aluminum-based alloys commonly employed in AM, such as AlSi10Mg, Al7075, and Scalmalloy, flowability is of particular significance owing to the distinctive physical and chemical characteristics of aluminum [194].

Compared to denser metallic powders such as titanium or steel, aluminum powders generally exhibit inferior flowability. This limitation arises primarily from their lower density, pronounced surface oxidation, and greater susceptibility to moisture uptake. The immediate formation of a native Al_2O_3 layer upon air exposure further increases particle surface roughness and interparticle friction, thereby impeding smooth powder flow [180]. These satellite particles create a rough and irregular surface texture and increase the likelihood of mechanical interlocking between particles, which further impairs powder flowability [68]. In aluminum powders, flowability is commonly evaluated using standard methods such as the Hall flowmeter and the angle of repose. The Hall flowmeter measures the time required for a fixed mass of powder, usually 50 g, to pass through a calibrated funnel, while the angle of repose indicates how steeply the powder accumulates when poured freely. For high-quality aluminum powders, a Hall flow time below 30 s is generally considered acceptable. However, very fine powders or powders with irregular particle shapes may show such poor flow behavior that they do not pass through the Hall funnel at all, highlighting serious handling and processing limitations [195].

Poor flowability can directly affect powder layer quality, leading to non-uniform deposition, uneven energy absorption, incomplete fusion, and increased surface roughness. These effects can ultimately translate into dimensional inaccuracies and reduced mechanical performance in the final part, which is particularly critical for AMed aluminum components [180,196]. To improve flowability, manufacturers usually optimize the gas atomization process to produce more spherical particles and to minimize satellite formation. Additional treatments, such as plasma spheroidization, may further smooth particle surfaces. Powder conditioning steps, including sieving, drying, and handling under inert atmosphere, are also important for removing fines, limiting moisture uptake, and reducing agglomeration. In summary, achieving high flowability in aluminum powders is both more challenging and more critical than with many other metals, and it directly influences the print quality, process stability, and final performance of AMed components [193,197].

Optical Reflectivity

Aluminum and its alloys exhibit inherently high optical reflectivity, particularly in the infrared (IR) wavelength range employed in AM processes such as L-PBF [32]. At wavelengths of around 1.06 μm, commonly used in fiber lasers, aluminum can reflect up to 95% of the incident energy, thereby limiting energy absorption and hindering efficient melting. This pronounced reflectivity contributes to melt pool instability, excessive spattering, and incomplete interlayer fusion. The challenge is especially critical during the initial build layers, when the substrate remains relatively cool, and heat conduction is high, often resulting in weak interlayer adhesion and diminished surface quality [198].

The high reflectivity of aluminum not only reduces laser energy absorption but also contributes to process instabilities such as keyhole formation and balling. Due to poor initial coupling between the laser beam and the powder surface, the applied energy often fails to

achieve uniform melting, leading to discontinuous melt tracks and increased porosity in the AMed components [199,200]. In addition, part of the incoming laser energy is scattered at the powder surface, especially when the particles are irregular in shape or non-uniform in size, which further increases reflective losses. As shown schematically in Figure 12, fresh aluminum powder with smooth particle surfaces generally exhibits high reflectivity and relatively low effective absorption. By contrast, reused powder, with rougher surfaces and thicker oxide layers, can encourage multiple reflections within the powder bed, which may locally increase energy absorption and assist melt-pool initiation. To compensate, higher laser power is often required to achieve sufficient energy density, which can in turn exacerbate issues such as spatter and material vaporization. Therefore, careful optimization of scan speed, beam focus, and hatch spacing is essential to mitigate reflectivity-related defects and to stabilize the melt pool in aluminum AM processes [201].

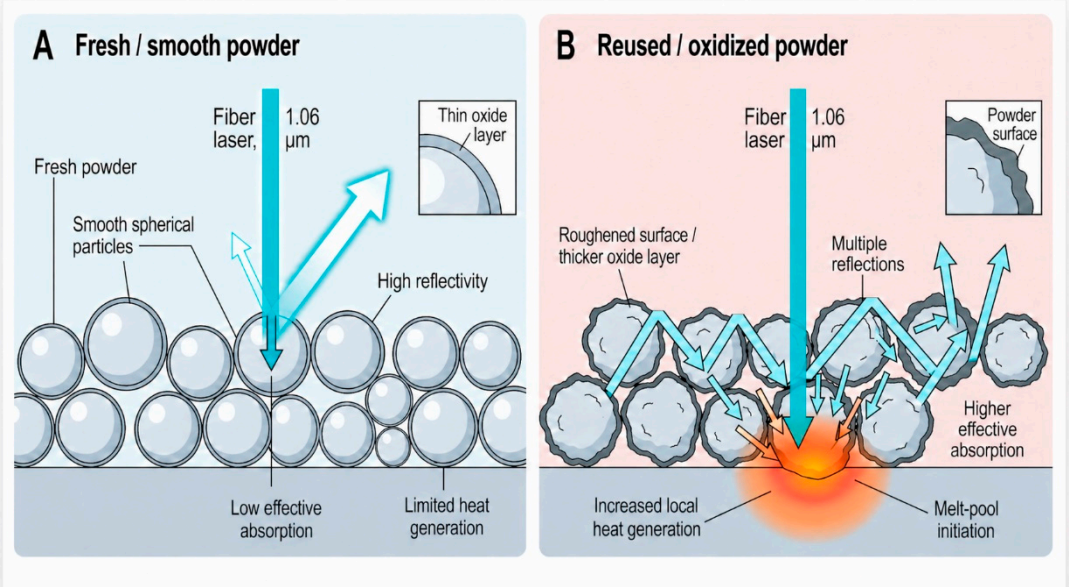

Figure 12. Schematic comparison of laser interaction with fresh and reused aluminum powders in L-PBF.

Several approaches have been proposed to reduce the negative effect of aluminum's high reflectivity in AM. One promising route is to modify the powder surface, either chemically or morphologically, to improve laser absorption. For example, applying light-absorbing coatings such as carbon black or certain metal oxides has been shown to lower reflectivity and promote more efficient energy uptake. Another effective strategy is to use lasers with shorter wavelengths. Compared with conventional infrared lasers, green and blue lasers are absorbed more readily by aluminum. Recent studies have shown that blue diode lasers (~450 nm) can achieve absorption values above 60% on aluminum surfaces, highlighting their strong potential for more stable and energy-efficient AM processing. Overall, these developments can reduce the laser power required and improve process reliability [202].

4.2.3. Powder Reusability of Aluminum Alloy Powders

Powder reusability denotes the ability to recycle and reutilize metal powders across multiple AM build cycles without inducing significant deterioration in powder characteristics or compromising the mechanical performance of the fabricated components. This concept is central to enhancing cost-effectiveness, promoting material sustainability, and supporting scalable metal AM production [25]. Nevertheless, achieving high levels of reusability in aluminum powders, such as AlSi10Mg and Scalmalloy, is considerably more

challenging than in more stable systems like stainless steel or titanium alloys. The difficulty arises from aluminum's inherently high chemical reactivity, its strong affinity for oxygen, and the rapid formation of Al_2O_3, all of which are exacerbated during repeated reuse [24,155]. Over successive recycling cycles, aluminum powders undergo both physical and chemical degradation. A notable transformation is the progressive thickening of the native oxide layer, which impairs powder meltability. In parallel, particle coarsening may occur as a result of partial melting, sintering, or redeposition of spattered material, leading to deterioration in particle morphology. The formation of satellite particles also becomes more prevalent, further disrupting powder sphericity and negatively affecting flowability and packing behavior [25,155].

As the number of build cycles increases, the likelihood of contamination also rises because partially melted particles, condensate, and spatter droplets gradually accumulate in the powder. These contaminants can interfere with uniform powder spreading, destabilize the melt pool, and eventually contribute to defects such as higher porosity and lack-of-fusion in the printed parts [81,102]. As a result, key powder properties, including flowability, apparent density, and laser absorptivity, can deteriorate in a measurable way. Reduced flowability hampers uniform layer deposition during the recoating process, while lower packing density can result in incomplete melting and inconsistencies in the density of the fabricated parts [25,81]. Due to its low melting point and high thermal conductivity, aluminum is particularly sensitive to process inconsistencies. Unlike steels, which tend to maintain their morphological and chemical stability over multiple reuse cycles, aluminum alloys often exhibit noticeable degradation after as few as 5 to 10 cycles, even under inert processing conditions, especially if the powder is exposed to air during handling, storage, or recycling [25,99].

To enhance the reusability of aluminum powders while maintaining the integrity of printed parts, strict powder management protocols must be implemented. These include regular sieving to eliminate oversized or irregular particles, blending recycled powder with virgin feedstock to dilute the effects of degradation, and handling powders under inert gas environments (such as argon or nitrogen) to minimize additional oxidation during processing and storage [26,154]. In addition, routine evaluation of powder condition before reuse should include techniques such as SEM, flow rate measurements, Hall flowmeter testing, and oxygen analysis. At present, standardized criteria for powder reusability are still evolving. Establishing such guidelines is important, since maintaining consistent powder quality is critical not only for ensuring reliable mechanical performance, but also for improving the economic and environmental sustainability of aluminum AM in large-scale industrial practice.

4.3. Chemical and Surface Properties of Fresh and Reused Aluminum Powder, Including Laser–Powder Interactions

4.3.1. Surface Chemistry

One of the most critical aspects influencing the reusability of aluminum powders is the evolution of surface chemistry, particularly the formation and thickness of oxide layers. Fresh aluminum powders are naturally coated with a thin native Al_2O_3 film, typically 2–5 nm in thickness for gas-atomized particles [155]. This passive oxide layer forms almost instantaneously upon exposure to air and provides initial stabilization of the powder surface. In virgin AlSi10Mg powder, the oxygen content associated with the native surface oxide is typically quite low, usually remaining within a few hundred parts per million by weight ($\leq$0.05%) [203]. With repeated reuse in AM, however, the oxygen level gradually rises as a result of continued surface oxidation and the accumulation of oxidized process by-products. For example, Fiegl et al. reported that the oxygen content in AlSi10Mg nearly doubled after extended reuse, increasing from about 0.06 to 0.12%, which indicates

a marked thickening of the oxide layer on the particle surfaces [154]. In a long-term 30-month investigation of AlSi10Mg reuse in L-PBF, Raza et al. likewise found a substantial increase in oxide thickness, from roughly 4 nm in virgin powder to nearly 38 nm in reused powder. Over the same period, the bulk oxygen content rose from around 500 ppm to about 1250 ppm. The authors linked this pronounced oxide growth mainly to two factors: continued oxidation of the powder during handling and repeated thermal exposure, and the gradual accumulation of oxide-rich spatter and condensate particles on the powder throughout successive build cycles. Notably, the oxide layer on aged aluminum particles may consist not only of Al_2O_3 but also of MgO or spinel phases such as $MgAl_2O_4$, as AlSi10Mg contains a minor amount of magnesium, which readily oxidizes during repeated use [155]. X-ray photoelectron spectroscopy (XPS) analysis in Raza's study confirmed that the surface of reused particles was covered with a thick, mixed Al–Mg oxide scale, whereas the virgin powder exhibited only a very thin Al_2O_3 film [155].

4.3.2. Chemical Stability vs. Contamination

Notably, apart from oxygen uptake, reused aluminum powders generally show no evidence of significant contamination or phase transformation. Multiple analytical investigations, including X-ray diffraction (XRD) and energy-dispersive X-ray spectroscopy (EDS), consistently confirm the absence of foreign elements or undesirable intermetallic phases in AlSi10Mg powders, even after repeated reuse cycles. The bulk alloy composition comprising aluminum with approximately 10% silicon and 0.4% magnesium remains essentially stable. Losses of low-boiling-point elements such as magnesium or zinc are minimal in AlSi10Mg, with any slight magnesium depletion largely restricted to surface oxide formation [29]. This behavior stands in contrast to higher-alloyed systems; for example, processing 7075 aluminum alloy often results in the evaporation of volatile elements like zinc and magnesium, which alters powder chemistry and compromises print quality [28].

Standard AlSi10Mg, however, demonstrates considerable thermal stability during L-PBF. Studies have reported no significant change in the silicon or magnesium content of reused powders, aside from the portion oxidized at the surface. As a result, the core chemical composition of the aluminum powder remains largely unchanged throughout multiple reuse cycles, with the primary chemical alteration being an increase in the surface oxygen content [29,155].

4.3.3. Surface Oxide and Moisture

As described, the oxide layer on aluminum powder thickens progressively with each reuse cycle. In addition, exposure to the atmosphere during recycling steps such as sieving or storage between builds, can introduce moisture into the powder environment. Over time, this can lead to the accumulation of hydroxide species on the powder surface, including $Al(OH)_3$ and $Mg(OH)_2$, particularly in the presence of ambient humidity [25]. As stated by Raza et al., evidence of $Mg(OH)_2$ formation on reused AlSi10Mg powder has been reported, correlating with moisture absorption. This hydroxide formation is particularly concerning, as it can lead to hydrogen release during melting, potentially contributing to porosity in the final part [155]. Hydrogen exhibits high solubility in molten aluminum and is a well-known contributor to porosity during solidification. The study further cautioned that the increased hydroxide content in aged powders could elevate hydrogen levels in the alloy melt, thereby promoting gas porosity in the AMed components [203].

These findings underscore the importance of proper storage, specifically, maintaining a dry, inert environment for minimizing moisture-induced degradation of aluminum powders between reuse cycles. Nevertheless, even with careful handling under argon, some degree of oxygen ingress is inevitable during processes such as recoating and powder

recovery. As a result, gradual oxide layer growth over time remains an expected outcome in aluminum AM operations [204].

4.3.4. Laser–Powder Interactions

During the AM process, the intense interaction between the laser and aluminum powder bed generates various by-products that can significantly alter the surface chemistry of the surrounding powder. Chief among these by-products are spatter particles and condensate fume.

Spatter Particles

Spatter refers to larger droplets of molten or partially molten metal that are ejected from the melt pool during processing. In L-PBF of aluminum, spatter particles are particularly prevalent. High-speed imaging has revealed both forward ejection from the front of the melt pool and backward ejection from the rear, driven by recoil pressure and Marangoni convection effects. These droplets typically solidify into near-spherical or irregularly shaped particles, ranging in size from tens to hundreds of microns [31]. Spatter particles often exhibit non-uniform chemical composition; for instance, they may be enriched in alloying elements with lower boiling points or may contain entrained oxides originating from the melt pool [205]. From a powder reuse perspective, spatter particles pose a critical concern, as many of them either settle back onto the powder bed or become mixed with the unused powder during collection. Because they are ejected at high temperatures into the chamber atmosphere, spatter particles typically develop thick oxide scales while in flight. In Raza's study, spatter particles in reused AlSi10Mg powder were found to have oxide layers ranging from 50 to 125 nm, significantly thicker than those on unused powder. Although spatter accounted for only approximately 3% of the total powder volume in long-term aged samples, its presence notably increased the overall oxygen content of the powder batch [155].

Condensate Fume

Condensate, also referred to as fume, is an ultrafine particulate generated from metal vapor during the AM process. In the case of aluminum, the vapor plume produced under intense laser irradiation can condense into nanoparticles composed of metal or metal oxides, which subsequently settle onto surrounding surfaces, including the powder bed. Santecchia et al. describe condensate in L-PBF as "a vapor plume due to evaporation of metals, which literally condenses inside the chamber," subsequently depositing on both the powder bed and AMed parts. Condensate particles are extremely fine, ranging from the nanometer to micron scale, and often adhere to the surfaces of powder particles, forming a coating that resembles a layer of fine dust [31]. If significant amounts of condensate redeposit onto the powder, they can substantially alter the surface chemistry and flow behavior of the powder. For example, a thin film of oxide condensate on aluminum particles can increase surface area and friability, ultimately reducing powder flowability and compromising uniform layer deposition during the AM process [81].

Condensate primarily consists of aluminum oxide and hydroxide in finely divided form, as aluminum vapor readily oxidizes upon cooling. Consequently, it contributes to the overall increase in oxygen content in reused powders. While modern AM systems are equipped with gas flow mechanisms designed to remove much of the condensate from the build chamber, some deposition on the powder bed is unavoidable. Over multiple build cycles, if not properly removed, this accumulation can progressively degrade powder quality [41,100].

Overall, the main chemical consequence of repeated reuse in aluminum powders is the gradual accumulation of surface-related degradation rather than a major bulk-alloy

transformation. In practical terms, the significance of these changes becomes most important when they begin to affect powder flowability, spreadability, melt-pool behavior, and defect formation, as discussed in the following section [29,54,154,155,206].

4.4. Flowability and Spreadability of Fresh and Reused Aluminum Powder, Including Defect Formation

Figure 13 schematically illustrates the cause-and-effect relationship between the evolution of reused aluminum powder characteristics, powder-bed behavior, melt-pool response, and final part quality. As the powder undergoes repeated reuse, changes in particle size distribution, morphology, surface oxidation, roughness, and cohesiveness may progressively reduce flowability and spreadability, leading to non-uniform layer deposition and local packing-density variations during recoating. These changes, together with altered laser absorptivity/reflectivity, can promote melt-pool instability, balling, spatter generation, and lack-of-fusion, which ultimately contribute to porosity, oxide-related defects, surface deterioration, microstructural variability, dimensional inconsistency, and reduced mechanical reliability in the fabricated components. The following subsections discuss these interrelated effects in greater detail, with particular emphasis on flowability, spreadability, and the resulting defect formation in reused aluminum powders.

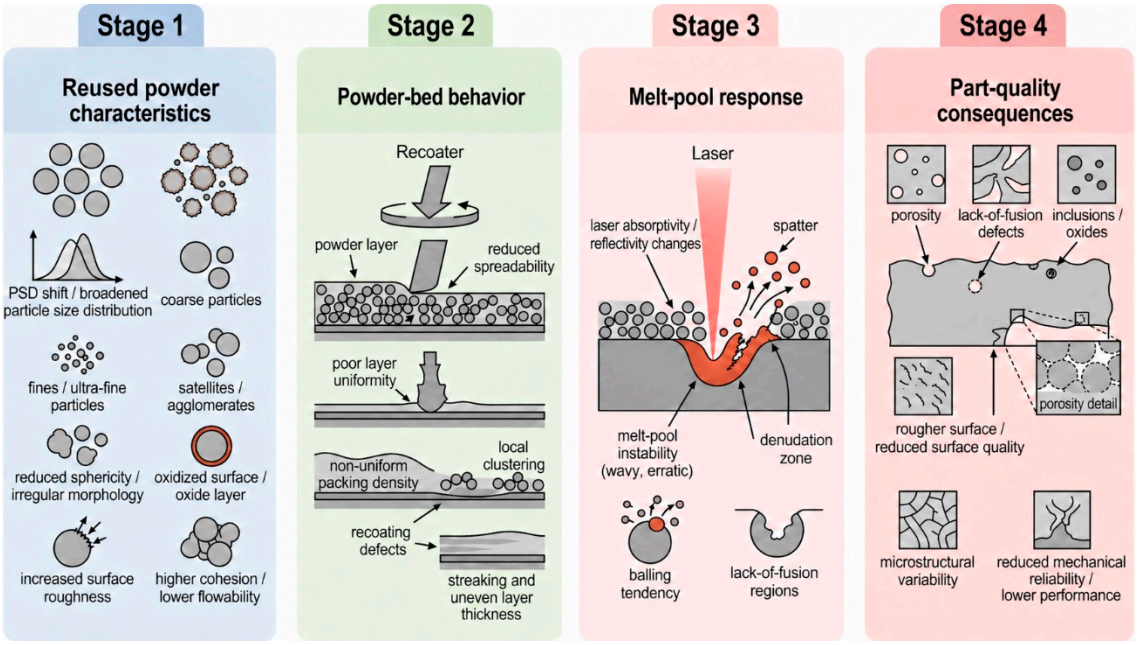

Figure 13. Schematic illustration of how reused powder characteristics influence powder-bed behavior, melt-pool response, and final part quality in metal additive manufacturing.

The practical importance of powder degradation in aluminum AM lies in the fact that its consequences are transmitted to the final part through a sequential process chain rather than through an immediate one-step effect. Changes such as PSD drift, loss of sphericity, surface roughening, oxide-layer thickening, moisture uptake, and particle clustering first modify powder flowability, spreadability, and local packing density during recoating. These powder-bed changes then affect laser–powder interaction and melt-pool stability, increasing the likelihood of lack-of-fusion defects, oxide-related inclusions, gas porosity, and local microstructural heterogeneity. As a result, the final component may exhibit reduced density, greater defect sensitivity, less stable mechanical performance, and in particular a higher risk of fatigue-relevant imperfections. For aluminum alloys, this link is especially important because degradation often remains moderate and surface-dominated at the powder level before becoming measurable in part performance; therefore, powder

qualification must be interpreted not only in terms of powder condition itself, but also in terms of its likely consequences for the final AMed part [25,54,99,154,155].

4.4.1. Flowability

Aluminum powders are generally recognized for their good flowability when fresh, owing to their spherical morphology and low density [207].

However, with reuse, changes in particle shape and surface condition can alter their flow behavior. Reused aluminum powder typically shows a slight reduction in flowability compared to the virgin powder [29]. Several factors contribute to this decline: particles tend to lose their spherical shape, increasing inter-particle friction; surface oxidation and roughness intensify, leading to higher surface friction and cohesion; and the presence of very fine particles or agglomerates can obstruct or hinder powder flow [31]. The most significant decline in flowability occurred after the first reuse, aligning with previously noted changes in particle size and aspect ratio. Beyond this point, flow characteristics stabilized, indicating that most problematic particles such as excessive fines or large spatter were likely introduced during the initial cycle and subsequently removed through sieving. Nonetheless, even slight reductions in flowability can be critical: Kiani et al. reference earlier studies showing that minor decreases in powder flow can result in disproportionately large reductions in the mechanical properties of fabricated parts [29,208].

Fine small particles, typically less than 10 μm, are often preferentially lost during recycling, either as spatter ejecta, through capture in filtration systems, or during sieving processes [54]. A reduction in the fine particle fraction can actually enhance flowability, as fine particles tend to absorb moisture, interlock, and agglomerate behaviors which lead to poor flow and increased cohesiveness [99]. By reducing or eliminating fines, the remaining powder becomes more free-flowing. For instance, Weiss et al. reported that after ten reuse cycles of AlSi10Mg, the powder flow behavior measured using the rotating drum avalanche angle improved noticeably. This improvement was correlated with the gradual loss of fine particles and a slight coarsening of the PSD [54]. Smolina et al. similarly observed that multiple reuses of AlSi7Mg0.6 powder did not lead to any deterioration in flow properties; in fact, the literature indicates that flowability can actually improve between approximately 6 to 15 reuse cycles, as the PSD becomes more favorable [99]. These findings highlight PSD as a key determinant of flowability: a narrow or refined PSD, free from excessive fines, helps to minimize the cohesive forces that hinder powder flow [54].

At the same time, other morphological changes in reused aluminum powders can negatively impact flowability. Repeated recycling and prolonged exposure to the AM environment often lead to more irregular particle shapes and rougher surface textures [209]. During laser processing, some particles partially melt or sinter into clusters; others are ejected as spatter and subsequently mix with the base powder, while some may experience superficial melting or oxidation [154]. As a result, reused powder often includes elongated or teardrop-shaped particles, along with spherical particles bearing smaller satellite particles attached to their surfaces. In AlSi10Mg powder reused 6 times, Cordova et al. reported an increase in non-spherical (deformed) particles and the appearance of fused satellite particles on their surfaces [42,210]. In a comparative study, Yusuf et al. quantified that the average particle circularity a measure of sphericity of AlSi10Mg powder, decreased by approximately 17% after reuse, while a stainless steel powder exhibited only about a 2% reduction in circularity under similar reuse conditions [210]. The reused aluminum powder particles exhibited rougher surfaces and more irregular shapes, which can increase inter-particle friction and impede flow. Irregular or jagged particles are more likely to mechanically interlock, thereby enhancing the powder cohesive strength and resistance to movement [211]. Olakanmi reported that highly irregular aluminum particles resulted in

more defect-prone parts, primarily due to poor particle packing and reduced powder-bed densities [212]. Thus, while the loss of fine particles during reuse may enhance flowability, the simultaneous increase in particle asphericity can partially counteract this benefit. In practice, however, researchers often observe that the overall flowability of recycled aluminum powder is either maintained or slightly improved compared to the virgin powder, as the positive impact of reduced fines often outweighs the negative effects of increased shape irregularity [54]. This suggests that, with proper handling such as sieving and the removal of fines and coarse debris, the flowability of aluminum powder can remain stable over multiple reuse cycles, which is a promising outcome for sustainable powder recycling.

4.4.2. Spreadability

Spreadability refers to the capability of a powder to form a uniform and defect-free layer during the recoating stage. While funnel-based flow tests may indicate good powder flow, this does not guarantee effective spreading, as segregation, streaking, or void formation can still occur within the powder bed. Critical factors influencing spreadability include particle cohesion, size distribution, and morphology. A broad PSD, for example, a bimodal mixture of coarse and fine particles, can improve packing density; however, fine particles may occupy interstitial sites between larger ones, resulting in localized density fluctuations or "wedging" effects during layer deposition [211,213]. Extremely fine or lightweight particles are also prone to displacement by the recoating blade or carrier gas flow, causing non-uniform powder coverage. Likewise, cohesive powders may adhere to the recoater or agglomerate, hindering smooth spreading [214]. Reused aluminum powders, due to changes in morphology and PSD, must therefore be carefully evaluated for spreadability. Talebi et al. emphasized that an excess of fine or irregularly shaped particles can produce uneven layer coverage and increase powder bed surface roughness [211]. Similarly, Ahmed et al. reported that patchy powder distribution impairs particle bonding during melting or sintering, ultimately degrading the quality of the manufactured part [215]. Experimental studies further confirm that powders with poor spreadability tend to generate powder layers containing thin regions or voids, which subsequently evolve into internal defects and surface irregularities in the finished component [191]. Importantly, insufficiently free-flowing powders exacerbate these issues under high recoating speeds or increased blade pressure, leading to further disruption in layer uniformity [213]. In aluminum alloys, which are inherently prone to oxide formation, surface oxides on powder particles can further reduce spreadability by increasing inter-particle adhesion and overall powder cohesion. With repeated reuse, the oxide layer on aluminum particles tends to thicken, potentially making them less able to roll or rearrange during the spreading process. However, this effect is generally secondary to mechanical factors such as particle size and shape. In practice, many researchers have reported that reused aluminum powders can still produce consistently uniform layers. For instance, Grainger et al. observed minimal degradation in powder bed quality across multiple reuse cycles of AlSi powder, provided that proper recycling procedures such as sieving and maintaining a controlled atmosphere were followed [52,216,217]. They also noted that conditioning the powder through shaking or gentle mixing before a build can help break up soft agglomerates formed during storage, thereby enhancing the first-layer spreading performance of reused powder. Overall, consistent spreadability with reused aluminum powder can be maintained through proper powder handling and maintenance, allowing the powder bed to retain a high relative density.

4.4.3. Defect Formation

A critical link between powder reuse and defect formation in aluminum alloys is the progressive increase in oxygen content during repeated build cycles. Fresh aluminum

powders are naturally coated with a thin native Al_2O_3 film; however, successive exposure to high temperatures and atmospheric conditions in L-PBF promotes additional oxygen uptake. Cordova et al., for example, observed that the oxygen concentration in AlSi10Mg nearly doubled after six reuse cycles, rising from ~0.06 to ~0.11 wt%. This increase is primarily attributed to the thickening of surface Al_2O_3 layers on powder particles, which can negatively influence melt dynamics and contribute to defect formation [54]. Although powder handling during printing typically occurs in an inert gas environment, brief but unavoidable exposures, such as during powder recovery, sieving, or transfer, and high-temperature contact with atmospheric oxygen can lead to an increased oxide content. As discussed earlier in Section 2.1.1, thickened oxide films on aluminum particles interfere with wetting, inter-particle fusion, and melt-pool stability. In the context of repeated powder reuse, these effects become increasingly relevant because the accumulated oxide content can intensify the tendency toward oxide-related defects and pore formation during processing. Because reused powder typically contains a higher oxide content, it is generally linked to an increased risk of oxide-induced porosity in printed parts. For example, Leung et al. observed that extensively reused Al–Mg powder, particularly when exposed to air, introduced fine oxide particles into the melt pool, which then acted as nucleation sites for pore formation in the fabricated samples [206]. That said, it is important to recognize that even virgin aluminum powder carries a native oxide layer on each particle, and the L-PBF process inherently incorporates some oxides into the solidified material. The main issue is the degree of oxidation, since excessive oxide buildup during prolonged powder reuse can eventually drive the material beyond acceptable limits. In practice, however, many studies performed under controlled argon atmospheres and proper storage conditions have not reported a noticeable increase in oxidation-related defects until the powder has undergone a relatively high number of reuse cycles. For example, Smolina et al. found no statistically significant change in porosity after up to five reuse cycles of AlSi7Mg0.6 powder, with the overall volumetric porosity remaining very low, at about 0.1% or less in all cases. Interestingly, they found that samples from the fifth reuse cycle exhibited the lowest average porosity (~0.03%), compared to ~0.06–0.09% in earlier cycles. This reduction was attributed either to random variability or to improved powder packing, which may have helped mitigate pore formation [99]. In Weiss's 10-cycle study on AlSi10Mg, the authors likewise observed no decrease in bulk part density with continued powder reuse the relative density consistently remained around 99.8–99.9% across all cycles, indicating no significant increase in lack-of-fusion voids [54]. These findings suggest that, under well-controlled reuse conditions, defect formation can be effectively minimized over a substantial number of reuse cycles. In such cases, the positive factors such as consistent powder layering, removal of out-of-spec particles, and strict atmospheric control appear to outweigh the negative impact of gradual oxidation. Nonetheless, other studies have reported a slight increase in defect content associated with reused powder [154].

The evidence discussed above shows that the effect of powder reuse on final part quality is mainly indirect and process-mediated. The following sections, therefore, examine whether these powder-level changes produce measurable consequences at the microstructural and mechanical levels.

4.5. Microstructural Changes in Am Parts Produced with Reused Aluminum Powder

Given the flow-, chemistry-, and defect-related mechanisms discussed in Sections 4.2–4.4, the key question is whether these powder-level changes translate into measurable microstructural differences in the final aluminum AMed parts. AM of aluminum alloys, such as Al-Si-Mg compositions, generally leads to a rapidly solidified microstructure characterized by fine cellular-dendritic grains and dispersed silicon-rich phases. In L-PBF, the

as-built microstructure of alloys like AlSi10Mg typically comprises an α-Al matrix with an interconnected network of interdendritic silicon-rich eutectic phases situated along the cell boundaries [123,218]. This occurs due to the high cooling rates, which trap supersaturated silicon within the aluminum matrix. Upon solidification, this silicon precipitates as fine filamentary structures along the grain boundaries. The grains in as-printed AlSi alloys typically exhibit a columnar morphology elongated along the build direction, a result of epitaxial growth. The dendrite arm spacing in these alloys generally measures just a few micrometers [219,220]. This intrinsic microstructure largely determines the alloy mechanical properties; for instance, the high strength arises from the presence of fine dendrites and silicon particles. Consequently, any modifications to the powder characteristics or processing conditions that influence solidification behavior could impact these microstructural features. A critical question, therefore, is whether the use of reused powder leads to any significant changes in the microstructure of the fabricated parts [154].

Current evidence indicates that powder reuse has little, if any, effect on the main microstructural features of aluminum parts produced by L-PBF, as long as the processing parameters are kept unchanged [54]. Smolina et al. carried out a detailed microstructural study on AlSi7Mg0.6 samples manufactured using both virgin powder and powder reused for up to five cycles. Based on optical microscopy and SEM observations, they found that the microstructure remained typical of AMed aluminum alloys, consisting of a fine semi-cellular dendritic α-Al matrix with intermetallic networks. The morphology was identical between parts built with virgin powder and those produced using reused powder. No new phases or grain structures emerged with powder reuse, and both grain size and dendrite arm spacing (DAS) exhibited no systematic variation related to the powder age. Quantitative DAS measurements across samples S0 (virgin) to S1, S2, S3, and S4 (reused 1 to 4 times) were all within the experimental margin of error. Figure 14 presents the average secondary DAS for each sample, showing that any minor differences were random and within the approximate ±1 μm standard deviation. The study concluded that powder reuse had no measurable effect on microstructural characteristics such as grain texture or cell spacing [99].

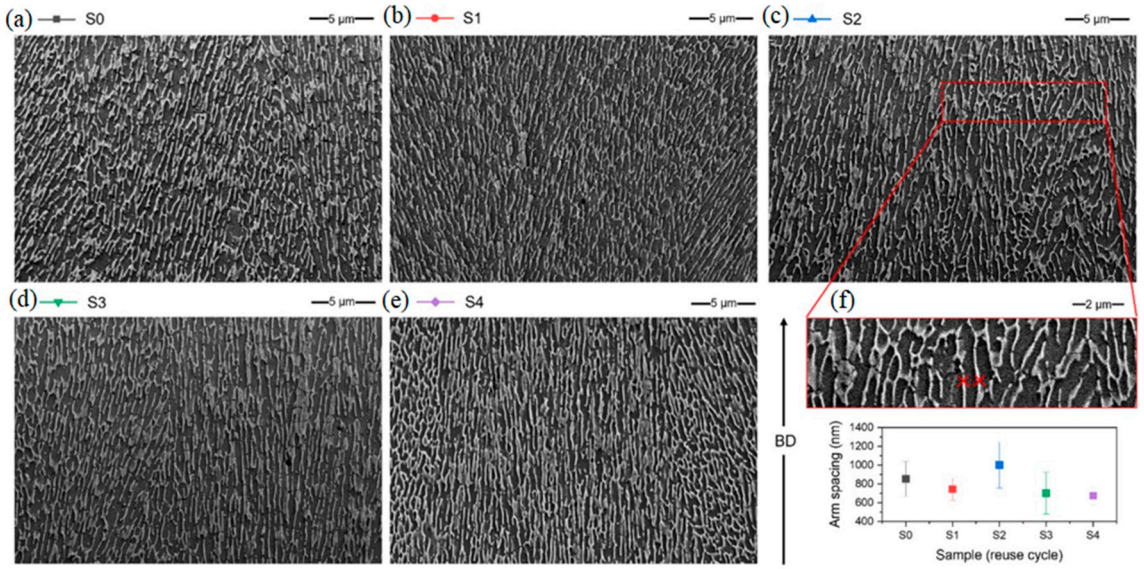

Figure 14. Microstructure of AlSi7Mg0.6 samples, SEM/BSE: (**a**) S0; (**b**) S1; (**c**) S2; (**d**) S3; (**e**) S4; and (**f**) an example of DAS measurement and the average DAS obtained from six random measurements for each sample from series S0 to S4. (Reproduced from [99], licensed under CC BY 4.0).

One potential microstructural concern associated with reused powder is the introduction of oxide inclusions or other impurities into the material matrix. As previously noted, reused aluminum powder generally exhibits a higher oxygen content due to the buildup of surface oxides over repeated use. If these oxides become entrained in the melt pool during processing, they may solidify as non-metallic inclusions such as Al_2O_3 particles or oxide films within the final microstructure [221]. Although such inclusions may not significantly alter the overall microstructure, particularly if they are sub-micron in size and sparsely distributed, they can still function as defects or stress concentrators [222].

However, most studies have reported that the oxide content, even after multiple reuse cycles, remains low and does not result in the formation of any new observable phases. For example, Mohd Yusuf et al. conducted XRD analyses comparing virgin and recycled AlSi10Mg powders. Their results showed no phase changes between the two powders (see Figure 15); the recycled powder exhibited only the expected face-centered cubic (FCC) aluminum phase and silicon peaks. No additional crystalline oxide peaks were detected, suggesting that any oxides present were either amorphous or present in quantities below the detection limit of the technique [210].

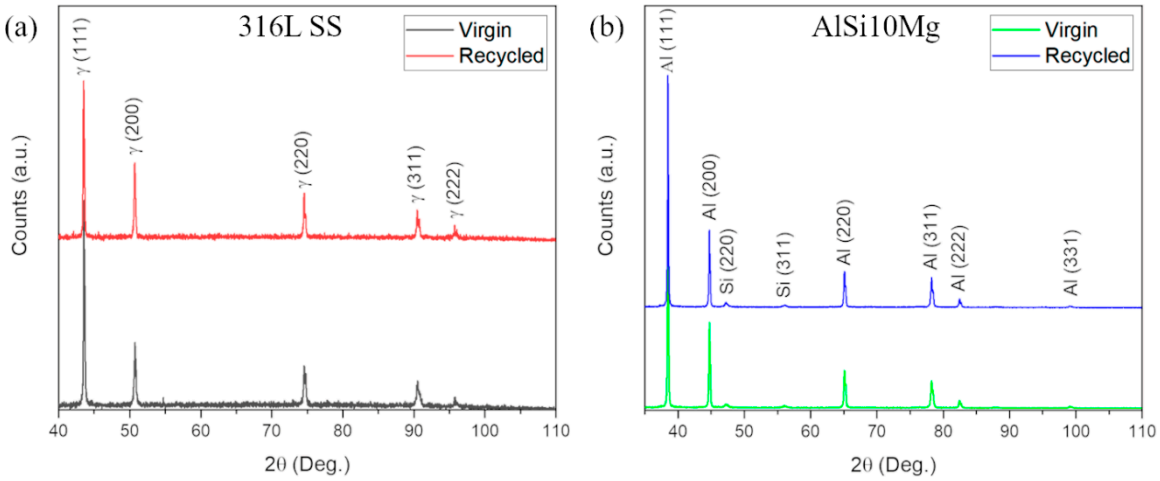

Figure 15. XRD spectra of virgin and recycled 316L SS (**a**) and AlSi10Mg (**b**) powders. (Reproduced from [210], licensed under CC BY 4.0).

Microstructural fidelity when using reused powder also applies to defect structures, such as porosity and cracking. One of the primary indicators of microstructural quality in AMed parts is porosity, both in terms of total volume and pore morphology. As previously mentioned, well-processed aluminum parts can reach densities exceeding 99.5%. While powder reuse could theoretically affect porosity by altering powder packing characteristics or introducing a higher number of inclusions (which may act as nucleation sites for pores), studies thus far have shown that such effects are minimal under controlled processing conditions [25]. In Barile's study, the use of reused powder did not lead to any increase in porosity or defect content within the microstructure. Neutral salt spray corrosion testing, together with microscopic examination, showed that surface roughness, density, and porosity were essentially the same in parts produced from virgin and recycled powder. In both cases, the porosity was around 0.2%, and the pore size distribution was also very similar. Most of the pores were small and spherical, consistent with gas porosity, while a few larger and more irregular voids were also observed, likely originating from process-related instabilities. These features appeared in both virgin and recycled powder specimens, with no evident increase in defect occurrence in the reused-powder builds [223]. These results are consistent with other studies, such as those by Kiani et al., who reported no significant changes in part density (approximately 99%) or pore morphology across five

reuse cycles of AlSi10Mg powder in DED. Although a slight increase in oxygen content was observed, it did not lead to the formation of widespread oxide inclusions or additional porosity detectable through density measurements or optical microscopy. In summary, as long as the process parameters remain constant and optimized, powder reuse does not significantly affect part density or defect levels, and the AMed components remain nearly fully dense [29].

Another important microstructural factor to consider is the elemental segregation or composition drift within the fabricated parts. If powder reuse led to the depletion or concentration of alloying elements, it could alter the resulting microstructure, for example, a loss of magnesium could reduce the material's age-hardening capability. This is particularly relevant for aluminum alloys such as AlSi10Mg, where magnesium plays a key role in precipitation hardening. However, studies have consistently shown that the overall composition remains stable throughout multiple reuse cycles, with no significant loss or accumulation of key alloying elements [29,224]. Smolina et al. specifically examined the Mg and Si contents in both the powder and the fabricated samples after multiple reuse cycles using X-ray fluorescence (XRF) analysis. They found that any variations in composition were within the margin of instrumental error. While they acknowledged that evaporation of volatile elements such as magnesium or zinc can be a concern in L-PBF processes, their results showed that magnesium loss was minimal. This negligible reduction in Mg content did not produce any measurable changes in the microstructure or degrade the mechanical properties of the material [99]. Similarly, no enrichment of impurity elements was detected, indicating that there was no unexpected segregation of contaminants such as iron or other trace elements. The only notable chemical change observed was a slight increase in oxygen content in the reused powder, which, as previously discussed, was minimal and also reflected as a modest rise in oxygen levels in the built parts still within the range of a few hundred parts per million (ppm). XRD analysis conducted by Yusuf et al. further confirmed that no undesired precipitates, such as Mg_2Si or other intermetallic compounds beyond those typically present in AlSi10Mg alloys, were formed in the recycled powder or in the AMed components. The recycled AlSi10Mg parts retained a supersaturated α-Al matrix with finely dispersed silicon, identical to that observed in parts produced from virgin powder. In essence, the alloy microchemistry remained stable despite powder reuse, which accounts for the observed consistency in microstructural characteristics [210].

Lastly, post-processing can effectively eliminate minor microstructural differences introduced by powder reuse. When parts undergo solution heat treatment followed by aging, a common practice for AlSi10Mg to enhance ductility, the as-built microstructure is homogenized, diminishing any residual effects of powder history. For instance, in both virgin and reused powder samples, subjected to aging will cause Mg_2Si precipitates and silicon particles to coarsen, ultimately resulting in metallurgically comparable microstructures. Therefore, from a microstructural perspective, any subtle variations caused by powder reuse can be mitigated through standard thermal post-treatment processes, if necessary [225].

In summary, the microstructure of aluminum AMed parts remains largely stable when reused powder is employed, at least within the typical reuse limits tested in research (commonly 5–10 cycles, and in some cases even more). The characteristic fine cellular-dendritic morphology and uniform dispersion of silicon particles in Al-Si alloys are preserved. No new phases, such as excessive oxides or unexpected intermetallics, have been observed to form as a result of powder reuse. Porosity levels remain low, with no significant increase, provided the powder continues to spread and melt effectively during processing.

These findings are encouraging because they indicate that moderate powder reuse does not significantly affect the bulk microstructural integrity of AMed aluminum compo-

nents. At the same time, it should be kept in mind that most published studies have been carried out under carefully controlled conditions, including inert-atmosphere handling, regular sieving, and limited exposure to ambient humidity. In more variable industrial environments, especially when powder is reused many times or handled without strict control, gradual microstructural degradation may still develop. Possible effects include a higher level of oxide inclusions or changes in precipitation behavior caused by the loss of important alloying elements such as magnesium.

Therefore, while current evidence supports the microstructural reliability of reused powder within practical limits, it is advisable to conduct periodic quality assessments when extending powder life. Overall, the research to date indicates that any changes in material properties due to powder reuse are more likely attributable to subtle variations in defect content or chemistry rather than significant microstructural transformations.

4.6. Mechanical Properties of Amed Parts Made from Aluminum Powder (Fresh vs. Reused)

The mechanical performance of AM aluminum components, including tensile strength, yield strength (YS), ductility, hardness, and fatigue resistance, is primarily dictated by the underlying microstructure and defect distribution. Given that powder reuse has been shown to exert minimal influence on the microstructure of aluminum alloys under controlled processing conditions, the corresponding mechanical properties also remain largely unaffected. Observed variations are generally minor and are typically linked to slight changes in porosity or the presence of inclusions rather than to substantial structural transformations. Over the past decade, numerous systematic studies have compared the mechanical behavior of parts fabricated from virgin and reused aluminum powders to assess the viability of powder recycling in AM. The prevailing consensus indicates that mechanical properties are reliably preserved over multiple reuse cycles. Even after extended recycling, variations in strength, ductility, and hardness remain small and within acceptable engineering limits. These findings underscore the feasibility of powder reuse from a mechanical standpoint, highlighting its potential to support cost-efficient and sustainable AM production [54,226–228]. When differences have been observed, they are typically minor, usually within a few percent, and often fall within the normal variability seen in AM test results. The following summarizes key findings from notable studies.

As summarized in Table 4, the literature does not support a single universal mechanical response to powder reuse in aluminum AM. Instead, the reported trend depends strongly on the severity of powder aging and on whether reuse is performed under controlled conditions. Most studies on AlSi10Mg and AlSi7Mg-based systems report little or no significant deterioration in static tensile properties and hardness over moderate reuse intervals, whereas noticeable mechanical losses tend to appear only in long-term or strongly degraded powder conditions. This comparison also shows that fatigue remains the least systematically documented property, highlighting an important gap between current powder qualification practice and the requirements of safety-critical applications.

Critical Interpretation

The literature indicates that the mechanical response of aluminum AM parts to powder reuse is governed mainly by the degree of powder aging and by the level of process control. Under controlled reuse conditions, especially in AlSi10Mg- and AlSi7Mg-based L-PBF systems, tensile strength, hardness, and general part integrity remain largely stable over moderate reuse intervals. In some cases, slight improvements in strength have even been reported, usually in connection with improved powder packing and reduced lack-of-fusion susceptibility [54,99,228].

Table 4. Representative literature summary of changes in the mechanical properties of AMed aluminum parts produced from reused powder.

Study	Alloy/AM Route	Reuse Condition	Tensile Response (YS/UTS/Elongation)	Hardness Response	Fatigue Response	Overall Trend/Interpretation
[99]	AlSi7Mg0.6/L-PBF	Powder reused up to 4 times (S0–S4)	UTS remained about 390–400 MPa; YS remained about 230–240 MPa; elongation stayed around 8–9%, with no statistically meaningful degradation.	HV0.3 remained about 120–125, with no systematic variation.	Not specifically reported.	Mechanical properties remained stable and repeatable over the studied reuse range.
[54]	AlSi10Mg/L-PBF	Up to 10 reuse cycles, without virgin top-up	YS and UTS showed a modest increase; elongation remained generally stable or showed only a slight decrease with scatter.	Microhardness remained within about 170–195 HV0.01, with no deterioration trend.	No direct fatigue dataset was reported; the authors highlighted fatigue as a future research need.	Controlled reuse did not degrade static properties and may slightly improve strength because of improved powder packing and densification.
[228]	AlSi10Mg/L-PBF	Multiple reuse cycles with fresh-powder addition; up to 8 cycles reported in the discussion	Static tensile properties remained nearly constant; only a small reduction was observed, with no consistent deterioration trend.	Not specifically emphasized.	Slight reduction in fatigue endurance limit after repeated reuse.	Under controlled top-up conditions, the mechanical effect of powder reuse remained limited.
[29]	AlSi10Mg/DED	Multiple reuse cycles in the DED context	Mechanical properties remained broadly comparable across reuse conditions.	Slight hardness increase after the first reuse, followed by essentially stable values.	Not specifically reported.	Reuse appeared mechanically feasible when powder handling and process conditions were controlled.
[154]	AlSi10Mg0.4/PBF-LB/M	Long-term reused/aged powder	UTS, YS, and elongation declined; the reduction in mechanical performance was reported to reach about 10–15% in the more degraded condition.	Microhardness also decreased.	Not specifically reported.	Excessive long-term degradation can eventually lead to measurable mechanical-property loss, especially when porosity and oxide-related degradation become severe.

In contrast, more noticeable property losses are mainly associated with long-term or poorly controlled reuse, where oxidation, morphology deterioration, or porosity-related effects become sufficiently severe to influence final part quality [154]. Available evidence therefore suggests that the main practical limitation of powder reuse is not an immediate collapse of mechanical performance, but the gradual emergence of conditions under which powder degradation begins to propagate into defect-sensitive properties. This point is especially relevant for fatigue, which remains less systematically documented than static tensile behavior and hardness [54,228].

5. Quality Assessment Methods for Reused Aluminum Powder

Ensuring the quality of reused aluminum powders is vital for the fabrication of reliable, defect-free components in AM. With successive build cycles, powder characteristics inevitably evolve due to processes such as oxidation, particle agglomeration, and repeated sieving. As a result, implementing rigorous powder quality evaluation protocols is essential to determine whether a feedstock remains suitable for reuse or requires rejuvenation or disposal [42,224]. In the absence of established international standards specifically dedicated to powder reuse, an area that remains under active development, both industry and academia rely on a combination of conventional powder characterization techniques and AM-specific

testing to assess powder condition. Key properties that require continuous monitoring include PSD, morphology, flowability, bulk and tapped density, and, critically, chemical composition with an emphasis on oxygen content [229]. Figure 16 schematically summarizes this multi-parameter characterization and qualification framework, highlighting the main property domains that should be evaluated before further powder reuse. Below is an overview of the commonly used methods for evaluating each of these characteristics in the context of reused Al powder.

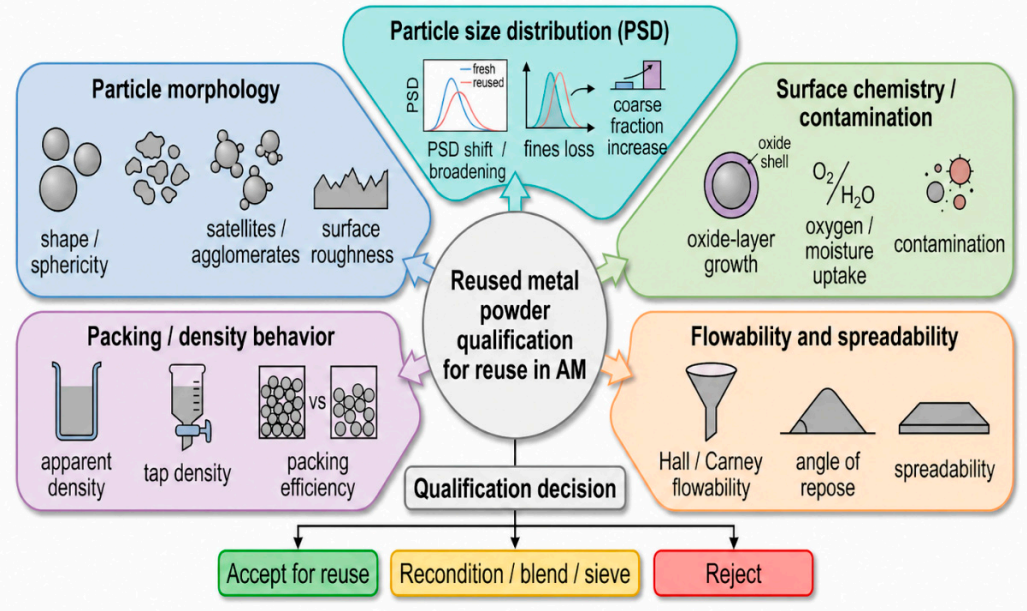

Figure 16. Multi-parameter characterization and qualification framework for reused metal powders in AM.

5.1. PSD Analysis

Since changes in PSD, typically a shift toward coarser particles and a reduction in fine particles, are among the most noticeable effects of reuse, it is essential to measure the PSD of the powder after each build or following a defined number of reuse cycles [25]. Widely used techniques for evaluating PSD include laser diffraction and sieve analysis. Laser diffraction, conducted according to ASTM B822 [230], offers a fast and reliable means of determining D_{10}, D_{50}, and D_{90} values, corresponding to the particle sizes below which 10%, 50%, and 90% of the particles are found, together with the full particle size distribution curve. In the reused powder, it is common to observe an increase in the D_{50} value and a reduction in the fine particle tail of the distribution curve [231]. Sieve analysis, such as using ASTM E11 [232] mesh sieves, serves as a complementary method by quantifying the proportion of powder below or above specific size thresholds (e.g., below 20 µm or above 63 µm). Many users routinely incorporate a sieving step, typically using a 63 µm or 75 µm mesh after each build to remove spatter particles and large agglomerates, helping to maintain powder consistency across reuse cycles [105,233]. The oversize material retained on the sieve can be weighed to assess the powder quality. An unusually high proportion of oversize particles may indicate abnormal events during the build process, such as excessive particle fusion, spatter formation, or contamination [234]. By monitoring PSD across reuse cycles, it becomes possible to establish thresholds for continued powder usability. For example, if D_{90} exceeds a specific limit or the fine fraction (percentage of particles < 10 µm) drops below a defined threshold, the powder may be approaching the end of its useful life for forming uniform layers. Since PSD has a direct impact on powder packing and flow behavior, it is crucial to keep it within the range for which the machine and process parameters were

originally optimized. Some companies implement a rapid screening process involving both a sieve cut and laser diffraction analysis on returned powder before approving it for reuse in the next build. This approach helps to ensure that the powder still meets critical size distribution criteria and is suitable for consistent layer deposition [62,235].

5.2. Particle Morphology and Surface Characterization

The shape and surface texture of particles are typically evaluated using SEM or optical imaging techniques. With repeated reuse, the powder can develop distinct features such as irregular particle shapes, the presence of satellites, and increased surface roughness due to oxide layer formation [236]. Image analysis software can be used to quantify particle shape descriptors such as circularity, aspect ratio, and roundness based on SEM micrographs or data obtained from dynamic image analyzers. These metrics provide objective assessments of morphological changes in reused powder that may affect flowability and packing behavior [237].

Many industrial laboratories use digital microscopes or particle image analysis systems to automatically capture and evaluate thousands of particle outlines. These tools generate detailed statistical information on shape-related parameters such as circularity, convexity, and aspect ratio. To ensure good flow behavior, the powder should remain largely spherical, with most particles showing a circularity above 0.9 [211].

If the morphological analysis shows an increasing amount of spatter, often identified by its rough, irregular, or shrapnel-like appearance, or reveals more fractured particles, this may indicate the need for additional sieving or blending with virgin powder to limit its effect. Surface chemistry is also an important factor. Techniques such as EDS or XPS can be used to detect oxide layers or trace contaminants on particle surfaces. For aluminum powders, a thin alumina layer is normal; however, an unusually thick oxide film or the presence of nitrides may be a sign of powder degradation. In practical settings, a quick EDS scan using SEM can be employed to compare the oxygen-to-aluminum (O: Al) ratio on the surfaces of fresh versus reused powder, providing a semi-quantitative measure of increased oxide content [238,239]. In a manufacturing environment, it is common practice to microscopically inspect a small powder sample from the hopper after each build. If the sample primarily contains smooth, spherical particles with only minor satellite attachments, the powder is typically approved for reuse. However, if the inspection reveals a high number of irregularly shaped particles or the presence of foreign debris, corrective measures such as additional sieving, blending, or disposal may be required to maintain build quality.

5.3. Flowability Tests

Powder flow behavior can be evaluated using both standardized and advanced techniques. A commonly used traditional method is the Hall flow rate, defined by ASTM B213 [240]. This test provides a quick indication of the powder flowability, with faster flow rates generally indicating better performance in spreading and recoating processes [195]. Many gas-atomized AlSi10Mg powders do not easily flow through the Hall funnel because of their fine particle size and slight cohesiveness. In such cases, the powder may be reported as having “no flow” if it takes longer than 15 min to pass through the funnel or if it forms arches that block flow. However, when the powder is coarser or contains flow-enhancing additives, the Hall flow time becomes a useful diagnostic. An increase in flow time over successive reuse cycles may indicate rising cohesiveness, potentially due to oxide buildup or moisture absorption. Conversely, a decrease in flow time could suggest improved flowability, often resulting from the loss of fine particles [72,216].

Modern powder rheometers, such as the Freeman FT4, offer a more detailed and comprehensive assessment of powder flow behavior by providing advanced flowability indices, including basic flow energy, specific energy, and conditioned bulk density. Additionally, rotating drum methods that measure avalanche angle and avalanche stability are particularly sensitive to inter-particle cohesion. A lower avalanche angle generally indicates better flowability, as it reflects reduced internal resistance and smoother movement of the powder mass. These techniques are valuable for detecting subtle changes in flow properties that may arise from repeated powder reuse. The Hausner ratio, calculated as the ratio of tapped density to loose (bulk) density, is a quick and practical indicator of powder flowability [241,242]. A Hausner ratio between 1.00 and 1.15 typically reflects very good flow behavior with low cohesion, while values exceeding 1.25 suggest poor flow and high cohesiveness. Monitoring the Hausner ratio of reused powder can provide useful insight into changes in cohesiveness, which may arise from oxidation, moisture absorption, or similar degradation effects. Paccou et al. proposed a five-step powder qualification procedure in which flowability and tapped density are treated as key indicators. According to their approach, reused powder should retain tap density and flow index values close to those of virgin powder in order to remain suitable for continued use and to ensure stable performance during AM processing [229].

If reused aluminum powder starts to show a noticeably higher Hausner ratio, this usually means that the powder compacts more readily under tapping, which is a sign of increased cohesiveness. In most cases, this may point to a larger fraction of fine or irregularly shaped particles that interfere with loose packing and may indicate developing problems in flowability and spreadability. In practice, many AM facilities monitor flow behavior using a layered or multi-step assessment approach. A quick Hall flow test (when the powder type allows) and a bulk density check are often performed routinely after each build. These are supplemented by more advanced flow tests, such as rheometry or avalanche angle measurements, when anomalies are detected or when deeper insight is needed to ensure the powder performance remains within acceptable limits [42,52].

5.4. Chemical Composition and Purity

Across successive reuse cycles, the chemical composition of powders may evolve through two primary pathways: the accumulation of interstitial elements such as oxygen, nitrogen, and hydrogen, and contamination from external sources, including foreign metallic particles, lubricants, or processing residues. In the case of aluminum powders, oxygen uptake represents the most critical issue, as previously highlighted. To monitor this, oxygen and, in some cases, nitrogen can be quantitatively assessed using inert gas fusion analysis, most commonly performed with LECO analyzers. Although ASTM E1409 [243] was originally developed for oxygen determination in titanium, its methodology can be effectively adapted for aluminum powders. This approach offers a highly sensitive and reliable means of detecting increases in interstitial elements that may impair powder processability and compromise the quality of AMed components [244,245].

Nitrogen uptake in aluminum powder is generally minimal, unless the powder has been exposed to a nitrogen-rich atmosphere or air during handling or processing. In such cases, measuring nitrogen content becomes relevant, as elevated levels may lead to the formation of aluminum nitride (AlN), which can affect material properties [246].

Hydrogen content in the powder is not usually measured directly. Nevertheless, hydrogen-related defects, particularly porosity in printed parts, are often associated with moisture absorbed by the powder. During melting, especially in laser-based AM processes, this moisture can promote hydrogen entrapment in the melt. To reduce this risk, some quality control procedures include drying or baking the powder to remove absorbed

moisture before reuse. Additional checks may then be performed to confirm that the powder does not release excessive hydrogen during processing. These checks can include trial builds or analytical techniques such as differential scanning calorimetry combined with mass spectrometry, which help detect hydrogen outgassing under simulated thermal conditions [74,247].

Another important factor in preserving the quality of aluminum powder is avoiding contamination by foreign metals. This type of contamination may occur when the same AM machine is used for different powders without proper cleaning between builds, or as a result of wear in machine components, which can introduce particles such as steel debris. To identify this issue, techniques such as XRF or SEM coupled with EDS are commonly employed, as they can detect unexpected elemental signals, including iron, copper, or other metallic contaminants in the powder sample [43,248]. For particularly sensitive or high-specification applications, some users also perform a ferrous contamination test by passing a strong magnet through the aluminum powder. While aluminum itself is non-magnetic, any ferrous contaminants, such as steel spatter from build plates or tooling wear, can be captured by the magnet. This provides a quick, practical way to detect potential steel-based contamination in reused powder [249].

5.5. Powder Bed Quality Tests

Beyond characterizing powders in isolation, certain quality assessment methods emphasize evaluating powder behavior directly within the machine environment. A prominent example is spreadability testing, in which a powder sample is deposited under controlled conditions designed to replicate the recoating process in AM. The resulting layer is then examined for uniformity, either through optical imaging to evaluate visual consistency or via surface profilometry to quantify roughness and thickness variations. Poor spreadability, manifested as uneven or patchy layers, may indicate elevated particle cohesion, irregular morphology, or contamination factors not always captured by conventional powder characterization techniques. As such, spreadability testing provides an important link between intrinsic powder properties and in-process performance during AM builds [213,215,250].

A practical method for assessing powder performance is the execution of test spreads on a flat substrate, designed to replicate the recoating stage of AM. In this method, the powder is spread using a recoater blade or a similar device, and the deposited layer is then examined with a high-resolution camera or laser scanner to detect streaks, gaps, or non-uniform coverage. This provides a direct and measurable way to assess spreadability. If reused powder continues to form a smooth and uniform layer similar to that produced by virgin powder, it can be considered suitable for further reuse. On the other hand, visible irregularities may indicate problems such as poor flowability, increased cohesion, or contamination, and should prompt further assessment or corrective action [251].

Some researchers employ calibration prints or witness specimens as part of their powder reuse assessment strategy. This involves printing standardized test geometries, such as small coupons or density cubes, using reused powder under fixed machine parameters. These specimens are then analyzed for part density and surface quality, providing a direct, application-based evaluation of powder performance. If, for example, a simple cube consistently achieves less than 99% density, it may indicate that the reused powder has degraded or that machine parameters need recalibration. In contrast, consistently high densities suggest that the powder remains viable. For instance, in the study by Smolina et al., all bulk sample densities measured via X-ray computed tomography (XCT) were approximately 99.9%, demonstrating that their reused powder met quality expectations and passed this form of functional validation with each cycle [99].

In industrial practice, companies may perform a qualification build when using recycled powder. For instance, EOS and other OEMs sometimes suggest printing a standard geometry, such as a stair-step or a pin array, and inspecting it for any defects when reclaimed powder is used. Although this is not done for every batch, it serves as part of the initial validation process in a powder reuse strategy.

6. Summary and Future Directions

The literature reviewed in this work shows that powder reuse in aluminum AM is governed by the coupled evolution of morphology, oxidation, moisture sensitivity, contamination, and flow-related behavior. Under controlled reuse conditions, especially for Al–Si-based powders processed by L-PBF, these changes are often gradual and manageable; however, they can eventually affect powder-bed uniformity, melt-pool stability, defect formation, and part reliability if degradation is allowed to accumulate without qualification.

Future progress should therefore focus on aluminum-specific qualification thresholds, improved control of oxygen and moisture pickup, and more application-oriented powder management strategies. In particular, closed-loop handling systems, real-time monitoring of powder-condition indicators, and clearer criteria for powder end-of-life are likely to become central to safer, more consistent, and more sustainable reuse of aluminum powders in additive manufacturing [96,97,99,252,253].

7. Conclusions

This review examined powder degradation and reuse in aluminum alloy powders used in powder-based additive manufacturing, with primary emphasis on L-PBF feedstocks. The available literature indicates that reused aluminum powders are primarily affected by progressive surface oxidation, morphological evolution, moisture sensitivity, and changes in flow-related behavior, whereas severe bulk-chemistry changes are less common under controlled conditions. Accordingly, the practical feasibility of powder reuse depends less on any single powder metric than on the combined effect of these changes on powder-bed behavior, defect formation, and final part performance. Overall, the evidence supports the mechanical and microstructural viability of moderate powder reuse in well-controlled aluminum AM workflows, while also highlighting the need for stronger critical qualification frameworks and alloy-specific reuse criteria.

Author Contributions: Conceptualization, S.R., S.B., F.B., D.U., P.F. and M.L.; Resources, P.F. and M.L.; Writing—original draft preparation, S.R.; Writing—review and editing, S.R., S.B., F.B., D.U., P.F. and M.L.; Visualization, S.R.; Supervision, S.B., F.B., D.U., P.F. and M.L.; Project administration, M.L.; Funding acquisition, P.F. and M.L. All authors have read and agreed to the published version of the manuscript.

Funding: This work was supported by the Italian Ministry of University and Research (MUR) under Next Generation EU—PNRR M4C2, DM 117/2023.

Institutional Review Board Statement: Not applicable.

Informed Consent Statement: Not applicable.

Data Availability Statement: No new data were created or analyzed in this study. Data sharing is not applicable to this article.

Acknowledgments: During the preparation of this manuscript, the authors used ChatGPT (GPT-5.3 Thinking; OpenAI, San Francisco, CA, USA) only to assist in the preparation of schematic illustrations. No AI tools were used to generate, analyze, or interpret scientific data or to draw scientific conclusions. All AI-assisted graphical outputs were carefully reviewed, edited, and validated by the authors, who take full responsibility for the content of this publication.

Conflicts of Interest: The authors declare no conflicts of interest.

References

1. *ISO/ASTM 52900:2021*; Additive Manufacturing—General Principles—Fundamentals and Vocabulary. ISO/TC 261: Berlin, Germany; ASTM-Komitee F42: West Conshohocken, PA, USA, 2021.
2. Pérez, M.; Carou, D.; Rubio, E.M.; Teti, R. Current advances in additive manufacturing. *Procedia CIRP* **2020**, *88*, 439–444. [CrossRef]
3. Fagundes, A.P.; Lira, J.O.D.B.; Padoin, N.; Soares, C.; Riella, H.G. Additive manufacturing of functional devices for environmental applications: A review. *J. Environ. Chem. Eng.* **2022**, *10*, 108049. [CrossRef]
4. Gohari, H.; Barari, A.; Kishawy, H.; Tsuzuki, M.S.G. Effect of Direct Slicing on Precision Additive Manufacturing. *IFAC-PapersOnLine* **2020**, *53*, 11982–11987. [CrossRef]
5. Christensen, K.H. The Difference Among Patient Acuity Levels and Consumer Satisfaction with Nursing Care Scores. Master's Thesis, University of Wyoming, Laramie, WY, USA, 1989.
6. Jin, L.; Zhang, K.; Xu, T.; Zeng, T.; Cheng, S. The fabrication and mechanical properties of SiC/SiC composites prepared by SLS combined with PIP. *Ceram. Int.* **2018**, *44*, 20992–20999. [CrossRef]
7. Duda, T.; Raghavan, L.V. 3D metal printing technology: The need to re-invent design practice. *AI Soc.* **2018**, *33*, 241–252. [CrossRef]
8. Duda, T.; Raghavan, L.V. 3D Metal Printing Technology. *IFAC-PapersOnLine* **2016**, *49*, 103–110. [CrossRef]
9. Atzeni, E.; Salmi, A. Economics of additive manufacturing for end-usable metal parts. *Int. J. Adv. Manuf. Technol.* **2012**, *62*, 1147–1155. [CrossRef]
10. Jiménez, M.; Romero, L.; Domínguez, I.A.; Espinosa, M.D.M.; Domínguez, M. Additive Manufacturing Technologies: An Overview about 3D Printing Methods and Future Prospects. *Complexity* **2019**, *2019*, 9656938. [CrossRef]
11. Constantin, L.; Wu, Z.; Li, N.; Fan, L.; Silvain, J.F.; Lu, Y.F. Laser 3D printing of complex copper structures. *Addit. Manuf.* **2020**, *35*, 101268. [CrossRef]
12. El-Wardany, T.; She, Y.; Jagdale, V.; Garofano, J.K.; Liou, J.; Schmidt, W. Challenges in 3D printing of high conductivity copper. In *ASME 2017 International Technical Conference and Exhibition on Packaging and Integration of Electronic and Photonic Microsystems, InterPACK 2017, Collocated with the ASME 2017 Conference on Information Storage and Processing Systems*; American Society of Mechanical Engineers (ASME): New York, NY, USA, 2017. [CrossRef]
13. Aboulkhair, N.T.; Simonelli, M.; Parry, L.; Ashcroft, I.; Tuck, C.; Hague, R. 3D printing of Aluminium alloys: Additive Manufacturing of Aluminium alloys using selective laser melting. *Prog. Mater. Sci.* **2019**, *106*, 100578. [CrossRef]
14. Stojanovic, B.; Bukvic; Epler, I. Application of aluminum and aluminum alloys in engineering. *Appl. Eng. Lett.* **2018**, *3*, 52–62. [CrossRef]
15. Al-Alimi, S.; Yusuf, N.K.; Ghaleb, A.M.; Lajis, M.A.; Shamsudin, S.; Zhou, W.; Altharan, Y.M.; Abdulwahab, H.S.; Saif, Y.; Didane, D.H.; et al. Recycling aluminium for sustainable development: A review of different processing technologies in green manufacturing. *Results Eng.* **2024**, *23*, 102566. [CrossRef]
16. Li, S.S.; Yue, X.; Li, Q.Y.; Peng, H.L.; Dong, B.X.; Liu, T.S.; Yang, H.Y.; Fan, J.; Shu, S.L.; Qiu, F.; et al. Development and applications of aluminum alloys for aerospace industry. *J. Mater. Res. Technol.* **2023**, *27*, 944–983. [CrossRef]
17. Mazzolani, F.M. Structural applications of aluminium in civil engineering. *Struct. Eng. Int. J. Int. Assoc. Bridge Struct. Eng. (IABSE)* **2006**, *16*, 280–285. [CrossRef]
18. Dalapati, G.K.; Masudy-Panah, S.; Kumar, A.; Tan, C.C.; Tan, H.R.; Chi, D. Aluminium alloyed iron-silicide/silicon solar cells: A simple approach for low cost environmental-friendly photovoltaic technology. *Sci. Rep.* **2015**, *5*, 17810. [CrossRef] [PubMed]
19. Demirkesen, A.; Uçar, M. Investigation of the Effects of Using Aluminum Alloys in Electric Vehicles Production. In Proceedings of the International Marmara Science Congress (IMASCON), Kocaeli, Turkey, 4–5 December 2020.
20. Gromov, A.; Ilyin, A.; Förter-Barth, U.; Teipel, U. Characterization of aluminum powders: II. Aluminum nanopowders passivated by non-inert coatings. *Propellants Explos. Pyrotech.* **2006**, *31*, 401–409. [CrossRef]
21. Popov, V.V.; Grilli, M.L.; Koptyug, A.; Jaworska, L.; Katz-Demyanetz, A.; Klobčar, D.; Balos, S.; Postolnyi, B.O.; Goel, S. Powder bed fusion additive manufacturing using critical raw materials: A review. *Materials* **2021**, *14*, 909. [CrossRef] [PubMed]
22. Ford, S.; Despeisse, M. Additive manufacturing and sustainability: An exploratory study of the advantages and challenges. *J. Clean. Prod.* **2016**, *137*, 1573–1587. [CrossRef]
23. Moghimian, P.; Poirié, T.; Habibnejad-Korayem, M.; Zavala, J.A.; Kroeger, J.; Marion, F.; Larouche, F. Metal powders in additive manufacturing: A review on reusability and recyclability of common titanium. nickel and aluminum alloys. *Addit. Manuf.* **2021**, *43*, 102017. [CrossRef]
24. Martucci, A.; Tam, P.L.; Aversa, A.; Lombardi, M.; Nyborg, L. The effect of powder reuse on the surface chemical composition of the Scalmalloy powder in Powder Bed Fusion—Laser Beam process. *Surf. Interface Anal.* **2022**, *55*, 388–395. [CrossRef]

25. Beal, M.; Azzougagh, M.N.; Pourchez, J.; Bertrand, P.; Cabrol, E.; Si-Mohand, H.; Keller, F.X. Effect of powder reuse on physical, chemical and toxicological properties of 6061-Zr aluminum alloy processed by Laser Powder Bed Fusion (L-PBF). *Mater. Tech.* **2023**, *111*, 103. [CrossRef] [PubMed]
26. Warner, J.H.; Ringer, S.P.; Proust, G. Strategies for metallic powder reuse in powder bed fusion: A review. *J. Manuf. Process.* **2024**, *110*, 263–290. [CrossRef]
27. Lanzutti, A.; Marin, E. The Challenges and Advances in Recycling/Re-Using Powder for Metal 3D Printing: A Comprehensive Review. *Metals* **2024**, *14*, 886. [CrossRef]
28. Zafar, F.; Reis, A.; Vieira, M.; Emadinia, O. Additively Manufactured High-Strength Aluminum Alloys: A Review. In *Recent Advancements in Aluminum Alloys*; IntechOpen: London, UK, 2024. [CrossRef]
29. Kiani, P.; Dupuy, A.D.; Ma, K.; Schoenung, J.M. The Reusability of AlSi10Mg Powder in Directed Energy Deposition. *Powders* **2024**, *3*, 28–43. [CrossRef]
30. Li, J.; Shi, W.; Lin, Y.; Li, J.; Liu, S.; Liu, B. Comparative study on MQL milling and hole making processes for laser beam powder bed fusion (L-PBF) of Ti-6Al-4V titanium alloy. *J. Manuf. Process.* **2023**, *94*, 20–34. [CrossRef]
31. Santecchia, E.; Spigarelli, S.; Cabibbo, M. Material reuse in laser powder bed fusion: Side effects of the laser—Metal powder interaction. *Metals* **2020**, *10*, 341. [CrossRef]
32. Patel, S.; Chen, H.; Vlasea, M.; Zou, Y. The influence of beam focus during laser powder bed fusion of a high reflectivity aluminium alloy—AlSi10Mg. *Addit. Manuf.* **2022**, *59*, 103112. [CrossRef]
33. Tassa, O.; Colaneri, A.; Fransesini, L.; Sammartino, F.; Demir, A.G. Developing the Additive Manufacturing Chain of AlSi7Mg with Laser Powder Bed Fusion and Tailored Heat Treatments for Railway Spare Parts. *J. Mater. Eng. Perform.* **2023**, *32*, 11479–11488. [CrossRef]
34. Mehta, B.; Svanberg, A.; Nyborg, L. Laser powder bed fusion of an Al-Mg-Sc-Zr alloy: Manufacturing. peak hardening response and thermal stability at peak hardness. *Metals* **2022**, *12*, 57. [CrossRef]
35. da Silva, L.J.; de Araújo, D.B.; Reis, R.P.; Palm, F.; Scotti, A. Wire Arc Additive Manufacturing of Scalmalloy® (Al-Mg-Sc-Zr): Thermal Management Effects on Direct Age-Hardening Response. *Coatings* **2025**, *15*, 237. [CrossRef]
36. Kvvssn, V.; Butt, M.M.; Laieghi, H.; Uddin, Z.; Salamci, E.; Kim, D.B.; Kizil, H. Recent progress in additive manufacturing of 7XXX aluminum alloys. *Int. J. Adv. Manuf. Technol.* **2025**, *137*, 4353–4399. [CrossRef]
37. Martin, J.H.; Yahata, B.D.; Hundley, J.M.; Mayer, J.A.; Schaedler, T.A.; Pollock, T.M. 3D printing of high-strength aluminium alloys. *Nature* **2017**, *549*, 365–369. [CrossRef] [PubMed]
38. Singh, A.; Ramakrishnan, A.; Baker, D.; Biswas, A.; Dinda, G.P. Laser metal deposition of nickel coated Al 7050 alloy. *J. Alloys Compd.* **2017**, *719*, 151–158. [CrossRef]
39. Yap, C.Y.; Chua, C.K.; Dong, Z.L.; Liu, Z.H.; Zhang, D.Q.; Loh, L.E.; Sing, S.L. Review of selective laser melting: Materials and applications. *Appl. Phys. Rev.* **2015**, *2*, 041101. [CrossRef]
40. Herzog, D.; Seyda, V.; Wycisk, E.; Emmelmann, C. Additive manufacturing of metals. *Acta Mater.* **2016**, *117*, 371–392. [CrossRef]
41. Slotwinski, J.A.; Garboczi, E.J.; Hebenstreit, K.M. Porosity measurements and analysis for metal additive manufacturing process control. *J. Res. Natl. Inst. Stand. Technol.* **2014**, *119*, 494–528. [CrossRef] [PubMed]
42. Cordova, L.; Campos, M.; Tinga, T. Revealing the Effects of Powder Reuse for Selective Laser Melting by Powder Characterization. *JOM* **2019**, *71*, 1062–1072. [CrossRef]
43. Powell, D.; Rennie, A.E.W.; Geekie, L.; Burns, N. Understanding powder degradation in metal additive manufacturing to allow the upcycling of recycled powders. *J. Clean. Prod.* **2020**, *268*, 122077. [CrossRef]
44. Leung, C.L.A.; Marussi, S.; Atwood, R.C.; Towrie, M.; Withers, P.J.; Lee, P.D. In situ X-ray imaging of defect and molten pool dynamics in laser additive manufacturing. *Nat. Commun.* **2018**, *9*, 1355. [CrossRef] [PubMed]
45. Liu, Y.; Yang, Y.; Mai, S.; Wang, D.; Song, C. Investigation into spatter behavior during selective laser melting of AISI 316L stainless steel powder. *Mater. Des.* **2015**, *87*, 797–806. [CrossRef]
46. Kellens, K.; Baumers, M.; Gutowski, T.G.; Flanagan, W.; Lifset, R.; Duflou, J.R. Environmental Dimensions of Additive Manufacturing: Mapping Application Domains and Their Environmental Implications. *J. Ind. Ecol.* **2017**, *21*, S49–S68. [CrossRef]
47. Faludi, J.; Bayley, C.; Bhogal, S.; Iribarne, M. Comparing environmental impacts of additive manufacturing vs traditional machining via life-cycle assessment. *Rapid Prototyp. J.* **2015**, *21*, 14–33. [CrossRef]
48. Derimow, N.; Hrabe, N. Oxidation in Reused Powder Bed Fusion Additive Manufacturing Ti-6Al-4V Feedstock: A Brief Review. *JOM* **2021**, *73*, 3618–3638. [CrossRef]
49. Son, J.Y.; Lee, K.Y.; Lee, S.H.; Choi, C.H. Effects of Oxidized Metal Powders on Pore Defects in Powder-Fed Direct Energy Deposition. *Micromachines* **2024**, *15*, 243. [CrossRef] [PubMed]
50. Brown, B.; Lough, C.; Wilson, D.; Newkirk, J.; Liou, F. Atmosphere Effects in Laser Powder Bed Fusion: A Review. *Materials* **2024**, *17*, 5549. [CrossRef] [PubMed]
51. Derimow, N.; Mansfield, E.; Holm, J.; Hrabe, N. Additive manufacturing titanium powder oxygen variation within a single powder bed due to differences in powder size and oxygen content. *Addit. Manuf. Lett.* **2023**, *5*, 100125. [CrossRef]

52. Shanbhag, G.; Vlasea, M. Powder reuse cycles in electron beam powder bed fusion—Variation of powder characteristics. *Materials* **2021**, *14*, 4602. [CrossRef] [PubMed]
53. Piscopo, G.; Atzeni, E.; Saboori, A.; Salmi, A. An Overview of the Process Mechanisms in the Laser Powder Directed Energy Deposition. *Appl. Sci.* **2023**, *13*, 117. [CrossRef]
54. Weiss, C.; Haefner, C.L.; Munk, J. On the Influence of AlSi10Mg Powder Recycling Behavior in the LPBF Process and Consequences for Mechanical Properties. *JOM* **2022**, *74*, 1188–1199. [CrossRef]
55. Stugelmayer, E.J. Characterization of Process Induced Defects in Laser Powder Bed Fusion Processed AlSi10Mg Alloy. Master's Thesis, Montana Technological University, Butte, MT, USA, 2018.
56. Yakubov, V.; Ostergaard, H.; Bhagavath, S.; Leung, C.L.A.; Hughes, J.; Yasa, E.; Khezri, M.; Löschke, S.K.; Li, Q.; Paradowska, A.M. Recycled aluminium feedstock in metal additive manufacturing: A state of the art review. *Heliyon* **2024**, *10*, e27243. [CrossRef] [PubMed]
57. Zapico, P.; Giganto, S.; Barreiro, J.; Martínez-Pellitero, S. Characterisation of 17-4PH metallic powder recycling to optimise the performance of the selective laser melting process. *J. Mater. Res. Technol.* **2020**, *9*, 1273–1285. [CrossRef]
58. Li, K.; Zhao, Z.; Zhou, H.; Zhou, H.; Yin, J.; Zhang, W.; Zhou, G. Numerical simulation of effect of different initial morphologies on melt hydrodynamics in laser polishing of Ti6Al4V. *Micromachines* **2021**, *12*, 581. [CrossRef] [PubMed]
59. Alnajjar, M.; Christien, F.; Wolski, K.; Bosch, C. Evidence of austenite by-passing in a stainless steel obtained from laser melting additive manufacturing. *Addit. Manuf.* **2019**, *25*, 187–195. [CrossRef]
60. Douglas, R.; Lancaster, R.; Jones, T.; Barnard, N.; Adams, J. The Influence of Powder Reuse on the Properties of Laser Powder Bed-Fused Stainless Steel 316L: A Review. *Adv. Eng. Mater.* **2022**, *24*, 2200596. [CrossRef]
61. Svozilova, S.; Zetková, I.; Marin, J.F.S.; Garay, J.A.T. Evaluation of Recycled and Reused Metal Powders for DMLS 3D Printing. *Materials* **2024**, *17*, 6184. [CrossRef] [PubMed]
62. Mahtabi, M.B.; Yadollahi, A.; Morgan-Barnes, C.; Priddy, M.W.; Rhee, H. Effects of Powder Reuse and Particle Size Distribution on Structural Integrity of Ti-6Al-4V Processed via Laser Beam Directed Energy Deposition. *J. Manuf. Mater. Process.* **2024**, *8*, 209. [CrossRef]
63. Liu, M.; Chiu, L.N.S.; Shen, H.; Fang, X.; Tao, Z.; Huang, A.; Davies, C.; Wu, X.; Yan, W. Effective thermal conductivities of metal powders for additive manufacturing. *Powder Technol.* **2022**, *401*, 117323. [CrossRef]
64. Nandy, J.; Sarangi, H.; Sahoo, S. A Review on Direct Metal Laser Sintering: Process Features and Microstructure Modeling. *Lasers Manuf. Mater. Process.* **2019**, *6*, 280–316. [CrossRef]
65. Montufar, E.B.; Tkachenko, S.; Casas-Luna, M.; Škarvada, P.; Slámečka, K.; Diaz-de-la-Torre, S.; Koutný, D.; Paloušek, D.; Koledova, Z.; Hernández-Tapia, L.; et al. Benchmarking of additive manufacturing technologies for commercially-pure-titanium bone-tissue-engineering scaffolds: Processing-microstructure-property relationship. *Addit. Manuf.* **2020**, *36*, 101516. [CrossRef]
66. Salehi, H.; Cummins, J.; Gallino, E.; Garg, V.; Deng, T.; Hassanpour, A.; Bradley, M. Optimising Spread-Layer Quality in Powder Additive Manufacturing: Assessing Packing Fraction and Segregation Tendency. *Processes* **2023**, *11*, 2276. [CrossRef]
67. Roy, S.; Shaheen, M.Y.; Pöschel, T. Effect of cohesion on structure of powder layers in additive manufacturing. *Granul. Matter* **2023**, *25*, 68. [CrossRef]
68. Chu, F.; Zhang, K.; Shen, H.; Liu, M.; Huang, W.; Zhang, X.; Liang, E.; Zhou, Z.; Lei, L.; Hou, J.; et al. Influence of satellite and agglomeration of powder on the processability of AlSi10Mg powder in Laser Powder Bed Fusion. *J. Mater. Res. Technol.* **2021**, *11*, 2059–2073. [CrossRef]
69. Haferkamp, L.; Haudenschild, L.; Spierings, A.; Wegener, K.; Riener, K.; Ziegelmeier, S.; Leichtfried, G.J. The influence of particle shape, powder flowability, and powder layer density on part density in laser powder bed fusion. *Metals* **2021**, *11*, 418. [CrossRef]
70. Juarez-Enriquez, E.; Olivas, G.I.; Zamudio-Flores, P.B.; Ortega-Rivas, E.; Perez-Vega, S.; Sepulveda, D.R. Effect of water content on the flowability of hygroscopic powders. *J. Food Eng.* **2017**, *205*, 12–17. [CrossRef]
71. Bertling, M.O.A. Moisture Mitigation and Analysis for the Powder Metallurgy Industry. Master's Thesis, KTH Royal Institute of Technology, Stockholm, Sweden, 2024.
72. Grubbs, J.; Sousa, B.C.; Cote, D. Exploration of the Effects of Metallic Powder Handling and Storage Conditions on Flowability and Moisture Content for Additive Manufacturing Applications. *Metals* **2022**, *12*, 603. [CrossRef]
73. Sandler, N.; Reiche, K.; Heinämäki, J.; Yliruusi, J. Effect of moisture on powder flow properties of theophylline. *Pharmaceutics* **2010**, *2*, 275–290. [CrossRef] [PubMed]
74. Kim, T.; Kim, M.K.; Fang, Y.; Suhr, J. Moisture Effects on Qualities and Properties of Laser Powder Bed Fusion (LPBF) Additive Manufacturing of As-Built 17-4PH Stainless Steel Parts. *Metals* **2023**, *13*, 1550. [CrossRef]
75. Brandão, A.D.; Gerard, R.; Gumpinger, J.; Beretta, S.; Makaya, A.; Pambaguian, L.; Ghidini, T. Challenges in Additive Manufacturing of space parts: Powder feedstock cross-contamination and its impact on end products. *Materials* **2017**, *10*, 522. [CrossRef] [PubMed]
76. Radchenko, O.K.; Gogaev, K.O. Requirements for Metal and Alloy Powders for 3D Printing (Review). *Powder Metall. Met. Ceram.* **2022**, *61*, 135–154. [CrossRef]

77. Rezaei, S.; Askari, A. Moulding of SS316L surgical component using palm-stearin feedstock: Rheological analysis, process window and parametric optimization. *Powder Metall.* **2024**, *67*, 246–261. [CrossRef]
78. Soundarapandiyan, G.; Johnston, C.; Khan, R.H.U.; Chen, B.; Fitzpatrick, M.E. A technical review of the challenges of powder recycling in the laser powder bed fusion additive manufacturing process. *J. Eng.* **2021**, *2021*, 97–103. [CrossRef]
79. Zhang, Y.; Wu, S.; Guo, Z.; Peng, G.; Wang, L.; Yan, W. Defects caused by powder spattering and entrainment in laser powder bed fusion process: High-fidelity modeling of gas, melt pool and powder dynamics. *Acta Mater.* **2025**, *288*, 120816. [CrossRef]
80. Raza, A.; Pauzon, C.; Hryha, E.; Markström, A.; Forêt, P. Spatter oxidation during laser powder bed fusion of Alloy 718: Dependence on oxygen content in the process atmosphere. *Addit. Manuf.* **2021**, *48*, 102369. [CrossRef]
81. Sutton, A.T.; Kriewall, C.S.; Leu, M.C.; Newkirk, J.W.; Brown, B. Characterization of laser spatter and condensate generated during the selective laser melting of 304L stainless steel powder. *Addit. Manuf.* **2020**, *31*, 100904. [CrossRef]
82. Kan, W.H.; Chiu, L.N.S.; Lim, C.V.S.; Zhu, Y.; Tian, Y.; Jiang, D.; Huang, A. A critical review on the effects of process-induced porosity on the mechanical properties of alloys fabricated by laser powder bed fusion. *J. Mater. Sci.* **2022**, *57*, 9818–9865. [CrossRef]
83. Bidare, P.; Jiménez, A.; Hassanin, H.; Essa, K. Porosity, cracks, and mechanical properties of additively manufactured tooling alloys: A review. *Adv. Manuf.* **2022**, *10*, 175–204. [CrossRef]
84. Rezaei, S.; Askari, A. Investigating metal injection molding of 4605 low-alloy steel powder-polymer mixture: Parametric optimization of the injection stage using RSM technique. *Iran. Polym. J. (Engl. Ed.)* **2024**, *34*, 453–464. [CrossRef]
85. LeBrun, T. Standardization Gaps in Powder Feedstock Characterization and Establishing Acceptability for Reuse in Additive Manufacturing. *JOM* **2024**, *76*, 1885–1889. [CrossRef]
86. Khairallah, S.A.; Sun, T.; Simonds, B.J. Onset of periodic oscillations as a precursor of a transition to pore-generating turbulence in laser melting. *Addit. Manuf. Lett.* **2021**, *1*, 100002. [CrossRef]
87. Li, Y.; Gu, D. Thermal behavior during selective laser melting of commercially pure titanium powder: Numerical simulation and experimental study. *Addit. Manuf.* **2014**, *1–4*, 99–109. [CrossRef]
88. Sun, W.; Ma, Y.; Li, P.; Zhang, W. Residual Stress Distribution and Its Effect on Fatigue Crack Path of Laser Powder Bed Fusion Ti6Al4V Alloy. *Aerospace* **2025**, *12*, 103. [CrossRef]
89. Cordova, L.; Bor, T.; de Smit, M.; Carmignato, S.; Campos, M.; Tinga, T. Effects of powder reuse on the microstructure and mechanical behaviour of Al–Mg–Sc–Zr alloy processed by laser powder bed fusion (LPBF). *Addit. Manuf.* **2020**, *36*, 101625. [CrossRef]
90. Wang, Z.; Lin, X.; Wang, J.; Kang, N.; Hu, Y.; Wang, D.; Li, H.; Huang, W.; Pan, F. Remarkable strength-impact toughness conflict in high-strength Al-Mg-Sc-Zr alloy fabricated via laser powder bed fusion additive manufacturing. *Addit. Manuf.* **2022**, *59*, 103093. [CrossRef]
91. Ren, S.; Zhang, Y.; Liu, Y.; Sakao, T.; Huisingh, D.; Almeida, C.M.V.B. A comprehensive review of big data analytics throughout product lifecycle to support sustainable smart manufacturing: A framework. challenges and future research directions. *J. Clean. Prod.* **2019**, *210*, 1343–1365. [CrossRef]
92. Gruber, K.; Smolina, I.; Stopyra, W. Assessing metal powder quality for additive manufacturing using diffuse light spectroscopy. *Powder Technol.* **2024**, *434*, 119366. [CrossRef]
93. Ahsan, F.; Razmi, J.; Ladani, L. Process Parameter Optimization in Metal Laser-Based Powder Bed Fusion Using Image Processing and Statistical Analyses. *Metals* **2022**, *12*, 87. [CrossRef]
94. DeWitte, L.; Saldana, C.; Kurfess, T.; Fu, K. Effect of coaxial nozzle wear on catchment efficiency in direct energy deposition built components. *J. Manuf. Syst.* **2022**, *63*, 524–538. [CrossRef]
95. Burke, P.; Kipouros, Y.G.; Judge, W.D.; Kipouros, G.J. Surprises and Pitfalls in the Development of Magnesium Powder Metallurgy Alloys. In *Magnesium and Its Alloys*; CRC Press: Boca Raton, FL, USA, 2019. [CrossRef]
96. Gibbons, D.W.; Govender, P.; van der Merwe, A.F. Metal powder feedstock evaluation and management for powder bed fusion: A review of literature. standards, and practical guidelines. *Prog. Addit. Manuf.* **2024**, *9*, 805–833. [CrossRef]
97. Riener, K.; Oswald, S.; Winkler, M.; Leichtfried, G.J. Influence of storage conditions and reconditioning of AlSi10Mg powder on the quality of parts produced by laser powder bed fusion (LPBF). *Addit. Manuf.* **2021**, *39*, 101896. [CrossRef]
98. Anderson, A.; Gallegos, S.; Rezaie, B.; Azarmi, F. Present and Future Sustainability Development of 3D Metal Printing. *Eur. J. Sustain. Dev. Res.* **2021**, *5*, em0168. [CrossRef] [PubMed]
99. Smolina, I.; Gruber, K.; Pawlak, A.; Ziółkowski, G.; Grochowska, E.; Schob, D.; Kobiela, K.; Roszak, R.; Ziegenhorn, M.; Kurzynowski, T. Influence of the AlSi7Mg0.6 Aluminium Alloy Powder Reuse on the Quality and Mechanical Properties of LPBF Samples. *Materials* **2022**, *15*, 5019. [CrossRef] [PubMed]
100. Lutter-Günther, M.; Bröker, M.; Mayer, T.; Lizak, S.; Seidel, C.; Reinhart, G. Spatter formation during laser beam melting of AlSi10Mg and effects on powder quality. *Procedia CIRP* **2018**, *74*, 33–38. [CrossRef]
101. Giganto, S.; Martínez-Pellitero, S.; Barreiro, J.; Zapico, P. Influence of 17-4 PH stainless steel powder recycling on properties of SLM additive manufactured parts. *J. Mater. Res. Technol.* **2022**, *16*, 1647–1658. [CrossRef]

102. Li, Z.; Li, H.; Yin, J.; Li, Y.; Nie, Z.; Li, X.; You, D.; Guan, K.; Duan, W.; Cao, L.; et al. A Review of Spatter in Laser Powder Bed Fusion Additive Manufacturing: In Situ Detection, Generation, Effects, and Countermeasures. *Micromachines* **2022**, *13*, 1366. [CrossRef] [PubMed]
103. Avrampos, P.; Vosniakos, G.C. A Simulation Study on Sieving as a Powder Deposition Method in Powder Bed Fusion Processes. *Materials* **2024**, *17*, 3382. [CrossRef] [PubMed]
104. Pereira, J.C.; Irastorza, U.; Solana, A.; Soriano, C.; García, D.; Ruiz, J.E.; Lamikiz, A. Effect of Powder Reuse on Powder Characteristics and Properties of DED Laser Beam Metal Additive Manufacturing Process with Stellite® 21 and UNS S32750. *Metals* **2024**, *14*, 1031. [CrossRef]
105. Huang, T.; Thu, K.S.; Zhang, Z.; Che, L.; Xu, P.; Fuh, J.Y.H.; Lee, H.P. Assessing the Impact of Top-Up Powder Reuse Strategy on MS1 Powder Characteristics and L-PBF Printed Part Properties. *Metals* **2025**, *15*, 181. [CrossRef]
106. Yamaguchi, M.; Kushima, K.; Ono, Y.; Sugai, T.; Oyama, T.; Furumoto, T. Humidity control in laser powder bed fusion using titanium alloy powder for quality assurance of built parts and reusability of metal powder. *J. Mater. Process. Technol.* **2023**, *311*, 117817. [CrossRef]
107. Cordova, L.; Bor, T.; de Smit, M.; Campos, M.; Tinga, T. Measuring the spreadability of pre-treated and moisturized powders for laser powder bed fusion. *Addit. Manuf.* **2020**, *32*, 101082. [CrossRef]
108. Abohelwa, M.; Wollmann, A.; Benker, B.; Plack, A.; Javadi, M.; Weber, A.P. Size Classification and Material Sorting of Fine Powders with a Deflector Wheel Air Classifier and an Electrostatic Separator. *Powders* **2024**, *3*, 550–573. [CrossRef]
109. Santana, D.; Rodríguez, J.M.; Macías-Machín, A. Modelling fluidized bed elutriation of fine particles. *Powder Technol.* **1999**, *106*, 110–118. [CrossRef]
110. Ding, W.; Chen, G.; Qin, M.; He, Y.; Qu, X. Low-cost Ti powders for additive manufacturing treated by fluidized bed. *Powder Technol.* **2019**, *350*, 117–122. [CrossRef]
111. Marchetti, L.; Mellin, P.; Hulme, C.N. Negative impact of humidity on the flowability of steel powders. *Part. Sci. Technol.* **2022**, *40*, 722–736. [CrossRef]
112. Mitterlehner, M.; Danninger, H.; Gierl-Mayer, C.; Gschiel, H. Investigation of the Influence of Powder Moisture on the Spreadability Using the Spreading Tester. *BHM Berg. Hüttenmänn. Monatshefte* **2021**, *166*, 14–22. [CrossRef]
113. Rescaglio, A.; Schockmel, J.; Vandewalle, N.; Lumay, G. Combined effect of moisture and electrostatic charges on powder flow. *EPJ Web Conf.* **2017**, *140*, 13009. [CrossRef]
114. Schwerz, C.; Moverare, J.; Kung, A.; Bircher, B.A.; Riabov, D.; Nyborg, L. Reduction of oxygen content in laser powder bed fusion process atmosphere—Effects on stochastic defect formation and mechanical properties. *J. Mater. Res. Technol.* **2024**, *30*, 4667–4681. [CrossRef]
115. Emminghaus, N.; Fritsch, S.; Büttner, H.; August, J.; Tegtmeier, M.; Huse, M.; Lammers, M.; Hoff, C.; Hermsdorf, J.; Kaierle, S. PBF-LB/M process under a silane-doped argon atmosphere: Preliminary studies and development of an innovative machine concept. *Adv. Ind. Manuf. Eng.* **2021**, *2*, 100040. [CrossRef]
116. Doutre, P.T.; Grandvallet, C.; Museau, M. A new method with ultrasonic mechanism for efficient depowdering of parts produced by electron beam melting. *Mech. Ind.* **2022**, *23*, 22. [CrossRef]
117. Janzen, K.; Kallies, K.J.; Waalkes, L.; Imgrund, P.; Emmelmann, C. Recycling of Ti-6Al-4V Powder in Metal Binder Jetting. *Funtai Oyobi Fummatsu Yakin/J. Jpn. Soc. Powder Powder Metall.* **2025**, *72*, S353–S360. [CrossRef]
118. Montanari, R.; Palombi, A.; Richetta, M.; Varone, A. Additive Manufacturing of Aluminum Alloys for Aeronautic Applications: Advantages and Problems. *Metals* **2023**, *13*, 716. [CrossRef]
119. Wang, A.; Wei, Q.; Luo, S.; Tang, Z.; Yang, H.; Wu, Y.; Leung, C.L.A.; Lee, P.D.; Wang, H.; Wang, H. Blue laser directed energy deposition of aluminum with synchronously enhanced efficiency and quality. *Addit. Manuf. Lett.* **2023**, *5*, 100127. [CrossRef]
120. Trevisan, F.; Calignano, F.; Lorusso, M.; Pakkanen, J.; Aversa, A.; Ambrosio, E.P.; Lombardi, M.; Fino, P.; Manfredi, D. On the selective laser melting (SLM) of the AlSi10Mg alloy: Process, microstructure, and mechanical properties. *Materials* **2017**, *10*, 76. [CrossRef] [PubMed]
121. Kempen, K.; Thijs, L.; Yasa, E.; Badrossamay, M.; Verheecke, W.; Kruth, J.P. Process optimization and microstructural analysis for selective laser melting of AlSi10Mg. In Proceedings of the 22nd Annual International Solid Freeform Fabrication Symposium—An Additive Manufacturing Conference, SFF 2011, Austin, TX, USA, 8–10 August 2011.
122. Javidani, M.; Arreguin-Zavala, J.; Danovitch, J.; Tian, Y.; Brochu, M. Additive Manufacturing of AlSi10Mg Alloy Using Direct Energy Deposition: Microstructure and Hardness Characterization. *J. Therm. Spray Technol.* **2017**, *26*, 587–597. [CrossRef]
123. Gong, J.; Wei, K.; Liu, M.; Song, W.; Li, X.; Zeng, X. Microstructure and mechanical properties of AlSi10Mg alloy built by laser powder bed fusion/direct energy deposition hybrid laser additive manufacturing. *Addit. Manuf.* **2022**, *59*, 103160. [CrossRef]
124. Kiani, P.; Dupuy, A.D.; Ma, K.; Schoenung, J.M. Directed energy deposition of AlSi10Mg: Single track nonscalability and bulk properties. *Mater. Des.* **2020**, *194*, 108847. [CrossRef]
125. Im, S.; Ghasri-Khouzani, M.; Muhammad, W.; Batmaz, R.; Esmati, K.; Chakraborty, A.; Natarajan, A.; Martin, É. Evaluation of Different Sintering Agents for Binder Jetting of Aluminum Alloy. *J. Mater. Eng. Perform.* **2023**, *32*, 9550–9560. [CrossRef]

126. Roberts, C.E.; Bourell, D.; Watt, T.; Cohen, J. A Novel Processing Approach for Additive Manufacturing of Commercial Aluminum Alloys. *Phys. Procedia* **2016**, *83*, 909–917. [CrossRef]
127. Rashid, R.; Masood, S.H.; Ruan, D.; Palanisamy, S.; Rashid, R.A.R.; Elambasseril, J.; Brandt, M. Effect of energy per layer on the anisotropy of selective laser melted AlSi12 aluminium alloy. *Addit. Manuf.* **2018**, *22*, 426–439. [CrossRef]
128. Baitimerov, R.; Lykov, P.; Zherebtsov, D.; Radionova, L.; Shultc, A.; Prashanth, K.G. Influence of powder characteristics on processability of AlSi12 alloy fabricated by selective laser melting. *Materials* **2018**, *11*, 742. [CrossRef] [PubMed]
129. Rashid, R.A.R.; Ali, H.; Palanisamy, S.; Masood, S.H. Effect of process parameters on the surface characteristics of AlSi12 samples made via Selective Laser Melting. *Mater. Today Proc.* **2017**, *4*, 8724–8730. [CrossRef]
130. Muñiz-Lerma, J.A.; Nommeots-Nomm, A.; Waters, K.E.; Brochu, M. A comprehensive approach to powder feedstock characterization for powder bed fusion additive manufacturing: A case study on AlSi7Mg. *Materials* **2018**, *11*, 2386. [CrossRef] [PubMed]
131. Rodríguez-González, P.; Zapico, P.; Robles-Valero, P.E.; Barreiro, J. Novel post-processing procedure to enhance casting molds manufactured by binder jetting AM. *Addit. Manuf.* **2022**, *59*, 103142. [CrossRef]
132. Kumar, M.; Gibbons, G.J.; Das, A.; Manna, I.; Tanner, D.; Kotadia, H.R. Additive manufacturing of aluminium alloy 2024 by laser powder bed fusion: Microstructural evolution, defects and mechanical properties. *Rapid Prototyp. J.* **2021**, *27*, 1388–1397. [CrossRef]
133. Pekok, M.A.; Setchi, R.; Ryan, M.; Han, Q.; Gu, D. Effect of process parameters on the microstructure and mechanical properties of AA2024 fabricated using selective laser melting. *Int. J. Adv. Manuf. Technol.* **2021**, *112*, 175–192. [CrossRef]
134. Ahmed, M.M.Z.; Seleman, M.M.E.-S.; Elfishawy, E.; Alzahrani, B.; Touileb, K.; Habba, M.I.A. The effect of temper condition and feeding speed on the additive manufacturing of AA2011 parts using friction stir deposition. *Materials* **2021**, *14*, 6396. [CrossRef] [PubMed]
135. Zhang, Y.; Gao, M.; Lu, Y.; Du, W. Deposition geometrical characteristics of wire arc additive-manufactured AA2219 aluminium alloy with cold metal transfer pulse advance arc mode. *Int. J. Adv. Manuf. Technol.* **2022**, *123*, 3807–3818. [CrossRef]
136. Kittichai, S. Effects of Very High Power Ultrasonic Additive Manufacturing Process Parameters on Hardness, Microstructure, and Texture of Aluminum 3003-H18 Alloy. Ph.D. Thesis, The Ohio State University, Columbus, OH, USA, 2015.
137. Pan, Q.; Kapoor, M.; Mileski, S.; Li, D.; Yang, J.; Zheng, Y.; Carsley, J.; Lou, X. Phase transformation and microstructural evolution in Al-Mn-Fe-Si 3104 aluminum alloy made by laser directed energy deposition. *Addit. Manuf.* **2023**, *77*, 103797. [CrossRef]
138. Rousseau, J.N.; Bois-Brochu, A.; Giguère, N.; Blais, C. Study of ultrasonic additive manufacturing and its utilization for the production of aluminum components made of alloys of the AA5XXX series. *Int. J. Adv. Manuf. Technol.* **2022**, *119*, 7983–8002. [CrossRef]
139. Horgar, A.; Fostervoll, H.; Nyhus, B.; Ren, X.; Eriksson, M.; Akselsen, O.M. Additive manufacturing using WAAM with AA5183 wire. *J. Mater. Process. Technol.* **2018**, *259*, 68–74. [CrossRef]
140. Bock, F.E.; Froend, M.; Herrnring, J.; Enz, J.; Kashaev, N.; Klusemann, B. Thermal analysis of laser additive manufacturing of aluminium alloys: Experiment and simulation. *AIP Conf. Proc.* **2018**, *1960*, 140004. [CrossRef]
141. Froend, M.; Ventzke, V.; Riekehr, S.; Kashaev, N.; Klusemann, B.; Enz, J. Microstructure and hardness evolution of laser metal deposited AA5087 wall-structures. *Procedia CIRP* **2018**, *74*, 131–135. [CrossRef]
142. Svetlizky, D.; Zheng, B.; Buta, T.; Zhou, Y.; Golan, O.; Breiman, U.; Haj-Ali, R.; Schoenung, J.M.; Lavernia, E.J.; Eliaz, N. Directed energy deposition of Al 5xxx alloy using Laser Engineered Net Shaping (LENS®). *Mater. Des.* **2020**, *192*, 108763. [CrossRef]
143. Mehta, A.; Zhou, L.; Huynh, T.; Park, S.; Hyer, H.; Song, S.; Bai, Y.; Imholte, D.D.; Woolstenhulme, N.E.; Wachs, D.M.; et al. Additive manufacturing and mechanical properties of the dense and crack free Zr-modified aluminum alloy 6061 fabricated by the laser-powder bed fusion. *Addit. Manuf.* **2021**, *41*, 101966. [CrossRef]
144. Loh, L.E.; Chua, C.K.; Yeong, W.Y.; Song, J.; Mapar, M.; Sing, S.L.; Liu, Z.H.; Zhang, D.Q. Numerical investigation and an effective modelling on the Selective Laser Melting (SLM) process with aluminium alloy 6061. *Int. J. Heat Mass Transf.* **2015**, *80*, 288–300. [CrossRef]
145. Dadbakhsh, S.; Mertens, R.; Vanmeensel, K.; Vleugels, J.; Van Humbeeck, J.; Kruth, J.P. In situ alloying and reinforcing of Al6061 during selective laser melting. *Procedia CIRP* **2018**, *74*, 39–43. [CrossRef]
146. Jeon, S.; Park, S.; Song, Y.; Park, J.; Park, H.; Lee, B.; Choi, H. Combinatorial Experiment for Al-6061 and Al-12Si alloy Based on Directed Energy Deposition (DED) Process. *J. Korean Powder Metall. Inst.* **2023**, *30*, 463–469. [CrossRef]
147. Patel, M.; Chaudhary, B.; Murugesan, J.; Jain, N.K. Additive Manufacturing of AA6063-ZrO2 Composite Using Friction Stir Surface Additive Manufacturing. *Trans. Indian Inst. Met.* **2023**, *76*, 581–588. [CrossRef]
148. Chen, X.; Duan, X.; Jiang, G. Numerical investigation of Transient Temperature Field on the Selective Laser Melting process with Al6063. *IOP Conf. Ser. Mater. Sci. Eng.* **2019**, *677*, 032070. [CrossRef]
149. Li, F.; Zhang, T.; Wu, Y.; Chen, C.; Zhou, K. Microstructure, mechanical properties, and crack formation of aluminum alloy 6063 produced via laser powder bed fusion. *J. Mater. Sci.* **2022**, *57*, 9631–9645. [CrossRef]

150. Blindheim, J.; Grong, Ø.; Welo, T.; Steinert, M. On the mechanical integrity of AA6082 3D structures deposited by hybrid metal extrusion & bonding additive manufacturing. *J. Mater. Process. Technol.* **2020**, *282*, 116684. [CrossRef]
151. Yoder, J.K.; Griffiths, R.J.; Yu, H.Z. Deformation-based additive manufacturing of 7075 aluminum with wrought-like mechanical properties. *Mater. Des.* **2021**, *198*, 109288. [CrossRef]
152. Xu, H.; Ren, W.; Ma, C.; Xu, L.; Han, Y.; Zhao, L.; Hao, K. Laser-directed energy deposition of ZrH2 particles reinforced Al7075 alloy: Cracks elimination and strength enhancement. *Addit. Manuf.* **2023**, *78*, 103877. [CrossRef]
153. Qi, T.; Zhu, H.; Zhang, H.; Yin, J.; Ke, L.; Zeng, X. Selective laser melting of Al7050 powder: Melting mode transition and comparison of the characteristics between the keyhole and conduction mode. *Mater. Des.* **2017**, *135*, 257–266. [CrossRef]
154. Fiegl, T.; Franke, M.; Raza, A.; Hryha, E.; Körner, C. Effect of AlSi10Mg0.4 long-term reused powder in PBF-LB/M on the mechanical properties. *Mater. Des.* **2021**, *212*, 110176. [CrossRef]
155. Raza, A.; Fiegl, T.; Hanif, I.; MarkstrÖm, A.; Franke, M.; Körner, C.; Hryha, E. Degradation of AlSi10Mg powder during laser based powder bed fusion processing. *Mater. Des.* **2021**, *198*, 109358. [CrossRef]
156. Sutton, A.T.; Kriewall, C.S.; Leu, M.C.; Newkirk, J.W. Powders for additive manufacturing processes: Characterization techniques and effects on part properties. In Proceedings of the Solid Freeform Fabrication 2016: Proceedings of the 27th Annual International Solid Freeform Fabrication Symposium—An Additive Manufacturing Conference, SFF 2016, Austin, TX, USA, 8–10 August 2016.
157. Zekovic, S.; Dwivedi, R.; Kovacevic, R. Numerical simulation and experimental investigation of gas-powder flow from radially symmetrical nozzles in laser-based direct metal deposition. *Int. J. Mach. Tools Manuf.* **2007**, *47*, 112–123. [CrossRef]
158. Nguyen, Q.B.; Nai, M.L.S.; Zhu, Z.; Sun, C.N.; Wei, J.; Zhou, W. Characteristics of Inconel Powders for Powder-Bed Additive Manufacturing. *Engineering* **2017**, *3*, 695–700. [CrossRef]
159. Tan, J.H.; Wong, W.L.E.; Dalgarno, K.W. An overview of powder granulometry on feedstock and part performance in the selective laser melting process. *Addit. Manuf.* **2017**, *18*, 228–255. [CrossRef]
160. Liu, W.; Huang, S.; Du, S.; Gao, T.; Zhang, Z.; Chen, X.; Huang, L. The Effects of Heat Treatment on Microstructure and Mechanical Properties of Selective Laser Melting 6061 Aluminum Alloy. *Micromachines* **2022**, *13*, 1059. [CrossRef] [PubMed]
161. Ngo, T.D.; Kashani, A.; Imbalzano, G.; Nguyen, K.T.Q.; Hui, D. Additive manufacturing (3D printing): A review of materials, methods, applications and challenges. *Compos. B Eng.* **2018**, *143*, 172–196. [CrossRef]
162. Dhillon, J.S.; Su, S.; Mata, O.S.; Ramakrishnan, T.; Brochu, M. Surface Roughness Studies on F357 Aluminum Alloy Fabricated Using Laser Powder Bed Fusion Process. *Eng. Proc.* **2023**, *43*, 8. [CrossRef]
163. Kumar, M.S.; Yang, C.H.; Farooq, M.U.; Kavimani, V.; Adesoji, A.A. Enhanced structural integrity of Laser Powder Bed Fusion based AlSi10Mg parts by attaining defect free melt pool formations. *Sci. Rep.* **2023**, *13*, 16672. [CrossRef] [PubMed]
164. Pelevin, I.A.; Nalivaiko, A.Y.; Ozherelkov, D.Y.; Shinkaryov, A.S.; Chernyshikhin, S.V.; Arnautov, A.N.; Zmanovsky, S.V.; Gromov, A.A. Selective laser melting of al-based matrix composites with al2o3 reinforcement: Features and advantages. *Materials* **2021**, *14*, 2648. [CrossRef] [PubMed]
165. Markovits, T.; Varga, L.F. Investigating the surface roughness of 3D printed metal parts in case of thin 20 µm build layer thickness. *J. Mater. Res.* **2024**, *39*, 1841–1851. [CrossRef]
166. Dixit, S.; Liu, S. Laser Additive Manufacturing of High-Strength Aluminum Alloys: Challenges and Strategies. *J. Manuf. Mater. Process.* **2022**, *6*, 156. [CrossRef]
167. Malakizadi, A.; Mallipeddi, D.; Dadbakhsh, S.; M'Saoubi, R.; Krajnik, P. Post-processing of additively manufactured metallic alloys—A review. *Int. J. Mach. Tools Manuf.* **2022**, *179*, 103908. [CrossRef]
168. Ren, P.; Ouyang, Y.; Mu, J.; Luo, S.; Tang, Z.; Wu, Y.; Leung, C.L.A.; Oliveira, J.P.; Zou, Y.; Wang, H.; et al. Metal powder atomization preparation, modification, and reuse for additive manufacturing: A review. *Prog. Mater. Sci.* **2025**, *152*, 101449. [CrossRef]
169. Dejene, N.D.; Tucho, W.M.; Lemu, H.G. Effects of Scanning Strategies, Part Orientation, and Hatching Distance on the Porosity and Hardness of AlSi10Mg Parts Produced by Laser Powder Bed Fusion. *J. Manuf. Mater. Process.* **2025**, *9*, 78. [CrossRef]
170. Hirata, T.; Kimura, T.; Nakamoto, T. Effect of Internal Pores on Fatigue Properties in Selective Laser Melted AlSi10Mg Alloy. *Mater. Trans.* **2022**, *63*, 1013–1020. [CrossRef]
171. Hastie, J.C.; Koelblin, J.; Kartal, M.E.; Attallah, M.M.; Martinez, R. Evolution of internal pores within AlSi10Mg manufactured by laser powder bed fusion under tension: As-built and heat treated conditions. *Mater. Des.* **2021**, *204*, 109645. [CrossRef]
172. Abdi, A.; Salehi, M.S.; Fatemi, S.A.; Iuliano, L.; Saboori, A. Microstructure-induced anisotropic tribological properties of Sc-Zr modified Al–Mg alloy (Scalmalloy®) produced via laser powder bed fusion process. *Int. J. Adv. Manuf. Technol.* **2024**, *130*, 755–779. [CrossRef]
173. Wang, L.; Zhang, Y.; Chia, H.Y.; Yan, W. Mechanism of keyhole pore formation in metal additive manufacturing. *npj Comput. Mater.* **2022**, *8*, 22. [CrossRef]
174. Sinha, S.; Mukherjee, T. Mitigation of Gas Porosity in Additive Manufacturing Using Experimental Data Analysis and Mechanistic Modeling. *Materials* **2024**, *17*, 1569. [CrossRef] [PubMed]

175. Rezaeifar, H.; Elbestawi, M. Porosity formation mitigation in laser powder bed fusion process using a control approach. *Opt. Laser Technol.* **2022**, *147*, 107611. [CrossRef]
176. Hafenstein, S.; Hitzler, L.; Sert, E.; Öchsner, A.; Merkel, M.; Werner, E. Hot Isostatic Pressing of Aluminum–Silicon Alloys Fabricated by Laser Powder-Bed Fusion. *Technologies* **2020**, *8*, 48. [CrossRef]
177. Engelhardt, A.; Kahl, M.; Richter, J.; Krooß, P.; Kroll, A.; Niendorf, T. Investigation of processing windows in additive manufacturing of AlSi10Mg for faster production utilizing data-driven modeling. *Addit. Manuf.* **2022**, *55*, 102858. [CrossRef]
178. Ibrahim, M.; Gobber, F.S.; Hulme, C.; Grasmo, G.; Aune, R.E. Influence of Atomizing Gas Pressure on Microstructure and Properties of Nickel Silicide Intended for Additive Manufacturing. *Metals* **2024**, *14*, 930. [CrossRef]
179. Gao, Z.; Zhang, F.; Li, H.; Ma, T.; Yang, H.; Wang, W.; Wei, W.; Wen, S.; Huang, H.; Wu, X.; et al. Process and Properties of Al-Mg-Er-Zr-Sc High-Strength Aluminum Alloy Powder Prepared by Vacuum Induction Melting Gas Atomization. *Materials* **2025**, *18*, 1763. [CrossRef] [PubMed]
180. Touzé, S.; Rauch, M.; Hascoët, J.Y. Flowability characterization and enhancement of aluminium powders for additive manufacturing. *Addit. Manuf.* **2020**, *36*, 101462. [CrossRef]
181. Yim, S.; Bian, H.; Aoyagi, K.; Yamanaka, K.; Chiba, A. Effect of powder morphology on flowability and spreading behavior in powder bed fusion additive manufacturing process: A particle-scale modeling study. *Addit. Manuf.* **2023**, *72*, 103612. [CrossRef]
182. Priyadarshi, A.; Shahrani, S.B.; Choma, T.; Zrodowski, L.; Qin, L.; Leung, C.L.A.; Clark, S.J.; Fezzaa, K.; Mi, J.; Lee, P.D.; et al. New insights into the mechanism of ultrasonic atomization for the production of metal powders in additive manufacturing. *Addit. Manuf.* **2024**, *83*, 104033. [CrossRef]
183. Sabard, A.; de Villiers Lovelock, H.L.; Hussain, T. Microstructural Evolution in Solution Heat Treatment of Gas-Atomized Al Alloy (7075) Powder for Cold Spray. *J. Therm. Spray Technol.* **2018**, *27*, 145–158. [CrossRef]
184. Shabanian, J.; Jafari, R.; Chaouki, J. Fluidization of Ultrafine Powders. *Int. Rev. Chem. Eng.* **2012**, *4*, 16–50.
185. Zheng, B.; Lin, Y.; Zhou, Y.; Lavernia, E.J. Gas atomization of amorphous aluminum powder: Part II. experimental investigation. *Metall. Mater. Trans. B Process Metall. Mater. Process. Sci.* **2009**, *40*, 995–1004. [CrossRef]
186. Martucci, A.; Aversa, A.; Lombardi, M. Ongoing Challenges of Laser-Based Powder Bed Fusion Processing of Al Alloys and Potential Solutions from the Literature—A Review. *Materials* **2023**, *16*, 1084. [CrossRef] [PubMed]
187. Altıparmak, S.C.; Yardley, V.A.; Shi, Z.; Lin, J. Challenges in additive manufacturing of high-strength aluminium alloys and current developments in hybrid additive manufacturing. *Int. J. Lightweight Mater. Manuf.* **2021**, *4*, 246–261. [CrossRef]
188. Marczyk, J.; Hebda, M. Effect of the Particle Size Distribution of Irregular Al Powder on Properties of Parts for Electronics Fabricated by Binder Jetting. *Electronics* **2023**, *12*, 2733. [CrossRef]
189. Mussatto, A.; Groarke, R.; O'Neill, A.; Obeidi, M.A.; Delaure, Y.; Brabazon, D. Influences of powder morphology and spreading parameters on the powder bed topography uniformity in powder bed fusion metal additive manufacturing. *Addit. Manuf.* **2021**, *38*, 101807. [CrossRef]
190. Marinucci, F.; Aversa, A.; Manfredi, D.; Lombardi, M.; Fino, P. Evaluation of a Laboratory-Scale Gas-Atomized AlSi10Mg Powder and a Commercial-Grade Counterpart for Laser Powder Bed Fusion Processing. *Materials* **2022**, *15*, 7565. [CrossRef] [PubMed]
191. Elambasseril, J.; Song, T.; Mendis, S.; Lui, E.; Leary, M.; Brandt, M.; Qian, M. Effect of powder characteristics on layer density, defects, and tensile properties of Ti-6Al-4V via laser powder bed fusion: Establishing benchmark parameters for quality. *Prog. Addit. Manuf.* **2025**, *10*, 7449–7470. [CrossRef]
192. Wang, P.; Salandari-Rabori, A.; Dong, Q.; Fallah, V. Effect of input powder attributes on optimized processing and as-built tensile properties in laser powder bed fusion of AlSi10Mg alloy. *J. Manuf. Process.* **2021**, *64*, 633–647. [CrossRef]
193. Pinotti, V.E.; Andreoli, A.F.; Gargarella, P. Gas atomization of AA2017 aluminum alloy: Effect of process parameters in the physical properties of powders for additive manufacturing. *J. Mater. Res. Technol.* **2024**, *30*, 3650–3662. [CrossRef]
194. Martin, J.H.; Barnes, J.E.; Rogers, K.A.; Hundley, J.; LaPlant, D.L.; Ghanbari, S.; Tsai, J.T.; Bahr, D.F. Additive manufacturing of a high-performance aluminum alloy from cold mechanically derived non-spherical powder. *Commun. Mater.* **2023**, *4*, 39. [CrossRef]
195. Kroeger, J.; Poirié, T.; Moghimian, P.; Marion, F.; Larouche, F. Flow rate ranges for spherical metallic powders for additive manufacturing. *Prog. Addit. Manuf.* **2022**, *7*, 411–418. [CrossRef]
196. Jalalahmadi, B.; Liu, J.; Rios, J.; Slotwinski, J.; Peitsch, C.; Goldberg, A.; Montalbano, T. In-process defect monitoring and correction in additive manufacturing of aluminum alloys. In *The Vertical Flight Society—Forum 75: The Future of Vertical Flight—Proceedings of the 75th Annual Forum and Technology Display*; Vertical Flight Society: Arlington, VA, USA, 2019. [CrossRef]
197. Iovane, P.; Borriello, C.; Pandolfi, G.; Portofino, S.; Mauro, A.D.G.D.; Sico, G.; Tammaro, L.; Fedele, N.; Galvagno, S. Spheroidization of Alumina Powders for Additive Manufacturing Applications by DC Plasma Technology. *Molecules* **2025**, *30*, 453. [CrossRef] [PubMed]
198. Thijs, L.; Verhaeghe, F.; Craeghs, T.; Van Humbeeck, J.; Kruth, J.P. A study of the microstructural evolution during selective laser melting of Ti-6Al-4V. *Acta Mater.* **2010**, *58*, 3303–3312. [CrossRef]
199. Guo, L.; Wang, H.; Liu, H.; Huang, Y.; Wei, Q.; Leung, C.L.A.; Wu, Y.; Wang, H. Understanding keyhole induced-porosities in laser powder bed fusion of aluminum and elimination strategy. *Int. J. Mach. Tools Manuf.* **2023**, *184*, 103977. [CrossRef]

200. Guo, Q.; Qu, M.; Escano, L.I.; Hojjatzadeh, S.M.H.; Young, Z.; Fezzaa, K.; Chen, L. Revealing melt flow instabilities in laser powder bed fusion additive manufacturing of aluminum alloy via in-situ high-speed X-ray imaging. *Int. J. Mach. Tools Manuf.* **2022**, *175*, 103861. [CrossRef]
201. Louvis, E.; Fox, P.; Sutcliffe, C.J. Selective laser melting of aluminium components. *J. Mater. Process. Technol.* **2011**, *211*, 275–284. [CrossRef]
202. Pinkerton, A.J. [INVITED] Lasers in additive manufacturing. *Opt. Laser Technol.* **2016**, *78*, 25–32. [CrossRef]
203. Fiegl, T.; Franke, M.; Körner, C. Correlation of powder degradation, energy absorption and gas pore formation in laser-based powder bed fusion process of AlSi10Mg0.4. *Addit. Manuf.* **2022**, *56*, 102917. [CrossRef]
204. Spierings, A.B.; Herres, N.; Levy, G. Influence of the particle size distribution on surface quality and mechanical properties in AM steel parts. *Rapid Prototyp. J.* **2011**, *17*, 195–202. [CrossRef]
205. Gasper, A.N.D.; Szost, B.; Wang, X.; Johns, D.; Sharma, S.; Clare, A.T.; Ashcroft, I.A. Spatter and oxide formation in laser powder bed fusion of Inconel 718. *Addit. Manuf.* **2018**, *24*, 446–456. [CrossRef]
206. Leung, C.L.A.; Marussi, S.; Towrie, M.; Atwood, R.C.; Withers, P.J.; Lee, P.D. The effect of powder oxidation on defect formation in laser additive manufacturing. *Acta Mater.* **2019**, *166*, 294–305. [CrossRef]
207. Zegzulka, J.; Gelnar, D.; Jezerska, L.; Prokes, R.; Rozbroj, J. Characterization and flowability methods for metal powders. *Sci. Rep.* **2020**, *10*, 21004. [CrossRef] [PubMed]
208. Kiani, P.; Bertoli, U.S.; Dupuy, A.D.; Ma, K.; Schoenung, J.M. A Statistical Analysis of Powder Flowability in Metal Additive Manufacturing. *Adv. Eng. Mater.* **2020**, *22*, 2000022. [CrossRef]
209. Kalina, T.; Chval, Z.; Sedlacek, F.; Spirk, S. Sensitivity Analysis and Influence Evaluation of Progressive Wall Thickness of Honeycomb Structures as Energy Absorber Produced by Additive Technology Multi-Jet Fusion. *Materials* **2025**, *18*, 1. [CrossRef] [PubMed]
210. Yusuf, S.M.; Choo, E.; Gao, N. Comparison between virgin and recycled 316l ss and alsi10mg powders used for laser powder bed fusion additive manufacturing. *Metals* **2020**, *10*, 1625. [CrossRef]
211. Talebi, F.A.; Haydari, Z.; Salehi, H.; Mehrabi, M.; Gardy, J.; Bradley, M.; Bayly, A.E.; Hassanpour, A. Spreadability of powders for additive manufacturing: A critical review of metrics and characterisation methods. *Particuology* **2024**, *93*, 211–234. [CrossRef]
212. Olakanmi, E.O. Selective laser sintering/melting (SLS/SLM) of pure Al; Al-Mg, and Al-Si powders: Effect of processing conditions and powder properties. *J. Mater. Process. Technol.* **2013**, *213*, 1387–1405. [CrossRef]
213. Hulme-Smith, C.N.; Hari, V.; Mellin, P. Spreadability Testing of Powder for Additive Manufacturing. *BHM Berg. Hüttenmänn. Monatshefte* **2021**, *166*, 9–13. [CrossRef]
214. Granutools. Understanding Powders Spreadability for a Recoater Process in Additive Manufacturing. Azom. 2019. Available online: https://www.azom.com/article.aspx?ArticleID=17650 (accessed on 8 March 2019).
215. Ahmed, M.; Pasha, M.; Nan, W.; Ghadiri, M. A simple method for assessing powder spreadability for additive manufacturing. *Powder Technol.* **2020**, *367*, 671–679. [CrossRef]
216. Li, J.; Liu, W.; Shen, J.; Zhang, X.; Li, S.; Wang, Z. Research progress of the metal powder reuse for powder bed fusion additive manufacturing technology. *Powder Technol.* **2024**, *441*, 119815. [CrossRef]
217. Capozzi, L.C.; Sivo, A.; Bassini, E. Powder spreading and spreadability in the additive manufacturing of metallic materials: A critical review. *J. Mater. Process. Technol.* **2022**, *308*, 117706. [CrossRef]
218. Zhang, X.; Zhang, X.; Liu, W.; Jiang, A.; Long, Y. Towards Understanding Formation Mechanism of Cellular Structures in Laser Powder Bed Fused AlSi10Mg. *Materials* **2024**, *17*, 2121. [CrossRef] [PubMed]
219. Bosio, F.; Phutela, C.; Ghisi, N.; Alhammadi, A.; Aboulkhair, N.T. Tuning the microstructure and mechanical properties of AlSi10Mg alloy via in-situ heat-treatments in laser powder bed fusion. *Mater. Sci. Eng. A* **2023**, *879*, 145268. [CrossRef]
220. Van Cauwenbergh, P.; Samaee, V.; Thijs, L.; Nejezchlebová, J.; Sedlák, P.; Iveković, A.; Schryvers, D.; Van Hooreweder, B.; Vanmeensel, K. Unravelling the multi-scale structure–property relationship of laser powder bed fusion processed and heat-treated AlSi10Mg. *Sci. Rep.* **2021**, *11*, 6423. [CrossRef] [PubMed]
221. Raza, A. Powder Degradation During Powder Bed Fusion Processing. Licentiate Thesis, Chalmers University of Technology, Gothenburg, Sweden, 2021.
222. Ilangovan, R.K.; Koundinya, N.T.B.N.; Krishnaswamy, H.; Kumar, G.S.; Amirthalingam, M.; Kottada, R.S. Influence of powder surface chemistry on the defect formation in AlSi10Mg alloy processed via laser powder bed fusion additive manufacturing. *Materialia* **2024**, *34*, 102102. [CrossRef]
223. Barile, C.; Casavola, C.; Kannan, V.P.; Renna, G. The influence of AlSi10Mg recycled powder on corrosion-resistance behaviour of additively manufactured components: Mechanical aspects and acoustic emission investigation. *Arch. Civ. Mech. Eng.* **2022**, *22*, 52. [CrossRef]
224. Fedina, T.; Belelli, F.; Lupi, G.; Brandau, B.; Casati, R.; Berneth, R.; Brueckner, F.; Kaplan, A.F.H. Influence of AlSi10Mg powder aging on the material degradation and its processing in laser powder bed fusion. *Powder Technol.* **2022**, *412*, 118024. [CrossRef]

225. Clement, C.D.; Masson, J.; Kabir, A.S. Effects of Heat Treatment on Microstructure and Mechanical Properties of AlSi10Mg Fabricated by Selective Laser Melting Process. *J. Manuf. Mater. Process.* **2022**, *6*, 52. [CrossRef]
226. Carroll, J.D.; Exil, A.N.; DeJong, S.A.; Valdez, I.A.; Laursen, C.M.; Deibler, L.A.; Finfrock, C.B.; Boyce, B.L. High-Throughput Statistical Interrogation of Mechanical Properties with Build Plate Location and Powder Reuse in AlSi10Mg. *JOM* **2021**, *73*, 3356–3370. [CrossRef]
227. Ponnusamy, P.; Rashid, R.A.R.; Masood, S.H.; Ruan, D.; Palanisamy, S. Mechanical properties of slm-printed aluminium alloys: A review. *Materials* **2020**, *13*, 4301. [CrossRef] [PubMed]
228. Del Re, F.; Contaldi, V.; Astarita, A.; Palumbo, B.; Squillace, A.; Corrado, P.; Di Petta, P. Statistical approach for assessing the effect of powder reuse on the final quality of AlSi10Mg parts produced by laser powder bed fusion additive manufacturing. *Int. J. Adv. Manuf. Technol.* **2018**, *97*, 2231–2240. [CrossRef]
229. Paccou, E.; Mokhtari, M.; Keller, C.; Nguejio, J.; Lefebvre, W.; Sauvage, X.; Boileau, S.; Babillot, P.; Bernard, P.; Bauster, E. Investigations of powder reusing on microstructure and mechanical properties of Inconel 718 obtained by additive manufacturing. *Mater. Sci. Eng. A* **2021**, *828*, 142113. [CrossRef]
230. *ASTM B822-25*; Standard Test Method for Particle Size Distribution of Metal Powders and Related Compounds by Light Scattering. ASTM International: West Conshohocken, PA, USA, 2025.
231. Ozeren, E.; Bilgin, G.M.; Ertekin, B.; Taş, A.; Cavcar, Z.; Gökcan, M.B.; Orhangül, A.; Kara, G. Characterization of Metal Powder Reused Multiple Times for Laser Powder Bed Fusion. *J. Addit. Manuf. Technol.* **2022**, *2*, 688–692. [CrossRef]
232. *ASTM E11-24*; Standard Specification for Woven Wire Test Sieve Cloth and Test Sieves. ASTM International: West Conshohocken, PA, USA, 2024.
233. Harkin, R.; Wu, H.; Nikam, S.; Quinn, J.; McFadden, S. Analysis of spatter removal by sieving during a powder-bed fusion manufacturing campaign in grade 23 titanium alloy. *Metals* **2021**, *11*, 399. [CrossRef]
234. Opatová, K.; Zetková, I.; Kučerová, L. Relationship between the size and inner structure of particles of virgin and re-used ms1 maraging steel powder for additive manufacturing. *Materials* **2020**, *13*, 956. [CrossRef] [PubMed]
235. Haferkamp, L. Effect of the Particle Size Distribution and Morphology on Powder Processability in Laser Powder Bed Fusion. Ph.D. Thesis, ETH Zurich, Zürich, Switzerland, 2022.
236. Gorji, N.E.; Saxena, P.; Corfield, M.; Clare, A.; Rueff, J.P.; Bogan, J.; González, P.G.M.; Snelgrove, M.; Hughes, G.; O'Connor, R.; et al. A new method for assessing the recyclability of powders within Powder Bed Fusion process. *Mater. Charact.* **2020**, *161*, 110167. [CrossRef]
237. Charbonneau, C.; Bernier, F.; Perrault, É.; Pelletier, R.; Lefebvre, L. Classification of Metallic Powder Morphology Using Traditional and Automated Static Image Analysis: A Comparative Study Classification of Metallic Powder Morphology Using Traditional and Automated Static Image Analysis: A Comparative Study. *Preprints* **2025**, 2025031784. [CrossRef]
238. Raza, A.; Hryha, E. Characterization of spatter and sublimation in alloy 718 during electron beam melting. *Materials* **2021**, *14*, 5953. [CrossRef] [PubMed]
239. Gorji, N.E.; O'Connor, R.; Brabazon, D. XPS and SEM characterization for powder recycling within 3d printing process. In Proceedings of the ESAFORM 2021—24th International Conference on Material Forming, Liège, Belgium, 14–16 April 2021. [CrossRef]
240. *ASTM B213-25*; Standard Test Methods for Flow Rate of Metal Powders Using the Hall Flowmeter Funnel. ASTM International: West Conshohocken, PA, USA, 2025.
241. Espiritu, E.R.L.; Kumar, A.; Nommeots-Nomm, A.; Lerma, J.A.M.; Brochu, M. Investigation of the rotating drum technique to characterise powder flow in controlled and low pressure environments. *Powder Technol.* **2020**, *366*, 925–937. [CrossRef]
242. Tan, Y.; Zhang, J.; Li, X.; Xu, Y.; Wu, C.Y. Comprehensive evaluation of powder flowability for additive manufacturing using principal component analysis. *Powder Technol.* **2021**, *393*, 925–937. [CrossRef]
243. *ASTM E1409-13(2021)*; Standard Test Method for Determination of Oxygen and Nitrogen in Titanium and Titanium Alloys by Inert Gas Fusion. ASTM International: West Conshohocken, PA, USA, 2021.
244. Bardo, R.; Dziurka, R.; Fryzowicz, K.; Bała, P. Exploring Elemental Powder Approach for Making Al and Ti Containing High-Entropy Alloys by Powder Bed Fusion. *Metall. Mater. Trans. A Phys. Metall. Mater. Sci.* **2024**, *55*, 2840–2854. [CrossRef]
245. Dörfert, R.; Zhang, J.; Clausen, B.; Freiße, H.; Schumacher, J.; Vollertsen, F. Investigation of the oxygen content of additively manufactured tool steel 1.2344. In Proceedings of the Solid Freeform Fabrication 2019: Proceedings of the 30th Annual International Solid Freeform Fabrication Symposium—An Additive Manufacturing Conference, SFF 2019, Austin, TX, USA, 12–14 August 2019.
246. Gromov, A.; Vereshchagin, V. Study of aluminum nitride formation by superfine aluminum powder combustion in air. *J. Eur. Ceram. Soc.* **2004**, *24*, 2879–2884. [CrossRef]
247. Weingarten, C.; Buchbinder, D.; Pirch, N.; Meiners, W.; Wissenbach, K.; Poprawe, R. Formation and reduction of hydrogen porosity during selective laser melting of AlSi10Mg. *J. Mater. Process. Technol.* **2015**, *221*, 112–120. [CrossRef]

248. Montazeri, M.; Yavari, R.; Rao, P.; Boulware, P. In-process monitoring of material cross-contamination defects in laser powder bed fusion. *J. Manuf. Sci. Eng. Trans. ASME* **2018**, *140*, 111001. [CrossRef]
249. Horn, M.; Langer, L.; Schafnitzel, M.; Dietrich, S.; Schlick, G.; Seidel, C.; Reinhart, G. Influence of metal powder cross-contaminations on part quality in Laser Powder Bed Fusion: Copper alloy particles in maraging steel feedstock. *Procedia CIRP* **2020**, *94*, 167–172. [CrossRef]
250. Hulme, C.N.; Mellin, P.; Marchetti, L.; Hari, V.; Uhlirsch, M.; Strandh, E.; Saeidi, K.; Goff, S.D.-L.; Saleem, S.; Pettersson, V.; et al. A practicable and reliable test for metal powder spreadability: Development of test and analysis technique. *Prog. Addit. Manuf.* **2023**, *8*, 505–517. [CrossRef]
251. Brika, S.E.; Brailovski, V. A Novel Apparatus for the Simulation of Powder Spreading Procedures in Powder-Bed-Based Additive Manufacturing Processes: Design, Calibration, and Case Study. *J. Manuf. Mater. Process.* **2023**, *7*, 135. [CrossRef]
252. Delacroix, T.; Lomello, F.; Schuster, F.; Maskrot, H.; Jacquier, V.; Lapouge, P.; Coste, F.; Garandet, J.P. Measurement of powder bed oxygen content by image analysis in laser powder bed fusion. *Mater. Des.* **2023**, *226*, 111667. [CrossRef]
253. Katagiri, J.; Nomoto, S.; Kusano, M.; Watanabe, M. Particle Size Effect on Powder Packing Properties and Molten Pool Dimensions in Laser Powder Bed Fusion Simulation. *J. Manuf. Mater. Process.* **2024**, *8*, 71. [CrossRef]

Disclaimer/Publisher's Note: The statements, opinions and data contained in all publications are solely those of the individual author(s) and contributor(s) and not of MDPI and/or the editor(s). MDPI and/or the editor(s) disclaim responsibility for any injury to people or property resulting from any ideas, methods, instructions or products referred to in the content.